

# An Efficient Multi-scale Leverage Effect Estimator under Dependent Microstructure Noise

Ziyang Xiong<sup>1</sup>, Zhao Chen<sup>\*1</sup>, and Christina Dan Wang<sup>†2</sup>

<sup>1</sup>School of Data Science, Fudan University

<sup>2</sup>Business Division, New York University Shanghai

June 12, 2025

## Abstract

Estimating the leverage effect from high-frequency data is vital but challenged by complex, dependent microstructure noise, often exhibiting non-Gaussian higher-order moments. This paper introduces a novel multi-scale framework for efficient and robust leverage effect estimation under such flexible noise structures. We develop two new estimators, the Subsampling-and-Averaging Leverage Effect (SALE) and the Multi-Scale Leverage Effect (MSLE), which adapt subsampling and multi-scale approaches holistically using a unique shifted window technique. This design simplifies the multi-scale estimation procedure and enhances noise robustness without requiring the pre-averaging approach. We establish central limit theorems and stable convergence, with MSLE achieving convergence rates of an optimal  $n^{-1/4}$  and a near-optimal  $n^{-1/9}$  for the noise-free and noisy settings, respectively. A cornerstone of our framework's efficiency is a specifically designed MSLE weighting strategy that leverages covariance structures across scales. This significantly reduces asymptotic variance and, critically, yields substantially smaller finite-sample errors than existing methods under both noise-free and realistic noisy settings. Extensive simulations and empirical analyses confirm the superior efficiency, robustness, and practical advantages of our approach.

**Keywords** High-frequency data; Market microstructure noise; Leverage effect; Subsampling; Multi-scale; Robust estimation; Efficiency

## 1 Introduction

The leverage effect, or the observed negative correlation between asset returns and their volatility changes, is a prominent stylized fact in financial econometrics (Black, 1976; Christie, 1982). It captures the asymmetry in volatility responses to positive and negative shocks in asset prices and is widely attributed to mechanisms such as financial leverage and asymmetric information in markets. Accurate estimation of the leverage effect is not only central to our understanding of asset price dynamics but also has critical implications for the pricing and hedging of derivative securities, especially in the presence of volatility skews.

One of the main challenges in the field of high-frequency financial data is the presence of market microstructure (MMS) noise. The well-known “volatility signature plot” demonstrates a key challenge: with high-frequency observations, simple realized volatility estimators are largely biased and thus inconsistent due to noise (Zhou, 1996; Andersen et al., 2000; Aït-Sahalia et al., 2005; Patton, 2011; Aït-Sahalia and Xiu, 2019); simple leverage effect estimators suffer from

\*Corresponding author: zchen.fdu@fudan.edu.cn

†Corresponding author: christina.wang@nyu.edu

a similar issue. Existing methods for leverage effect estimation have primarily focused on mitigating the impact of such noise by either adopting the pre-averaging technique (Jacod et al., 2009; Podolskij and Vetter, 2009; Mykland and Zhang, 2016) under the assumption of independent and identically distributed (iid) Gaussian noise or using extra information. For instance, Wang and Mykland (2014) and Aït-Sahalia et al. (2017) utilize the pre-averaging methods to estimate leverage effect under iid Gaussian noise, Yuan et al. (2020) adopts the parametric setting for microstructure noise proposed by Li et al. (2016) that incorporates trading information to address noise, Chong and Todorov (2024) utilizes high-frequency short-dated option to recover spot volatility process, thereby estimating leverage effect, while some other works (e.g. Bandi and Renò, 2012; Kalnina and Xiu, 2017; Curato and Sanfelici, 2022; Yang, 2023) estimate leverage effect without explicitly addressing microstructure noise. While these methods represent significant advances, their reliance on iid Gaussian noise-related assumptions or auxiliary data remains restrictive in practice. Specifically, empirical evidence has consistently shown that microstructure noise exhibits serial dependence and higher-order moments (Jacod et al., 2017; Aït-Sahalia and Xiu, 2019; Li et al., 2020; Da and Xiu, 2021; Li and Linton, 2022). These features not only violate standard modeling assumptions, but also exacerbate bias and variance in leverage effect estimation, underscoring the need for more flexible methodologies that can accommodate complex noise structures.

In this paper, we propose a novel multi-scale framework for estimating the leverage effect that explicitly accounts for microstructure noise exhibiting more flexible noise structures, allowing for stationary, dependent noise with nontrivial higher-order moments, which are commonly observed in empirical financial data. Specifically, we introduce two new estimators: the Subsampling-and-Averaging Leverage Effect (SALE) estimator and the Multi-Scale Leverage Effect (MSLE) estimator. Both estimators are constructed by adapting a base estimator modified from an estimator studied by Aït-Sahalia et al. (2017). In particular, the MSLE estimator aggregates a series of weighted SALE estimators computed across multiple time scales, exploiting their complementary properties to achieve improved convergence rates. Our methodology draws inspiration from the principles underlying the Two-Scale Realized Volatility (TSRV) and Multi-Scale Realized Volatility (MSRV) estimators (Zhang et al., 2005; Zhang, 2006; Aït-Sahalia et al., 2011), but adapts and extends them for the specific task of estimating the leverage effect. Crucially, we do not merely use their methods as plug-in estimators for spot volatility; we develop a holistic multi-scale approach for the leverage effect itself. A key innovation in our construction is the use of a shifted window for estimating spot volatility, as illustrated schematically in Figure 1a and 1b. This shift is important as it not only helps decouple noise components to achieve unbiasedness and variance reduction with respect to noise, but also fundamentally simplifies certain aspects of the multi-scale estimation procedure compared with the classical constructions in TSRV and MSRV.

The second primary contribution of this work is the explicit demonstration and optimization of multi-scale benefits beyond mere noise mitigation. Specifically, for the noise-free setting, we show that our MSLE estimator, through a proper weighting scheme, achieves a notable reduction in asymptotic variance compared with the base estimator by exploiting the covariance structure of SALE estimators of different subsampling scales. Our focus on improving estimator efficiency through structural design and weighting design resonates with some recent research such as Yang (2023), which explores efficient estimation for leverage effect through nonuniform kernel functions in spot volatility estimation.

Recognizing a potential gap between standard theoretical assumptions and empirical reality regarding MMS noise, another major contribution of this work lies in the in-depth study of optimal weight assignment under diverse and realistic noise magnitudes. Classical asymptotic analyses often assume that noise variance is of constant order, thus dominating the shrinking latent increments as the sampling frequency increases. However, empirical evidence suggests a more complex picture. For instance, Aït-Sahalia and Xiu (2019) finds that improvements

in market liquidity allow employing simple volatility estimators at higher frequencies, while [Kalnina and Linton \(2008\)](#) and [Da and Xiu \(2021\)](#) also explore the case of shrinkage MMS noise. A recent work by [Chong et al. \(2025\)](#) investigates the rough noise model that captures a more subtle interplay between the latent price process and noise. This implies that weighting schemes based solely on the strict noise-dominance assumption might suffer from modeling error when applied to real data. Motivated by this, we conduct a fine-grained analysis of the MSLE’s asymptotic variance components across different subsampling scales and noise conditions. Moreover, implementing truly optimal weights would require precise values of asymptotic covariances between SALE estimators at sampling scales, which are infeasible in practice. To overcome this, we develop a computationally efficient approximate weighting strategy that works for a wide spectrum of noise conditions, yielding robust finite-sample performance as demonstrated in Monte Carlo simulations.

Our theoretical analysis establishes central limit theorems and stable convergence results for both the noise-free and noisy settings, demonstrating that the proposed estimators achieve consistency and asymptotic normality. Under the noise-free setting, both estimators attain the optimal convergence rate of order  $n^{-1/4}$ . In the presence of MMS noise, the MSLE estimator achieves a convergence rate of order  $n^{-1/9}$ , which is slightly slower than the optimal  $n^{-1/8}$  but remains highly competitive. Furthermore, to support feasible inference, we construct consistent estimators for the asymptotic variances in both noise-free and noisy regimes, enabling the implementation of feasible central limit theorems. Monte Carlo simulations, employing both iid and dependent noise with various distributions, validate both the feasible and infeasible central limit theorems. To assess the finite-sample performance of the proposed estimators, we conduct another extensive simulation study, where a variety of settings concerning realistic time horizons and noise conditions, verifying the outstanding efficiency of the proposed MSLE estimator with the approximate weighting strategy. The result shows that, under the noise-free setting, our method outperforms the base estimator, while under the noisy setting, our method outperforms the pre-averaging strategy implemented in [Aït-Sahalia et al. \(2017\)](#). This superior finite-sample behavior is attributable to a combination of factors, further detailed in Section 6.3: (i) the more advantageous noise-free asymptotic variance of the SALE estimator, (ii) the relatively smaller impact of noise under realistic settings, and (iii) the enhanced performance of MSLE over the individual SALE estimators.

To examine the performance of our estimators in practical applications, we also conduct an empirical analysis using high-frequency financial data. The high-frequency trading data of 30 assets including ETFs and individual stocks from the U.S. stock market are utilized. The leverage effects are estimated adaptively based on the microstructure noise characteristics in each period, and general negative correlation between the returns and volatility changes is verified. This study demonstrates the practical effectiveness of the MSLE estimator in capturing the leverage effect under realistic market conditions, further validating the advantages observed in the simulation experiments.

The remaining paper is arranged as follows. Section 2 introduces the model settings and notations. Section 3 presents the construction of the estimators, covering the original estimator, the all-observation estimator, the subsample estimator, and the development of the SALE and MSLE estimators. Section 4 states the main theoretical results, including limit theorems for the SALE and MSLE estimators under both noise-free and noisy conditions. Section 5 discusses the issue of variance reduction, including variance approximations under both noise-free and noisy settings, and proposes practical strategies for optimizing the performance of MSLE. Section 6 provides a detailed simulation study to validate the theoretical properties, examining the asymptotic behavior and finite-sample performance under various settings of microstructure noise. Section 7 reports the results of an empirical study using real-world high-frequency data to demonstrate the practical utility of the proposed methods. Appendices A and B contain the proofs of the main propositions, theorems, and technical lemmas supporting the results

presented in the paper.

## 2 Model settings and notations

**Underlying processes** We assume that the log-price  $(X_t)_{t \geq 0}$  and volatility  $(\sigma_t)_{t \geq 0}$  processes are both Itô processes defined on a filtered probability space  $(\Omega, \mathcal{F}, (\mathcal{F}_t)_{t \geq 0}, \mathbb{P})$ :

$$\begin{aligned} X_t &= X_0 + \int_0^t \mu_s ds + \int_0^t \sigma_s dW_s, \\ \sigma_t &= \sigma_0 + \int_0^t a_s ds + \int_0^t f_s dW_s + \int_0^t g_s dB_s, \end{aligned} \quad (2.1)$$

where  $(\mu_t)_{t \geq 0}$ ,  $(a_t)_{t \geq 0}$ ,  $(f_t)_{t \geq 0}$  and  $(g_t)_{t \geq 0}$  are adapted càdlàg locally bounded random processes, and  $(W_t)_{t \geq 0}$  as well as  $(B_t)_{t \geq 0}$  are independent Wiener processes. Moreover, the process  $(\sigma_t^2)_{t \geq 0}$  is assumed to be bounded away from zero.

**Parameter of interest** The leverage effect is defined as the quadratic covariation of  $X$  and  $\sigma^2$ ,

$$\langle X, \sigma^2 \rangle_T = \int_0^T 2\sigma_s^2 f_s ds, \quad (2.2)$$

which is our parameter of interest.

**Observation scheme and notations** The log-price process contaminated by MMS noise is observed at equidistant time points  $t_0, t_1, \dots, t_n$  on  $[0, T]$ , where  $t_i = i\Delta_n = iT/n$ ,  $i = 0, 1, \dots, n$ . For convenience, we adopt the following three conventions regarding the notations in this work: (i) with a slight abuse of notation, we use the observation time index to index the process at that time, *i.e.*,  $V_i = V_{t_i}$ , whenever there is no ambiguity; (ii) we define the difference over the subsequent time interval as  $\Delta V_i = V_{i+1} - V_i$  for  $i = 0, 1, \dots, n-1$ ; and (iii) similarly,  $\Delta_k V_i = V_{i+k} - V_i$  for  $i = 0, 1, \dots, n-k$ .

**Microstructure noise** The observed log-price can be described as

$$Y_i = X_i + \varepsilon_i, \quad (2.3)$$

where  $\varepsilon_i$  is the MMS noise at time  $t_i$ . We assume that the MMS noise sequence  $\{\varepsilon_i\}_{i=0}^n$  satisfies: (i)  $\{\varepsilon_i\}_{i=0}^n$  is mean zero, identically distributed, and independent of  $\mathcal{F}$ ; and (ii)  $\{\varepsilon_i\}_{i=0}^n$  is independent. We will later see that, in some of the proposed estimators, the condition (ii) can be relaxed to a weaker condition, namely: (ii')  $\{\varepsilon_i\}_{i=0}^n$  is strictly stationary and  $q$ -dependent, which means there exists a non-negative integer  $q$  such that  $\varepsilon_i \perp \varepsilon_j$  for  $|i - j| > q$ . The  $k$ th moment of the noise is denoted as  $\nu_k = \mathbb{E}[\varepsilon_i^k]$  for any  $k \geq 1$ .

**Notations of subsamples** A subsample of observations is defined by a pair of integers  $(H, h)$ . For a subsample scale  $H$ , we choose one observation from every  $H$  observations, resulting in  $H$  subsamples indexed by  $h \in \{1, \dots, H\}$ . The  $j$ th observations in subsample  $(H, h)$  can be denoted as  $(H, h, j)$ , where  $j \in \{0, 1, \dots, n_{H,h}\}$  and  $n_{H,h} = \lfloor (n - h + 1)/H \rfloor$ . The observation  $(H, h, j)$  is indexed by  $j_{H,h} = jH + h - 1$  in all observations, and it corresponds to the time point  $\tau_{H,h,j} = t_{j_{H,h}} = (jH + h - 1)\Delta_n$ .

**Table 1:** Notations of estimators and their definitions.

Estimator	Sequence of observations		Definition
	Noise-free	Noisy	
Ait-Sahalia et al. (2017)	$[X, \sigma^2]_T^{\text{[AFLWY17]}}$	$\widehat{[X, \sigma^2]_T}^{\text{[AFLWY17]}}$	Equation (3.1) and (3.2)
All-observation	$[X, \sigma^2]_T^{(\text{all})}$	$\widehat{[X, \sigma^2]_T}^{(\text{all})}$	Equation (3.4) and (3.5)
Subsample	$[X, \sigma^2]_T^{(H_n, h)}$	$\widehat{[X, \sigma^2]_T}^{(H_n, h)}$	Equation (3.9) and (3.10)
SALE	$[X, \sigma^2]_T^{(H_n)}$	$\widehat{[X, \sigma^2]_T}^{(H_n)}$	Equation (3.12) and (3.13)
MSLE	$[X, \sigma^2]_T^{(\text{MS})}$	$\widehat{[X, \sigma^2]_T}^{(\text{MS})}$	Equation (3.20) and (3.21)

**Notations of estimators** The notations of estimators are clarified here. Given the sample size, an estimator can be viewed as a function that maps a sequence of observations to an estimated value, whether the observations are contaminated by noise or not. However, our main interest is to investigate its behavior when applied to both the noise-free sequence  $\{X_i\}_{i=0}^n$  and the noisy sequence  $\{Y_i\}_{i=0}^n$ . Therefore, with a slight abuse of notations, we denote  $[X, \sigma^2]_T$  as the estimate with the noise-free sequence, and  $\widehat{[X, \sigma^2]_T}$  as the estimate with the noisy sequence. In contrast,  $\langle X, \sigma^2 \rangle_T$  is used to denote the true value of leverage effect, as defined in Equation (2.2). Specifically, the notations and definitions of the estimators in this paper are listed in Table 1. In addition, the subscript  $T$  in any estimator  $[X, \sigma^2]_T$ ,  $\widehat{[X, \sigma^2]_T}$  or parameter  $\langle X, \sigma^2 \rangle_T$  may be omitted when there is no ambiguity.

**Expectations and variances** By using  $\mathbb{E}[h]$  for some function  $h$ , we mean that the expectation is taken with respect to the joint distribution of processes  $(X_t)_{t \geq 0}$ ,  $(\sigma_t)_{t \geq 0}$  and the noise  $\{\varepsilon_i\}_{i=1}^n$ . We also consider the conditional expectation given processes  $(X_t)_{t \geq 0}$  and  $(\sigma_t)_{t \geq 0}$ , which is denoted as  $\mathbb{E}[h|\mathcal{F}]$ . The notations for variances and covariances should be interpreted similarly.

**Overview of methodologies** For an estimator of interest, we focus on two aspects:

1. Ensuring that it is *unbiased with respect to noise*; that is,

$$\underbrace{\mathbb{E} \left( \widehat{[X, \sigma^2]_T} \middle| \mathcal{F} \right) - [X, \sigma^2]_T}_{\text{bias due to noise}} = 0. \quad (2.4)$$

2. Assessing its total variance by decomposing it into the *variance due to discretization* and the expected *variance due to noise*:

$$\begin{aligned} \text{Var} \left( \widehat{[X, \sigma^2]_T} \right) &= \text{Var} \left[ \mathbb{E} \left( \widehat{[X, \sigma^2]_T} \middle| \mathcal{F} \right) \right] + \mathbb{E} \left[ \text{Var} \left( \widehat{[X, \sigma^2]_T} \middle| \mathcal{F} \right) \right] \\ &= \underbrace{\text{Var} \left( [X, \sigma^2]_T \right)}_{\text{variance due to discretization}} + \mathbb{E} \left[ \underbrace{\text{Var} \left( \widehat{[X, \sigma^2]_T} \middle| \mathcal{F} \right)}_{\text{variance due to noise}} \right]. \end{aligned} \quad (2.5)$$

To establish the limit theorems, the idea of Equation (2.5) needs to be made more rigorous. Yet, a primary goal of this paper is to balance the asymptotic variances arising from these two sources by developing new estimators and tuning hyperparameters.

### 3 Construction of estimators

#### 3.1 Original estimator

We start with an existing continuous leverage effect estimator proposed by [Aït-Sahalia et al. \(2017\)](#). This estimator uses the threshold technique to deal with the jump in the observed log-price process. However, since we are not including jumps in this paper, we will only consider its form without threshold. When the noise is absent, their estimator is given by

$$[X, \sigma^2]_T^{[\text{AFLWY17}]} = \frac{1}{k_n \Delta_n} \sum_{i=k_n}^{n-k_n-1} (\Delta X_i) \left( \sum_{j=i+1}^{i+k_n} (\Delta X_j)^2 - \sum_{j=i-k_n}^{i-1} (\Delta X_j)^2 \right). \quad (3.1)$$

Notice that  $(k_n \Delta_n)^{-1} \sum_{j=i+1}^{i+k_n} (\Delta X_j)^2$  and  $(k_n \Delta_n)^{-1} \sum_{j=i-k_n}^{i-1} (\Delta X_j)^2$  are spot volatility estimates for  $\sigma_{i+1}^2$  and  $\sigma_i^2$  respectively, where  $k_n \rightarrow \infty$  and  $k_n \Delta_n \rightarrow 0$  as  $n \rightarrow \infty$ . By directly substituting  $Y_i$  for  $X_i$  in this estimator, the estimator becomes

$$\widehat{[X, \sigma^2]_T}^{[\text{AFLWY17}]} = \frac{1}{k_n \Delta_n} \sum_{i=k_n}^{n-k_n-1} (\Delta Y_i) \left( \sum_{j=i+1}^{i+k_n} (\Delta Y_j)^2 - \sum_{j=i-k_n}^{i-1} (\Delta Y_j)^2 \right). \quad (3.2)$$

Given the processes, the conditional expectation of the noisy estimator is

$$\mathbb{E} \left( \widehat{[X, \sigma^2]_T}^{[\text{AFLWY17}]} \middle| \mathcal{F} \right) = [X, \sigma^2]_T^{[\text{AFLWY17}]} + 2 \frac{n - 2k_n}{k_n \Delta_n} \nu_3. \quad (3.3)$$

Therefore, the dominant term is the noise term whenever  $\nu_3$  is non-zero. This is because, for the  $i$ th summand in the estimator, the noise terms at  $i$  and  $i + 1$  exist simultaneously in the estimates of  $\Delta X_i$  and  $\Delta \sigma_i^2$ . In fact, the estimator is inconsistent even when  $\nu_3$  is zero, as the variance due to noise diverges as  $n \rightarrow \infty$ .

#### 3.2 All-observation estimator

Therefore, our first attempt is to shift the windows for spot volatility estimates outward by  $\Delta_n$ , which does not affect the asymptotic behavior of the noise-free version of estimator. The resulting estimator is called an *all-observation Leverage Effect* (LE) estimator, and its noise-free version is

$$[X, \sigma^2]_T^{(\text{all})} = \frac{1}{k_n \Delta_n} \sum_{i \in I} (\Delta X_i) \left( \sum_{j \in I^+(i)} (\Delta X_j)^2 - \sum_{j \in I^-(i)} (\Delta X_j)^2 \right), \quad (3.4)$$

where  $I^+(i) = \{i+2, \dots, i+k_n+1\}$ ,  $I^-(i) = \{i-k_n-1, \dots, i-2\}$ , and  $I = \{k_n+1, \dots, n-k_n-2\}$ . It is clear that  $|I^+(i)| = |I^-(i)| = k_n$  and  $|I| = n - 2k_n - 2$ . The noisy version of this estimator is

$$\widehat{[X, \sigma^2]_T}^{(\text{all})} = \sum_{i \in I} (\Delta Y_i) \left( \hat{\sigma}_{(i+1)+}^2 - \hat{\sigma}_{i-}^2 \right), \quad (3.5)$$

where the spot volatility estimates are

$$\hat{\sigma}_{(i+1)+}^2 = \frac{1}{k_n \Delta_n} \sum_{j \in I^+(i)} (\Delta Y_j)^2, \quad \hat{\sigma}_{i-}^2 = \frac{1}{k_n \Delta_n} \sum_{j \in I^-(i)} (\Delta Y_j)^2. \quad (3.6)$$

The bias and variance due to noise are described by the following proposition. The proof, as well as a more precise version, is given in [Appendix A.1](#).

**Proposition 1.** *If  $\{\varepsilon_i\}_{i=0}^n$  satisfies the condition (i) and (ii) concerning the noise in Section 2, given the processes, the all-observation estimator is unbiased, i.e.*

$$\mathbb{E} \left( \widehat{[X, \sigma^2]}_T^{(\text{all})} \middle| \mathcal{F} \right) = [X, \sigma^2]_T^{(\text{all})}. \quad (3.7)$$

and its conditional variance satisfies

$$\Delta_n^3 k_n^2 \text{Var} \left( \widehat{[X, \sigma^2]}_T^{(\text{all})} \middle| \mathcal{F} \right) \xrightarrow{p} (8\nu_2\nu_4 + 16\nu_2^3 + 8\nu_3^2)T, \quad \text{as } n \rightarrow \infty. \quad (3.8)$$

Although the all-observation estimator is unbiased due to noise, its variance is of order  $O(n^3 k_n^{-2})$ , and therefore diverges. According to the asymptotic results derived in [Aït-Sahalia et al. \(2017\)](#), the variance due to discretization is of order  $O(k_n^{-1} + n^{-1}k_n)$ . Therefore, it is never possible to achieve a balance between the discretization variance and the noise variance by simply choosing an appropriate  $k_n$ .

However, this estimator is the foundation for the subsequent sections. We will show that the variance due to noise can be controlled using subsampling, averaging, and multi-scale techniques, allowing us to strike a balance with the variance due to discretization.

### 3.3 Subsample estimator

We now consider using a sparse subsample of the observations. Recall the notations defined in Section 2. Hereafter, we assume that  $k_n \rightarrow \infty$ ,  $H_n \rightarrow \infty$  and  $k_n H_n \Delta_n \rightarrow 0$  as  $n \rightarrow \infty$ . The noise-free version of the estimator based on the subsample  $(H_n, h)$  is defined as

$$[X, \sigma^2]_T^{(H_n, h)} = \frac{1}{k_n H_n \Delta_n} \sum_{i \in I_{H_n, h}} (\Delta_{H_n} X_{i_h}) \left( \sum_{j \in I^+(i)} (\Delta_{H_n} X_{j_h})^2 - \sum_{j \in I^-(i)} (\Delta_{H_n} X_{j_h})^2 \right), \quad (3.9)$$

where  $I^+(i) = \{i + 2, \dots, i + k_n + 1\}$ ,  $I^-(i) = \{i - k_n - 1, \dots, i - 2\}$ , and  $I_{H_n, h} = \{k_n + 1, \dots, n_{H_n, h} - k_n - 2\}$ . Clearly,  $|I^+(i)| = |I^-(i)| = k_n$ , and  $|I| = n_{H_n, h} - 2k_n - 2$ . The noisy version of this estimator is

$$\widehat{[X, \sigma^2]}_T^{(H_n, h)} = \sum_{i \in I_{H_n, h}} (\Delta_{H_n} Y_{i_h}) \left( \hat{\sigma}_{(i+1)_{H_n, h}}^2 - \hat{\sigma}_{i_{H_n, h}}^2 \right), \quad (3.10)$$

where the spot volatility estimates are

$$\hat{\sigma}_{(i+1)_{H_n, h}}^2 = \frac{1}{k_n H_n \Delta_n} \sum_{j \in I^+(i)} (\Delta_{H_n} Y_{j_h})^2, \quad \hat{\sigma}_{i_{H_n, h}}^2 = \frac{1}{k_n H_n \Delta_n} \sum_{j \in I^-(i)} (\Delta_{H_n} Y_{j_h})^2. \quad (3.11)$$

The variance of the subsample estimator can be directly derived from the properties of all-observation estimator by substituting  $n$  with  $n_{H_n, h} \approx n/H$ . Thus, the variance due to discretization is of order  $O(k_n^{-1} + n^{-1}H_n k_n)$ , while the variance due to noise is of order  $O(n^3 H_n^{-3} k_n^{-2})$ . Although the variance due to noise is much smaller than that of the all-observation estimator, it still diverges because of the assumption that  $k_n H_n \Delta_n \rightarrow \infty$  as  $n \rightarrow \infty$ .

### 3.4 SALE: subsampling-and-averaging estimator

Since we have  $H_n$  subsamples, we can average the subsample estimators to reduce the variance due to noise. The *Subsampling-and-Averaging Leverage Effect* (SALE) estimator for a noise-free sequence is defined as

$$[X, \sigma^2]_T^{(H_n)} = \frac{1}{H_n} \sum_{h=1}^{H_n} [X, \sigma^2]_T^{(H_n, h)}, \quad (3.12)$$



and the noisy version is defined as

$$\widehat{[X, \sigma^2]}_T^{(H_n)} = \frac{1}{H_n} \sum_{h=1}^{H_n} \widehat{[X, \sigma^2]}_T^{(H_n, h)}. \quad (3.13)$$

The SALE is unbiased due to noise, as implied by Proposition 1. It also allows the noise to be strictly stationary and dependent up to a certain lag. Specifically, when the noise is independent, there is no covariance due to noise between subsample estimators. Consequently, the variance of SALE due to noise can be significantly reduced compared to the subsample estimator. The following proposition describes the variance of SALE estimator due to noise. The proof, along with a more precise version, is given in Appendix A.2.

**Proposition 2.** *If  $\{\varepsilon_i\}_{i=0}^n$  satisfies the condition (i) and (ii') concerning the noise in Section 2, denoting the generalized autocorrelation functions (acfs) of noise as*

$$\begin{aligned} \rho_2(l) &= \text{Corr}(\varepsilon_i, \varepsilon_{i+l}) = \frac{\mathbb{E}[\varepsilon_i \varepsilon_{i+l}]}{\nu_2}, \\ \rho_3(l) &= \text{Corr}(\varepsilon_i, \varepsilon_{i+l}^2) = \frac{\mathbb{E}[\varepsilon_i \varepsilon_{i+l}^2]}{\sqrt{\nu_2(\nu_4 - \nu_2^2)}}, \\ \rho_4(l) &= \text{Corr}(\varepsilon_i^2, \varepsilon_{i+l}^2) = \frac{\mathbb{E}[\varepsilon_i^2 \varepsilon_{i+l}^2] - \nu_2^2}{\nu_4 - \nu_2^2}, \end{aligned} \quad (3.14)$$

for  $l \in \mathbb{Z}$ , assuming  $2q < H_n$ , we have

$$\Delta_n^3 H_n^4 k_n^2 \text{Var} \left( \widehat{[X, \sigma^2]}_T^{(H_n)} \middle| \mathcal{F} \right) \xrightarrow{p} \Phi T, \quad \text{as } n \rightarrow \infty, \quad (3.15)$$

where

$$\Phi = 8\nu_2 (\nu_4 - \nu_2^2) \sum_{l=-q}^q \left( \rho_2(l) \rho_4(l) + \rho_3(l) \rho_3(-l) \right) + 24\nu_2^3 \sum_{l=-q}^q \rho_2^3(l). \quad (3.16)$$

Specifically, if  $\{\varepsilon_i\}_{i=0}^n$  is independent, we have

$$\Phi = 8\nu_2 \nu_4 + 16\nu_2^3 + 8\nu_3^2. \quad (3.17)$$

Although the variance due to noise can be significantly reduced to  $O(n^3 H_n^{-4} k_n^{-2})$  by subsampling and averaging, the variance due to discretization does not improve significantly. As Theorem 1 will demonstrate, the variance due to discretization is  $O(k_n^{-1} + n^{-1} H_n k_n)$ , the same as the subsample estimator. Suppose  $H_n \asymp n^a$  and  $k_n \asymp (n/H)^b$ . Then, the minimum order of total variance is  $O(n^{-1/7})$  when  $a = 5/7$  and  $b = 1/2$ , resulting in an optimal convergence rate of  $n^{-1/14}$ . Although the variance of SALE estimator converges, the convergence rate is not satisfactory.

The SALE estimator can also be viewed as being composed of overlapping sparse increments. That is,

$$\widehat{[X, \sigma^2]}_T^{(H_n)} = \frac{1}{H_n} \sum_{i=(k_n+1)H_n}^{n-(k_n+2)H_n} (\Delta_{H_n} Y_i) \left( \hat{\sigma}_{H_n, i+}^2 - \hat{\sigma}_{H_n, i-}^2 \right), \quad (3.18)$$

where the spot volatility estimations are

$$\hat{\sigma}_{H_n, i+}^2 = \frac{1}{k_n H_n \Delta_n} \sum_{j=i+2H_n}^{i+(k_n+1)H_n} (\Delta_{H_n} Y_j)^2, \quad \hat{\sigma}_{H_n, i-}^2 = \frac{1}{k_n H_n \Delta_n} \sum_{j=i-(k_n+1)H_n}^{i-2H_n} (\Delta_{H_n} Y_j)^2. \quad (3.19)$$



### 3.5 MSLE: multi-scale estimator

Finally, we consider combining SALE estimators at different scales to achieve improved performance. The *Multi-Scale Leverage Effect* (MSLE) estimator is defined as a weighted average of SALE estimators at different scales. In general, consider a set of scales  $1 \leq H_1 < \dots < H_{M_n} \leq n^a$  for some  $a \in (0, 1)$  and  $M_n > 0$ . The noise-free version of the MSLE estimator is defined as

$$[X, \sigma^2]_T^{(\text{MS})} = \sum_{p=1}^{M_n} w_p [X, \sigma^2]_T^{(H_p)}, \quad (3.20)$$

and the noisy version is defined as

$$\widehat{[X, \sigma^2]_T}^{(\text{MS})} = \sum_{p=1}^{M_n} w_p \widehat{[X, \sigma^2]_T}^{(H_p)}, \quad (3.21)$$

where the weight vector  $\mathbf{w} = (w_1, \dots, w_{M_n})$  satisfies  $\mathbf{w}^T \mathbf{1}_{M_n} = 1$  and  $\|\mathbf{w}\|_\infty$  bounded.

It is clear that the MSLE is unbiased due to noise, and its variance due to noise is determined by the covariance due to noise between SALE estimators at different scales. However, the behavior of covariance due to noise can be very different depending on the assumption on noise. If the noise is independent, the covariance due to noise between SALE estimators at different scale is simply zero. The only exception occurs when one scale is exactly twice the other, in which case the covariance is non-zero but small (for normal distributed noise, the correlation coefficient equals to 0.1). For dependent noise, the covariance due to noise can be non-zero, especially for scales that are close to each other, but it is tiny between most of the scales. The following proposition describes the variance of MSLE due to noise when the noise is independent, and its proof is given in Appendix A.3. For dependent noise, we do not derive a closed-form expression for the variance due to noise, because the covariances due to noise is influenced by too many factors, but it can be calculated using the algorithm described in Appendix A.3, which has been validated through simulation.

**Proposition 3.** Suppose  $\{\varepsilon_i\}_{i=0}^n$  satisfies conditions (i) and (ii) concerning the noise in Section 2. Moreover, suppose  $k_p = \lfloor \beta \lfloor n/H_p \rfloor^b \rfloor$  holds for all  $p \in \{1, \dots, M_n\}$ , with some constant  $\beta > 0$  and  $b \in (0, 1)$ , and define the matrix  $\mathbf{F} \in \mathbb{R}^{M_n \times M_n}$  as

$$F_{p,q} = (8\nu_2\nu_4 + 16\nu_2^3 + 8\nu_3^2)1_{\{p=q\}} + 2\nu_2(\nu_4 - \nu_2^2)(1_{\{H_p/H_q=2\}} + 1_{\{H_q/H_p=2\}}). \quad (3.22)$$

Then, for any  $p, q \in \{1, \dots, M_n\}$ , we have

$$\Delta_n^3 H_p^2 H_q^2 k_p k_q \text{Cov} \left( \widehat{[X, \sigma^2]_T}^{(H_p)}, \widehat{[X, \sigma^2]_T}^{(H_q)} \middle| \mathcal{F} \right) \xrightarrow{p} F_{p,q} T. \quad (3.23)$$

Therefore, the variance due to noise of MSLE is given by

$$\frac{\text{Var} \left( \widehat{[X, \sigma^2]_T}^{(\text{MS})} \middle| \mathcal{F} \right)}{\Delta_n^{-3} \sum_{p=1}^{M_n} \sum_{q=1}^{M_n} \frac{w_p}{H_p^2 k_p} \cdot F_{p,q} \cdot \frac{w_q}{H_q^2 k_q}} \xrightarrow{p} T. \quad (3.24)$$

*Remark 1.* Although under the iid noise setting, SALE estimators at different scales can be correlated due to noise when the ratio of scales is 2 or 1/2, such correlation is weak. For example, it is easy to see that  $\mathbf{F}$  is a strictly diagonally dominant matrix satisfying  $\sum_{q \neq p} |F_{p,q}| < \frac{1}{2} |F_{p,p}|$ . As a result, the variance due to noise in MSLE estimator is dominated by the diagonal elements of  $\mathbf{F}$ , so its order is equivalent to that of the “independent case” where  $\mathbf{F}$  is diagonal. Figure 1

compares our all-observation estimator with the continuous leverage effect estimator in Aït-Sahalia et al. (2017), and also illustrate a shifted version of all-observation estimator. This shifted all-observation estimator can be used to construct SALE estimators that are completely uncorrelated with each other due to noise and have smaller asymptotic variances due to noise. A similar proposition can be established, with the corresponding version of Equation (3.22) being  $F_{p,q}^{(\text{shifted})} = (8\nu_2\nu_4 + 8\nu_2^3 + 8\nu_3^2)1_{\{p=q\}}$ .

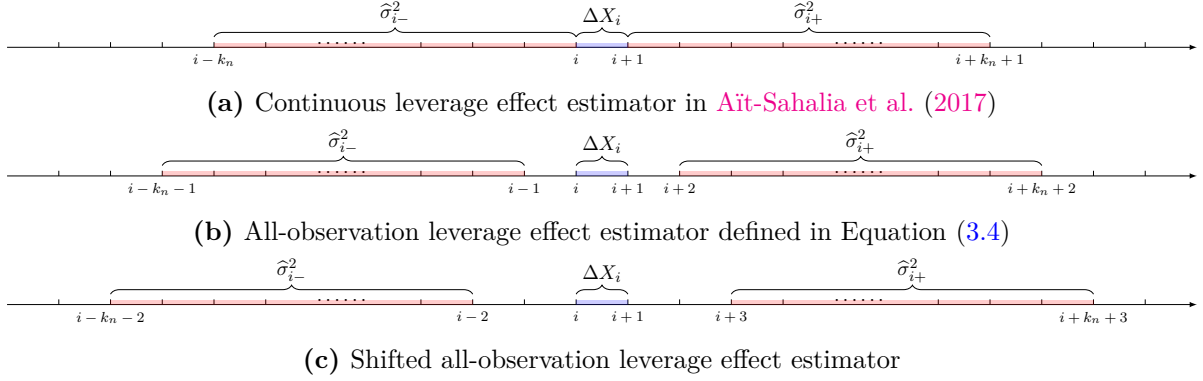


**Figure 1:** Increments in base leverage effect estimators with different positions of spot volatility estimation windows, used as proxies for  $\int_{t_i}^{t_{i+1}} d\langle X, \sigma^2 \rangle_t$ . The noise-free versions of these base estimators share the same asymptotic property, but their noisy versions differ. Based on (a), we construct (b) as an estimator that is unbiased due to noise and has a smaller variance due to noise. We also claim that (c) can be used to ensure that the errors due to noise of SALE estimators with different scales are completely uncorrelated under iid noise setting, and can also be used to reduce the variance due to noise.

The MSLE estimator provide an effective way to reduce the variance due to noise. For example, with  $H_p = p$  for  $p = 1, \dots, M_n$  and  $M_n = \lfloor n^a \rfloor$ , and taking  $w_p \propto p^{4-2b}$ , the order of variance due to noise becomes  $O(M_n^{-2}(n/M_n)^{3-2b}) = O(n^{3-5a-2b+2ab})$ , as shown in Proposition 3. In contrast, as Theorem 4 will demonstrate, the variance due to discretization is of order  $O((n/M_n)^{-b\wedge(1-b)}) = O(n^{-(1-a)(b\wedge(1-b))})$ . Therefore, as the maximum scale  $M_n$  increases, the variance due to noise decreases, while the variance due to discretization increases. Thus, by selecting  $a = 5/9$  and  $b = 1/2$ , the minimum order of total variance is  $O(n^{-2/9})$ , resulting in an optimal convergence rate of  $n^{-1/9}$ .

In fact, even in the noise-free setting, the MSLE estimator can be used to reduce the variance of the all-observation LE estimator. Theorem 4 provides the explicit form of the asymptotic variance of the MSLE estimator, so that the weights  $w_p$  can be chosen to minimize the variance of the estimator.

## 4 Main results

### 4.1 Central limit theorems for SALE

We start by establishing the following theorem for the noise-free version of SALE. Specifically, two scenarios for the scale  $H_n$  are considered for the noise-free setting: either it is a fixed positive integer  $H$ , or it goes to infinity as  $n \rightarrow \infty$ . The first scenario is appropriate for finite-sample analysis and includes the all-observation LE estimator as a special case, while the second is suitable for asymptotic analysis.

**Theorem 1.** *The normalized error process of the noise-free SALE estimator converges stably to a limiting process on an extension of the original probability space. Specifically, we have the following two results.*

1. Suppose  $H_n$  is a given positive integer  $H$ ,  $k_n = \lfloor \beta \lfloor n/H \rfloor^b \rfloor$  for some  $\beta > 0$  and  $b \in (0, 1)$ . Let  $u_n = \sqrt{k_n \wedge (k_n H \Delta_n)^{-1}}$ . We have

$$u_n \left( [X, \sigma^2]_T^{(H)} - \langle X, \sigma \rangle_T \right) \xrightarrow{\text{st}} \int_0^T \zeta_{1,t} dW_{1,t}, \quad (4.1)$$

as  $n \rightarrow \infty$ , where  $(W_{1,t})_{t \geq 0}$  is a standard Brownian motion process independent of  $\mathcal{F}$ , and the predictable process  $(\zeta_{1,t})_{t \geq 0}$  satisfies

$$\int_0^T \zeta_{1,t}^2 dt = \frac{u_n^2}{k_n} \left( \frac{8}{3} + \frac{4}{3H^2} \right) \int_0^T \sigma_s^6 dt + u_n^2 k_n H \Delta_n \frac{2}{3} \int_0^T \sigma_t^2 d\langle \sigma^2, \sigma^2 \rangle_t. \quad (4.2)$$

2. Suppose  $H_n = \lfloor \alpha n^a \rfloor$ ,  $k_n = \lfloor \beta \lfloor n/H_n \rfloor^b \rfloor$  for some  $\alpha, \beta > 0$  and  $a, b \in (0, 1)$ . We have

$$n^{\frac{1}{2}(1-a)(b \wedge (1-b))} \left( [X, \sigma^2]_T^{(H_n)} - \langle X, \sigma^2 \rangle_T \right) \xrightarrow{\text{st}} \int_0^T \zeta_{1,t} dW_{1,t}, \quad (4.3)$$

as  $n \rightarrow \infty$ , where  $(W_{1,t})_{t \geq 0}$  is a standard Brownian motion process independent of  $\mathcal{F}$ , and the predictable process  $(\zeta_{1,t})_{t \geq 0}$  satisfies

$$\int_0^T \zeta_{1,t}^2 dt = \frac{8\alpha^b}{3\beta} \int_0^T \sigma_t^6 dt \cdot 1_{(0,1/2]}(b) + \frac{2\alpha^{1-b}\beta T}{3} \int_0^T \sigma_t^2 d\langle \sigma^2, \sigma^2 \rangle_t \cdot 1_{[1/2,1)}(b). \quad (4.4)$$

*Remark 2.* Note that in Theorem 1, if we take  $H = 1$  in the first scenario, the result is consistent with that of the all-observation estimator, which has the same asymptotic variance as the continuous leverage effect estimator in Aït-Sahalia et al. (2017).

*Remark 3.* Similar to existing work on leverage effect estimation such as Wang and Mykland (2014), Aït-Sahalia and Jacod (2014), Aït-Sahalia et al. (2017), Kalnina and Xiu (2017) and Yang (2023), the convergence rate is determined by the spot volatility estimation, which again consists of two sources of errors. Aït-Sahalia et al. (2017) refers to them as *price variation error* and *volatility variation error*, respectively, corresponding to the first and second terms in Equation (4.2) or Equation (4.4). Intuitively, increasing  $k_n$  leads to a wider spot volatility estimation window and thus a larger sample for that estimation, which reduces the price variation error. However, this also increases the volatility variation error, because the estimated volatility becomes less “local”. The optimal choice of  $k_n$  is a trade-off between these two sources of error. This can be achieved by setting  $b = 1/2$  in the asymptotic scenario, and by estimating and minimizing the asymptotic variance in the finite-sample scenario.

Next, we establish the following theorem for the noisy version of SALE. The convergence rate of the SALE estimator is determined by the variances due to discretization and noise. However, when the scale is fixed at a constant  $H$ , from an asymptotic perspective, the variance due to noise ends up diverging as  $n \rightarrow \infty$ , according to Proposition 2. For this reason, we only consider the second scenario in Theorem 1 for the following result.

**Theorem 2.** Suppose  $H_n = \lfloor \alpha n^a \rfloor > 2q$  and  $k_n = \lfloor \beta \lfloor n/H_n \rfloor^b \rfloor$  for some  $\alpha, \beta > 0$  and  $a, b \in (0, 1)$ . When  $4a + 2b - 2ab > 3$ , the normalized error process of the noisy SALE estimator converges stably to a limiting process on an extension of the original probability space. That is,

$$n^{\frac{1}{2}r} \left( \widehat{[X, \sigma^2]_T}^{(H_n)} - \langle X, \sigma^2 \rangle_T \right) \xrightarrow{\text{st}} \int_0^T \zeta_{2,t} dW_{2,t}, \quad (4.5)$$

as  $n \rightarrow \infty$ , where  $r = [(1-a)(b \wedge (1-b))] \wedge [4a + 2b - 2ab - 3]$ ,  $(W_{2,t})_{t \geq 0}$  is a standard Brownian motion process independent of  $\mathcal{F}$ , and the predictable process  $(\zeta_{2,t})_{t \geq 0}$  satisfies

$$\begin{aligned} \int_0^T \zeta_{2,t}^2 dt &= \frac{8\alpha^b}{3\beta} \int_0^T \sigma_t^6 dt \cdot 1_{\{r\}}((1-a)b) + \frac{2\alpha^{1-b}\beta T}{3} \int_0^T \sigma_t^2 d\langle \sigma^2, \sigma^2 \rangle_t \cdot 1_{\{r\}}((1-a)(1-b)) \\ &\quad + \frac{1}{\alpha^{4-2b}\beta^2 T^3} \int_0^T \Phi dt \cdot 1_{\{r\}}(4a + 2b - 2ab - 3), \end{aligned} \quad (4.6)$$

with  $\Phi$  defined in Equation (3.16).

Note that Theorem 1 and Theorem 2 are infeasible CLTs because their asymptotic variances cannot be observed directly. To address this, we proceed to develop feasible versions of these theorems. This can be achieved by constructing consistent estimators for the quantities in asymptotic variances in both the noise-free and noisy settings, including  $\int_0^T \sigma_t^6 dt$ ,  $\int_0^T \sigma_t^2 d\langle \sigma^2, \sigma^2 \rangle_t$  as well as  $\Phi$ . For the noise-free case, the following estimators can be established:

$$G_n^{(1)} = \frac{1}{15\Delta_n^2} \sum_{i=0}^{n-1} (\Delta X_i)^6 \xrightarrow{p} \int_0^T \sigma_t^6 dt, \quad (4.7)$$

$$G_n^{(2)} = \frac{1}{k_n \Delta_n} \sum_{i \in I} (\Delta X_i)^2 \left( \frac{3}{2} (\hat{\sigma}_{(j+1)+}^2 - \hat{\sigma}_{j-}^2)^2 - \frac{1}{k_n^2 \Delta_n^2} \sum_{j \in I^{\pm(i)}} (\Delta X_j)^4 \right) \xrightarrow{p} \int_0^T \sigma_t^2 d\langle \sigma^2, \sigma^2 \rangle_t. \quad (4.8)$$

For the noisy case, we estimate process-related terms and noise-related terms in asymptotic variance separately. For the process-related terms, the pre-averaging technique is applied. A sequence of non-overlapping windows of length  $A_n$ , satisfying  $A_n \rightarrow \infty$  as well as  $A_n \Delta_n \rightarrow \infty$  as  $n \rightarrow \infty$  (for example,  $A_n = \lfloor n^{1/2} \rfloor$ ), is used to pre-average the noisy observations. The resulting pseudo-observations are denoted as  $\bar{X}_i = A_n^{-1} \sum_{j=iA_n}^{(i+1)A_n} Y_j$ , with  $i = 0, 1, \dots, \bar{n}$ , where  $\bar{n} = \lfloor (n+1)/A_n \rfloor - 1$ . We also define  $\bar{\Delta}_n = A_n \Delta_n$  and other notations, such as  $\bar{I}$ ,  $\bar{k}_n$  and  $\hat{\sigma}^2$ , similarly. The following estimators for process-related terms can be established:

$$\widehat{G}_n^{(1)} = \frac{9}{40\bar{\Delta}_n} \sum_{i=0}^{\bar{n}-1} (\bar{\Delta} X_i)^6 \xrightarrow{p} \int_0^T \sigma_t^6 dt, \quad (4.9)$$

$$\widehat{G}_n^{(2)} = \frac{27}{8\bar{k}_n \bar{\Delta}_n} \sum_{i \in \bar{I}} (\bar{\Delta} \bar{X}_i)^2 \left( \frac{3}{2} (\hat{\sigma}_{(j+1)+}^2 - \hat{\sigma}_{j-}^2)^2 - \frac{1}{\bar{k}_n^2 \bar{\Delta}_n^2} \sum_{j \in \bar{I}^{\pm(i)}} (\bar{\Delta} \bar{X}_j)^4 \right) \xrightarrow{p} \int_0^T \sigma_t^2 d\langle \sigma^2, \sigma^2 \rangle_t. \quad (4.10)$$

For the noise-related terms, we need to estimate  $\nu_2$ ,  $\nu_4$ ,  $\rho_2(l)$ ,  $\rho_3(l)$  and  $\rho_4(l)$  in Equation (3.16). Existing methods have been established to estimate these quantities, such as [Jacod et al. \(2017\)](#) and [Li and Linton \(2022\)](#). Here, the Realized moMents of Disjoint Increments (ReMeDI) approach proposed by [Li and Linton \(2022\)](#) is used to estimate the moments of MMS noise. Applying their method in our setting, it can be derived that, for any fixed integer  $l$ , suppose that  $k'_n > 0$  satisfies  $k'_n \rightarrow \infty$  and  $k'_n \Delta_n \rightarrow 0$  as  $n \rightarrow \infty$ , we have

$$\frac{1}{n} \sum_{i=k'_n}^{n-m-k'_n} (Y_{i+l} - Y_{i+l+k'_n})(Y_i - Y_{i-k'_n}) \xrightarrow{p} \mathbb{E}[\varepsilon_i \varepsilon_{i+l}], \quad (4.11)$$

$$\frac{1}{n} \sum_{i=2k'_n}^{n-m-k'_n} (Y_{i+l} - Y_{i+l+k'_n})(Y_{i+l} - Y_{i+l-k'_n})(Y_i - Y_{i-2k'_n}) \xrightarrow{p} \mathbb{E}[\varepsilon_i \varepsilon_{i+l}^2], \quad (4.12)$$

$$\frac{1}{n} \sum_{i=3k'_n}^{n-m-k'_n} (Y_{i+l} - Y_{i+l+k'_n})(Y_{i+l} - Y_{i+l-k'_n})(Y_i - Y_{i-2k'_n})(Y_i - Y_{i-3k'_n}) \xrightarrow{p} \mathbb{E}[\varepsilon_i^2 \varepsilon_{i+l}^2]. \quad (4.13)$$

The estimators for the noise moments  $\hat{\nu}_2$ ,  $\hat{\nu}_4$  and the generalized acfs  $\hat{\rho}_2(l)$ ,  $\hat{\rho}_3(l)$ ,  $\hat{\rho}_4(l)$  can be constructed accordingly. Thus, by plugging these estimators into Equation (3.16), the following estimator for  $\Phi$  can be derived:

$$\widehat{\Phi}_n = 8\hat{\nu}_2(\hat{\nu}_4 - \hat{\nu}_2^2) \sum_{l=-q}^q \hat{\rho}_2(l) \hat{\rho}_4(l) + 24\hat{\nu}_2^3 \sum_{l=-q}^q \hat{\rho}_2^3(l) + 8\hat{\nu}_2(\hat{\nu}_4 - \hat{\nu}_2^2) \sum_{l=-q}^q \hat{\rho}_3(l) \hat{\rho}_3(-l) \xrightarrow{p} \Phi. \quad (4.14)$$

Putting all these estimators together, we can establish the following feasible CLT for SALE.

**Theorem 3.**

1. Suppose  $H_n$  is a given positive integer  $H$ ,  $k_n = \lfloor \beta \lfloor n/H \rfloor^b \rfloor$  for some  $\beta > 0$  and  $b \in (0, 1)$ . Let  $u_n = \sqrt{k_n \wedge (k_n H \Delta_n)^{-1}}$ . The feasible CLT for noise-free SALE is

$$\frac{u_n}{\sqrt{V_{1,n}}} \left( [X, \sigma^2]_T^{(H)} - \langle X, \sigma \rangle_T \right) \xrightarrow{\text{st}} \mathcal{N}(0, 1), \quad (4.15)$$

as  $n \rightarrow \infty$ , where the standard normal on the right hand side is independent of  $\mathcal{F}$ , and

$$V_{1,n} = \frac{u_n^2}{k_n} \left( \frac{8}{3} + \frac{4}{3H^2} \right) G_n^{(1)} + u_n^2 k_n H \Delta_n \frac{2}{3} G_n^{(2)}. \quad (4.16)$$

2. Suppose  $H_n = \lfloor \alpha n^a \rfloor$ ,  $k_n = \lfloor \beta \lfloor n/H_n \rfloor^b \rfloor$  for some  $\alpha, \beta > 0$  and  $a, b \in (0, 1)$ . The feasible CLT for noise-free SALE is

$$\frac{n^{\frac{1}{2}(1-a)(b \wedge (1-b))}}{\sqrt{V_{1,n}}} \left( [X, \sigma^2]_T^{(H_n)} - \langle X, \sigma^2 \rangle_T \right) \xrightarrow{\text{st}} \mathcal{N}(0, 1), \quad (4.17)$$

as  $n \rightarrow \infty$ , where the standard normal on the right hand side is independent of  $\mathcal{F}$ , and

$$V_{1,n} = \frac{8\alpha^b}{3\beta} G_n^{(1)} \cdot 1_{(0,1/2]}(b) + \frac{2\alpha^{1-b}\beta T}{3} G_n^{(2)} \cdot 1_{[1/2,1)}(b). \quad (4.18)$$

When  $H_n > 2q$  and  $4a + 2(1-a)b > 3$ , the feasible CLT for noisy SALE is

$$\frac{n^{\frac{1}{2}r}}{\sqrt{V_{2,n}}} \left( \widehat{[X, \sigma^2]_T}^{(H_n)} - [X, \sigma^2]_T^{(H_n)} \right) \xrightarrow{\text{st}} \mathcal{N}(0, 1), \quad (4.19)$$

as  $n \rightarrow \infty$ , where  $r = [(1-a)(b \wedge (1-b))] \wedge [4a + 2(1-a)b - 3]$ , the standard normal on the right hand side is independent of  $\mathcal{F}$  and  $(B_t^{(H_n)})_{t \geq 0}$ , and

$$\begin{aligned} V_{2,n} = & \frac{8\alpha^b}{3\beta} \widehat{G}_n^{(1)} \cdot 1_{\{r\}}((1-a)b) + \frac{2\alpha^{1-b}\beta T}{3} \widehat{G}_n^{(2)} \cdot 1_{\{r\}}((1-a)(1-b)) \\ & + \frac{1}{\alpha^{4-2b}\beta^2 T^3} \int_0^T \widehat{\Phi}_n dt \cdot 1_{\{r\}}(4a + 2b - 2ab - 3). \end{aligned} \quad (4.20)$$

## 4.2 Central limit theorems for MSLE

In this section, we consider MSLE, the weighted average of SALEs at different scales. For a general set of scales  $1 \leq H_1 < \dots < H_{M_n} \leq n^a$  for some  $a \in (0, 1)$ ,  $M_n > 0$ . For now, we do not expose any explicit asymptotic assumptions on  $M_n$  and  $\{H_p\}_{p=1}^{M_n}$ . The MSLE estimators, defined as

$$[X, \sigma^2]_T^{(\text{MS})} = \sum_{p=1}^{M_n} w_p [X, \sigma^2]_T^{(H_p)} \quad \text{and} \quad \widehat{[X, \sigma^2]_T}^{(\text{MS})} = \sum_{p=1}^{M_n} w_p \widehat{[X, \sigma^2]_T}^{(H_p)}, \quad (4.21)$$

are specified by a weight vector  $\mathbf{w} = (w_1, \dots, w_{M_n})$  satisfying  $\mathbf{w}^T \mathbf{1}_{M_n} = 1$  and  $\|\mathbf{w}\|_\infty$  bounded. The asymptotic variance of MSLE is determined by the asymptotic covariance between SALE estimators at different scales, as the following proposition establishes.

**Proposition 4.** Suppose  $k_p = \lfloor \beta \lfloor n/H_p \rfloor^b \rfloor$  holds for all  $p \in \{1, \dots, M_n\}$ , with some constant  $\beta > 0$  and  $b \in (0, 1)$ . For any  $1 \leq q \leq p \leq M_n$ , the asymptotic covariance between the noise-free version of SALE estimators of scales  $H_q$  and  $H_p$  is given by

$$\text{ACOV}_{p,q}^{(\text{disc})} = \frac{1}{k_p} \cdot 4v_{p,q}^{(1)} \frac{H_q}{H_p} \cdot \int_0^T \sigma_t^6 dt + k_p H_p \Delta_n \cdot \frac{2}{3} v_{p,q}^{(2)} \left( \frac{k_q H_q}{k_p H_p} \right)^2 \cdot \int_0^T \sigma_t^2 d\langle \sigma^2, \sigma^2 \rangle_t, \quad (4.22)$$

such that for  $u_n = \sqrt{k_p \wedge (k_p H_p \Delta_n)^{-1}}$ , we have

$$u_n \begin{pmatrix} [X, \sigma^2]_T^{(H_p)} - \langle X, \sigma^2 \rangle_T \\ [X, \sigma^2]_T^{(H_q)} - \langle X, \sigma^2 \rangle_T \end{pmatrix} \xrightarrow{d} \mathcal{N} \left( 0, u_n^2 \begin{bmatrix} \text{ACOV}_{p,p}^{(\text{disc})} & \text{ACOV}_{p,q}^{(\text{disc})} \\ \text{ACOV}_{p,q}^{(\text{disc})} & \text{ACOV}_{q,q}^{(\text{disc})} \end{bmatrix} \right), \quad (4.23)$$

as  $n \rightarrow \infty$ . Here,  $v_{p,q}^{(1)}, v_{p,q}^{(2)} \in [0, 1)$  are adjustment factors depending on  $p, q, n$ , and are defined in Definition 1 in Appendix B.5.

*Remark 4.* The non-negative adjustment factors  $v_{p,q}^{(1)}$  and  $v_{p,q}^{(2)}$  are determined by the grid structures of scales  $H_p$  and  $H_q$ , and correspond to the price variation error and volatility variation error in the spot volatility estimation (Remark 3), respectively. These factors can be interpreted as follows. When the  $(\Delta X)$  terms in increments of  $H_p$ -scaled and  $H_q$ -scaled SALEs overlap, as defined in Equation (3.18), their cross product contributes a term to the asymptotic covariance. This contribution depends on the overlapping region of their spot volatility estimation windows. Specifically, the price variation error is proportional to the sum of the squares of small segments within the overlapping region. These segments are defined by the grid points of  $H_p$  and  $H_q$ . In contrast, the volatility variation error is proportional to the cubed length of the entire overlapping region. The adjustment factors  $v_{p,q}^{(1)}$  and  $v_{p,q}^{(2)}$  can thus be thought of as the normalized averages of these respective quantities.

Although the precise values of adjustment factors  $v_{p,q}^{(1)}$  and  $v_{p,q}^{(2)}$  can be calculated based on their definitions provided in Definition 1 in Appendix B.5, the following proposition establishes the asymptotic behavior of the  $v_{p,q}^{(1)}$  and  $v_{p,q}^{(2)}$ .

**Proposition 5.** *Under the condition of Proposition 4, the asymptotic behavior of  $v_{p,q}^{(1)}$  and  $v_{p,q}^{(2)}$  is as follows. Specifically, we assume that there are two sequences of scales  $H_p$  and  $H_q$  indexed by  $n$ , such that  $H_p \geq H_q$  for all  $n$ , and  $H_p, H_q \rightarrow \infty$ ,  $H_q/H_p \rightarrow c$  for some constant  $c \in (0, 1]$  as  $n \rightarrow \infty$ . We have*

$$v_{p,q}^{(1)} \rightarrow 1 - \frac{c}{3} \quad \text{and} \quad v_{p,q}^{(2)} \rightarrow 1, \quad \text{as } n \rightarrow \infty. \quad (4.24)$$

*Remark 5.* The asymptotic behavior of the adjustment factors  $v_{p,q}^{(1)}$  and  $v_{p,q}^{(2)}$  in Proposition 5 aligns with the intuition that the asymptotic covariance between SALE estimators at different scales is determined by the overlapping regions of their spot volatility estimation windows. The conditions in Proposition 5 guarantee that the spot volatility estimation windows of two scales are of the same order, and their overlapping regions also have the same order. In this case, the adjustment factors turn out to have non-vanishing limits with simple forms.

**Theorem 4.** *Suppose  $1 \leq H_1 < \dots < H_{M_n} \leq n^a$  for some  $a \in (0, 1)$ ,  $k_p = \lfloor \beta \lfloor n/H_p \rfloor^b \rfloor$  holds for all  $p \in \{1, \dots, M_n\}$  with some  $\beta > 0$  and  $b \in (0, 1)$ , and the weight vector  $\mathbf{w} = (w_1, \dots, w_{M_n})$  satisfies that  $\mathbf{w}^T \mathbf{1}_{M_n} = 1$  and  $\|\mathbf{w}\|_\infty$  is bounded. The normalized error process of the noise-free MSLE estimator converges stably to a limiting process on an extension of the original probability space. Specifically, the following two results hold.*

1. *Without any explicit assumptions on  $M_n$  and  $\{H_p\}_{p=1}^{M_n}$ , we have*

$$\frac{[X, \sigma^2]_T^{(\text{MS})} - \langle X, \sigma^2 \rangle_T}{\sqrt{\sum_{p=1}^{M_n} \sum_{q=1}^{M_n} w_p w_q \text{ACOV}_{p,q}^{(\text{disc})}}} \xrightarrow{\text{st}} \mathcal{N}(0, 1), \quad (4.25)$$

*as  $n \rightarrow \infty$ , where  $\text{ACOV}_{p,q}^{(\text{disc})}$  is defined in Equation (4.22), and the standard normal on the right hand side is independent of  $\mathcal{F}$ .*

2. *Suppose  $H_p = m_n + p$  for all  $p \in \{1, \dots, M_n\}$ . Denote  $H_n^* = H_{M_n} = m_n + M_n$ , and suppose that  $H_n^*/n^a \rightarrow \alpha$ ,  $m_n/H_n^* \rightarrow c$  for some constant  $\alpha > 0$ ,  $a \in (0, 1)$ ,  $c \in (0, 1)$  as*

$n \rightarrow \infty$ . Moreover, suppose there exists a continuous bounded function  $\phi : [c, \infty) \rightarrow \mathbb{R}$ , such that  $\int_c^1 \phi(x) dx = 1$ , and  $w_p = \frac{1-c}{M_n} \phi(c + \frac{p}{H_n^*})$ . We have

$$n^{\frac{1}{2}(1-a)(b \wedge (1-b))} \left( [X, \sigma^2]_T^{(\text{MS})} - \langle X, \sigma^2 \rangle_T \right) \xrightarrow{\text{st}} \int_0^T \zeta_{4,t} dW_{4,t}, \quad (4.26)$$

as  $n \rightarrow \infty$ , where  $(W_{4,t})_{t \geq 0}$  is a standard Brownian motion independent of  $\mathcal{F}$ , and the predictable process  $(\zeta_{4,t})_{t \geq 0}$  satisfies

$$\begin{aligned} \int_0^T \zeta_{4,t}^2 dt &= \frac{8\alpha^b}{\beta} \int_c^1 \int_c^x \phi(x) \phi(y) x^b \left( \frac{y}{x} - \frac{y^2}{3x^2} \right) dy dx \cdot \int_0^T \sigma_t^6 dt \cdot 1_{(0,1/2]}(b) \\ &\quad + \frac{4\alpha^{1-b}\beta T}{3} \int_c^1 \int_c^x \phi(x) \phi(y) \frac{y^{2(1-b)}}{x^{1-b}} dy dx \cdot \int_0^T \sigma_t^2 d\langle \sigma^2, \sigma^2 \rangle_t \cdot 1_{[1/2,1)}(b). \end{aligned} \quad (4.27)$$

The feasible version of this theorem can be established with  $G_n^{(1)}$  and  $G_n^{(2)}$  defined in Equation (4.7) and Equation (4.8).

*Remark 6.* Note that in Theorem 4, the first scenario is a general result without any explicit assumptions on  $M_n$  and  $\{H_p\}_{p=1}^{M_n}$ , while the second scenario is under a specific choice of consecutive scales in  $(m_n, m_n + M_n]$ , with  $m_n \approx c\alpha n^a \gg 1$  as  $n \rightarrow \infty$ . The latter is mainly based on theoretical considerations. This assumption avoids the case in Proposition 5 where the asymptotic covariance between widely separated scales may vanish. In such cases, Equation (4.27) may be inaccurate, particularly for weight functions  $\phi(x)$  that concentrate too much density near 0 and 1. However, if the observations are not contaminated by noise, one should start from the scale  $H_1 = 1$  and put more weight on the smaller scales to construct a better estimator, as the convergence rates of these scales are much faster than the larger scales.

**Theorem 5.** Under the second scenario of Theorem 4, if the noise is independent, and  $5a + 2b - 2ab > 3$ , the normalized error process of the noisy MSLE estimator converges stably to a limiting process on an extension of the original probability space. Specifically,

$$n^{\frac{1}{2}r} \left( \widehat{[X, \sigma^2]_T}^{(\text{MS})} - [X, \sigma^2]_T^{(\text{MS})} \right) \xrightarrow{\text{st}} \int_0^T \zeta_{5,t} dW_{5,t}, \quad (4.28)$$

as  $n \rightarrow \infty$ , where  $r = [(1-a)(b \wedge (1-b))] \wedge [5a + 2b - 2ab - 3]$ ,  $(W_{5,t})_{t \geq 0}$  is a standard Brownian motion independent of  $\mathcal{F}$  and  $(\zeta_{5,t})_{t \geq 0}$  satisfies

$$\begin{aligned} \int_0^T \zeta_{5,t}^2 dt &= \frac{8\alpha^b}{\beta} \int_c^1 \int_c^x \phi(x) \phi(y) x^b \left( \frac{y}{x} - \frac{y^2}{3x^2} \right) dy dx \cdot \int_0^T \sigma_t^6 dt \cdot 1_{\{r\}}((1-a)b) \\ &\quad + \frac{4\alpha^{1-b}\beta T}{3} \int_c^1 \int_c^x \phi(x) \phi(y) \frac{y^{2(1-b)}}{x^{1-b}} dy dx \cdot \int_0^T \sigma_t^2 d\langle \sigma^2, \sigma^2 \rangle_t \cdot 1_{\{r\}}((1-a)(1-b)) \\ &\quad + \frac{1}{\alpha^{5-2b}\beta^2 T^3} \int_c^1 \phi^2(x) x^{-(4-2b)} dx \cdot \int_0^T F_1 dt \cdot 1_{\{r\}}(5a + 2b - 2ab - 3) \\ &\quad + \frac{1_{(0,1/2]}(c)}{2^{2-b}\alpha^{5-2b}\beta^2 T^3} \int_c^{1/2} \phi(x) \phi(2x) x^{-(4-2b)} dx \cdot \int_0^T F_2 dt \cdot 1_{\{r\}}(5a + 2b - 2ab - 3), \end{aligned} \quad (4.29)$$

where  $F_1 = 8\nu_2\nu_4 + 16\nu_2^3 + 8\nu_3^2$  and  $F_2 = 2\nu_2(\nu_4 - \nu_2^2)$ . The feasible version of this theorem can be established with  $\widehat{G}_n^{(1)}$  and  $\widehat{G}_n^{(2)}$  defined in Equation (4.7) and Equation (4.8), as well as  $\widehat{F}_1$  and  $\widehat{F}_2$  constructed similarly as Equation (4.14).

*Remark 7.* Although only the second scenario of Theorem 4 is considered in Theorem 5, the CLT for the first scenario can be established similarly. The asymptotic covariance due to noise,



denoted by  $\text{ACOV}_{p,q}^{(\text{noise})} = \text{Cov}(\widehat{[X, \sigma^2]_T^{(H_p)}}, \widehat{[X, \sigma^2]_T^{(H_q)}} | \mathcal{F})$ , allows us to establish that

$$\frac{\widehat{[X, \sigma^2]_T^{(\text{MS})}} - [X, \sigma^2]_T^{(\text{MS})}}{\sqrt{\sum_{p=1}^{M_n} \sum_{q=1}^{M_n} w_p w_q (\text{ACOV}_{p,q}^{(\text{disc})} + \text{ACOV}_{p,q}^{(\text{noise})})}} \xrightarrow{\text{st}} \mathcal{N}(0, 1), \quad (4.30)$$

where the standard normal on the right hand side is independent of  $\mathcal{F}$ . The reason we do not include the first scenario in Theorem 5 is that the closed-form expression for  $\text{ACOV}_{p,q}^{(\text{noise})}$  is not provided in this paper when the noise is dependent. As an alternative solution, the variance due to noise can be calculated with the algorithm described in Appendix A.3, as is mentioned in Section 3.5.

## 5 Variance reduction

In this section, we consider the important problem of variance reduction for the MSLE estimator. This includes the variance reduction in both noise-free setting and noisy setting. For a given set of scales  $1 \leq H_1 < \dots < H_{M_n} \ll n$ , one can always calculate the optimal weights  $\mathbf{w}^*$  that minimize the asymptotic variance in Equation (4.25) or Equation (4.30). Let  $\Sigma \in \mathbb{R}^{M_n \times M_n}$  denote the total asymptotic covariance matrix between scales, where  $\Sigma_{p,q} = \text{ACOV}_{p,q}^{(\text{disc})} + \text{ACOV}_{p,q}^{(\text{noise})}$ . The optimal weights can be calculated by solving the following optimization problem:

$$\begin{aligned} & \underset{\mathbf{w} \in \mathbb{R}^{M_n}}{\text{minimize}} && V(\mathbf{w}) = \mathbf{w}^T \Sigma \mathbf{w}, \\ & \text{subject to} && \mathbf{w}^T \mathbf{1}_{M_n} = 1. \end{aligned} \quad (5.1)$$

The solution is given by

$$\mathbf{w}^* = \frac{1}{\mathbf{1}_{M_n}^T \Sigma^{-1} \mathbf{1}_{M_n}} \Sigma^{-1} \mathbf{1}_{M_n}, \quad \text{with} \quad V(\mathbf{w}^*) = \frac{1}{\mathbf{1}_{M_n}^T \Sigma^{-1} \mathbf{1}_{M_n}} = \left( \sum_{p=1}^{M_n} \sum_{q=1}^{M_n} (\Sigma^{-1})_{p,q} \right)^{-1}. \quad (5.2)$$

Since the asymptotic covariance matrix  $\Sigma$  cannot be observed directly, its estimate,  $\widehat{\Sigma}$ , through consistent estimators of quantities, such as  $\int_0^T \sigma_t^6 dt$ ,  $\int_0^T \sigma_t^2 d\langle \sigma^2, \sigma^2 \rangle_t$  and  $\Phi$ , can be used. However, from an asymptotic point of view, the inversion operation of  $\Sigma$  can be numerically expensive, especially when the number of scales  $M_n$  is large, because matrix inversion has a time complexity of  $O(M_n^3)$ . Moreover, the accurate solution  $\mathbf{w}^*$  can be numerically unstable, exhibiting, for example, zigzagging weights and sensitivity to estimation errors  $\widehat{\Sigma}$ . These issues motivate the development of computationally efficient and numerically stable variance reduction methods.

Therefore, we develop the approximation methods for variance reduction under different settings when  $M_n$  is large. We consider a specific set of consecutive scales  $H_p = m_n + p$  for all  $p \in \{1, \dots, M_n\}$ , where  $H_n^* = m_n + M_n$ . We also assume  $b = 1/2$ , so that a medium-sized spot volatility estimation window is adopted in the asymptotic sense. In the noise-free case, the special structure of  $\Sigma$  allows us to derive a closed-form expression for the optimal weights. In the noisy case, we utilized the Fredholm integral equation of the second kind to approximate the optimal weights.

### 5.1 Approximation under noise-free setting

Under the noise-free setting, the covariance matrix between scales is simply given by  $\Sigma_{p,q} = \text{ACOV}_{p,q}^{(\text{disc})}$ . In order to minimize the variance of MSLE, the best choice of scales might be a set of scales that starts from  $H_1 = 1$ , because the all-observation estimator (which is SALE with  $H = 1$ ) has the minimal asymptotic variance. To ensure mathematical tractability, we begin

with the first scenario of Proposition 5, so that  $v_{p,q}^{(1)} \rightarrow 1 - \frac{H_q}{3H_p}$  and  $v_{p,q}^{(2)} \rightarrow 1$  as  $n \rightarrow \infty$ . In this case, denoting  $x_p = H_p/H_n^*$ , the asymptotic version of covariance matrix can be written as

$$\Sigma_{p,q} = (s_1 + s_2)(n/H_n^*)^{-1/2}(x_p \vee x_q)^{1/2} \left[ \frac{x_p \wedge x_q}{x_p \vee x_q} - \frac{s_1}{3(s_1 + s_2)} \left( \frac{x_p \wedge x_q}{x_p \vee x_q} \right)^2 \right], \quad (5.3)$$

where the positive constants  $s_1$  and  $s_2$  are defined as

$$s_1 = \frac{4}{\beta} \int_0^T \sigma_t^6 dt, \quad s_2 = \frac{2\beta T}{3} \int_0^T \sigma_t^2 d\langle \sigma^2, \sigma^2 \rangle_t. \quad (5.4)$$

Although  $s_1$  and  $s_2$  are process-related stochastic quantities, they are treated as constants in this section for a given sample. The inverse of the matrix  $\Sigma$  is approximately a tridiagonal matrix (as can be seen by examining the cofactors), meaning that its elements are approximately zero except for the main diagonal and the two adjacent diagonals. Moreover, we have the following lemma.

**Lemma 1.** *Let  $n > 0$  be an integer, and let  $m \in \mathbb{R}$ . The matrix  $\mathbf{B} \in \mathbb{R}^{n \times n}$  is defined as*

$$\mathbf{B}_{p,q} = f((m+p) \vee (m+q)) \frac{g((m+p) \wedge (m+q))}{g((m+p) \vee (m+q))}, \quad \text{for all } p, q \in \{1, \dots, n\}, \quad (5.5)$$

where  $f, g$  are well-defined functions such that all expressions in this lemma are valid. Define

$$h(p, q) = f(m+p) - \frac{g^2(m+p)}{g^2(m+q)} f(m+q). \quad (5.6)$$

The inverse  $\mathbf{A} = \mathbf{B}^{-1}$  is tridiagonal. Its superdiagonal and subdiagonal elements are given by

$$\mathbf{A}_{p,p+1} = \mathbf{A}_{p+1,p} = -\frac{g(m+p)}{g(m+p+1)} \frac{1}{h(p, p+1)}, \quad p = 1, \dots, n-1, \quad (5.7)$$

and its main diagonal elements are given by

$$\mathbf{A}_{1,1} = \frac{1}{h(1, 2)}, \quad (5.8)$$

$$\mathbf{A}_{p,p} = \frac{h(p-1, p+1)}{h(p-1, p)h(p, p+1)}, \quad p = 2, \dots, n-1, \quad (5.9)$$

$$\mathbf{A}_{n,n} = \frac{f(m+n-1)}{f(m+n)} \frac{1}{h(n-1, n)}. \quad (5.10)$$

Intuitively, since  $s_1/(3(s_1 + s_2)) \in (0, 1/3)$  and  $(x_p \wedge x_q)/(x_p \vee x_q) \geq (x_p \wedge x_q)^2/(x_p \vee x_q)^2$ , it is reasonable to expect that the first term in the brackets of Equation (5.3) contributes more significantly than the second term. Therefore, neglecting the second term in the bracket (for now), we obtain

$$\tilde{\Sigma}_{p,q} = (s_1 + s_2)(n/H_n^*)^{-1/2}(x_p \vee x_q)^{1/2} \frac{x_p \wedge x_q}{x_p \vee x_q} = (s_1 + s_2)n^{-1/2} \mathbf{B}_{p,q}, \quad (5.11)$$

with  $\mathbf{B}_{p,q}$  given in Lemma 1 with  $f(x) = \sqrt{x}$  and  $g(x) = x$ . With  $\omega = \mathbf{B}^{-1} \mathbf{1}_{M_n}$ , the optimal weights obtained by solving Equation (5.1) with  $\tilde{\Sigma}$  are  $\mathbf{w} = (\mathbf{1}_{M_n}^T \omega)^{-1} \omega$ . From Lemma 1, it follows that for  $p = 2, \dots, M_n - 1$ ,

$$\omega_1 = \left( \frac{m_n + 2}{m_n + 1} \right)^{1/2} \frac{1}{(m_n + 2)^{3/2} - (m_n + 1)^{3/2}} \quad (5.12)$$

$$\omega_p = (m_n + p)^{1/2} \left( \frac{(m_n + p)^{1/2} - (m_n + p - 1)^{1/2}}{(m_n + p)^{3/2} - (m_n + p - 1)^{3/2}} - \frac{(m_n + p + 1)^{1/2} - (m_n + p)^{1/2}}{(m_n + p + 1)^{3/2} - (m_n + p)^{3/2}} \right), \quad (5.13)$$

$$\omega_{M_n} = (m_n + M_n)^{1/2} \frac{(m_n + M_n)^{1/2} - (m_n + M_n - 1)^{1/2}}{(m_n + M_n)^{3/2} - (m_n + M_n - 1)^{3/2}}. \quad (5.14)$$

As  $m_n \rightarrow \infty$ , these values can be further approximated as

$$\omega_1 \rightarrow \frac{2}{3(m_n + 1)^{1/2}}, \quad \omega_p \rightarrow \frac{1}{3(m_n + p)^{3/2}}, \quad \omega_{M_n} \rightarrow \frac{1}{3(m_n + M_n)^{1/2}}. \quad (5.15)$$

This provides an approximation of the optimal weights in noise-free settings.

**Table 2:** Variance increase ratio with the approximate weights.  $m_n = 10, M_n = 10$ .

$s_1/s_2$	0	...	$10^{-2}$	$10^{-1}$	1	$10^1$	$10^2$	...	$\infty$
<b>VIR (%)</b>	0.000	...	0.000	0.004	0.173	1.088	1.544	...	1.614

Table 2 shows the variance increase ratio with the approximate weights  $\tilde{\mathbf{w}}$ , as defined in Equation (5.15), under different settings of  $s_1/s_2$ , compared with using optimal solution in Equation (5.2). In this case,  $m_n = 10$  and  $M_n = 10$ , and the variance increase ratio (VIR) is defined as

$$\text{Variance Increase Ratio (VIR)} = \frac{V(\tilde{\mathbf{w}}) - V(\mathbf{w}^*)}{V(\mathbf{w}^*)} \times 100\%. \quad (5.16)$$

The asymptotic covariance matrix  $\Sigma$  in Equation (5.3) is used to evaluate the variance. Numerical experiment indicate that the VIR increases as  $m_n$  decreases and  $M_n$  increases. However, even with  $m_n = 0$ ,  $M_n = 10000$  and  $s_1/s_2 \rightarrow \infty$ , the VIR remains relatively small, at 3.787%. These results suggest that the approximation is adequate for practical applications.

Furthermore, the approximate weights exhibit numerical stability. As  $m_n, M_n \rightarrow \infty$ , the distribution of approximate weights satisfies the following asymptotic properties:

$$\tilde{w}_1 \approx \frac{2(m_n + M_n)^{1/2}}{4(m_n + M_n)^{1/2} - (m_n + 1)^{1/2}} > \frac{1}{2}, \quad (5.17)$$

$$\tilde{w}_2 + \dots + \tilde{w}_{M_n-1} \approx \frac{2(m_n + M_n)^{1/2} - 2(m_n + 1)^{1/2}}{4(m_n + M_n)^{1/2} - (m_n + 1)^{1/2}} < \frac{1}{2}, \quad (5.18)$$

$$\tilde{w}_{M_n} \approx \frac{(m_n + 1)^{1/2}}{4(m_n + M_n)^{1/2} - (m_n + 1)^{1/2}} < \frac{1}{3}. \quad (5.19)$$

In conjunction with Equation (5.15), it can be observed that the approximate weights tend to assign the majority of the weight to  $\tilde{w}_1$  and a significant portion to  $\tilde{w}_{M_n}$ , while the combined weight of all other scales remains less than one-half. This property is shared by the approximate weights and the optimal weights obtained using Equation (5.3). Figure 2 illustrates the approximate and optimal weights under the setting of Table 2, confirming this observation. Another property of the approximate weights is that they are all positive, implying that the sum of their absolute values equals one, which contributes to the relative stability of the values of  $\tilde{\mathbf{w}}$ . However, the optimal weights with  $s_1/s_2 \rightarrow \infty$  may exhibit negative values, although this does not present any issues in this particular case.

Having derived the approximate weights, we now return to the original scenario outlined at the beginning of this section. Specifically, we set  $m_n = 0$  to utilize a set of scales starting from  $H_1 = 1$ , and we employ the non-asymptotic form of  $\Sigma$  instead of the asymptotic approximation provided by Proposition 5. In this context, we assess the performance of the approximate weights in terms of variance reduction. A randomly selected sample path from the simulation study (see Section 6) is used to determine the values of  $s_1$  and  $s_2$ . Specifically, the path consists of one-second observations ( $n = 23400$ ) in one trading day ( $T = 1/252$ ), and we set  $\beta = 1$  for the spot volatility estimation window. In this case, partly due to a small  $T$ , the value of  $s_1/s_2$  is 132.47, which is pretty large.

Three weights are compared: the optimal weights  $\mathbf{w}^\dagger$  obtained by solving Equation (5.2) using the non-asymptotic covariance matrix (calculated using the definition of adjustment factors

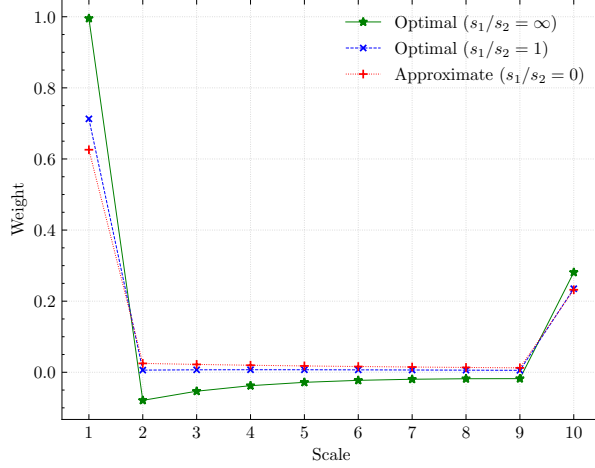


**Figure 2:** Approximate and optimal weights.  $m_n = 10, M_n = 10$ .

in Definition 1 in Appendix B.5), the optimal weights  $\mathbf{w}^*$  obtained by solving Equation (5.2) using the asymptotic covariance matrix in Equation (5.3), and the approximate weights  $\tilde{\mathbf{w}}$ . The variance of MSLEs using these weights are evaluated using the non-asymptotic (true) covariance matrix, and the variance increase ratios of  $\mathbf{w}^*$  and  $\tilde{\mathbf{w}}$  relative to  $\mathbf{w}^\dagger$  are calculated.

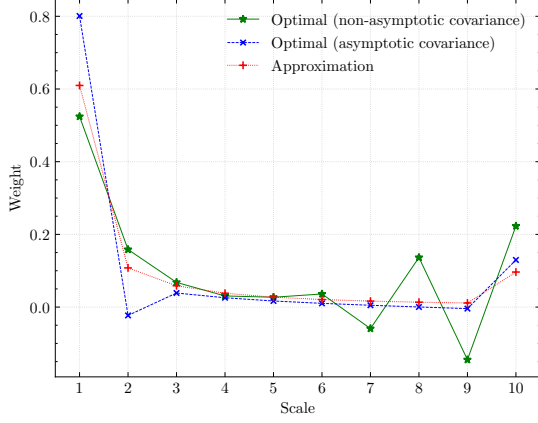
**Table 3:** Variance of MSLE with optimal and approximate weights.

$M_n$	$V(\mathbf{w}^\dagger)$	$V(\mathbf{w}^*)$	$V(\tilde{\mathbf{w}})$	VIR of $\mathbf{w}^*$ (%)	VIR of $\tilde{\mathbf{w}}$ (%)
10	$8.335 \times 10^{-10}$	$8.975 \times 10^{-10}$	$8.436 \times 10^{-10}$	7.672	1.214
20	$8.072 \times 10^{-10}$	$8.728 \times 10^{-10}$	$8.172 \times 10^{-10}$	8.123	1.235
30	$7.809 \times 10^{-10}$	$8.633 \times 10^{-10}$	$8.071 \times 10^{-10}$	10.549	3.347
40	$7.574 \times 10^{-10}$	$8.546 \times 10^{-10}$	$7.981 \times 10^{-10}$	12.832	5.361
50	$7.450 \times 10^{-10}$	$8.508 \times 10^{-10}$	$7.938 \times 10^{-10}$	14.194	6.541
100	$7.105 \times 10^{-10}$	$8.374 \times 10^{-10}$	$7.788 \times 10^{-10}$	17.851	9.612
150	$6.965 \times 10^{-10}$	$8.327 \times 10^{-10}$	$7.728 \times 10^{-10}$	19.555	10.959
200	$6.865 \times 10^{-10}$	$8.302 \times 10^{-10}$	$7.696 \times 10^{-10}$	20.929	12.094
250	$6.808 \times 10^{-10}$	$8.277 \times 10^{-10}$	$7.666 \times 10^{-10}$	21.570	12.600
300	$6.754 \times 10^{-10}$	$8.263 \times 10^{-10}$	$7.649 \times 10^{-10}$	22.338	13.238

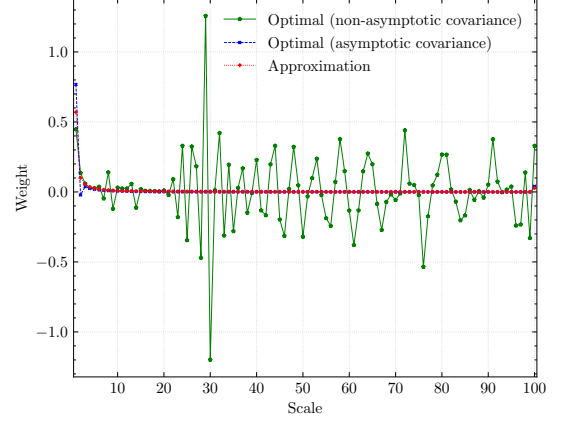
As Table 3 shows, all sets of weights considered result in smaller variances compared to the all-observation LE estimator, which has a variance of  $1.102 \times 10^{-9}$ . Surprisingly, the approximate weights perform better than the optimal weights obtained using the asymptotic covariance matrix in terms of variance reduction. This may be attributed to the inaccuracy of the asymptotic covariance approximation when the scales are small. Moreover, although the VIR of  $\tilde{\mathbf{w}}$  increases with  $M_n$ , the results are still satisfactory for two reasons. First,  $V(\tilde{\mathbf{w}})$  continues to decrease as  $M_n$  increases, and its VIR remains below 15% even for a large value of  $M_n = 300 \approx n^{0.567}$ . Second, as illustrated in Figure 3,  $\mathbf{w}^\dagger$  can be highly unstable and exhibit zigzagging patterns. Therefore, improving  $V(\mathbf{w}^\dagger)$  to a limited extent may not be worthwhile, given the potential for numerical instability, particularly when an estimate of  $\Sigma$  is used.

## 5.2 Approximation under noisy setting

Under the noisy setting, the covariance matrix is given by  $\Sigma_{p,q} = \text{ACOV}_{p,q}^{(\text{disc})} + \text{ACOV}_{p,q}^{(\text{noise})}$ . For simplicity, we only consider the iid noise, and disregard the correlation between SALE estimators when  $H_p/H_q = 2$  or  $1/2$ , due to its limited contribution. This simplification can be



(a)  $m_n = 0, M_n = 10$



(b)  $m_n = 0, M_n = 100$

**Figure 3:** Approximate and optimal weights for different values of  $M_n$ .

made more rigorous by considering  $c \in [1/2, 1]$ . As a result, we have

$$\text{ACOV}_{p,q}^{(\text{noise})} = \frac{\Phi T}{\Delta_n^3 H_p^4 k_p^2} \delta_{p,q} \approx \frac{\Phi}{\beta^2 T^2} n^2 (H_n^*)^{-3} x_p^{-3} \delta_{p,q}. \quad (5.20)$$

According to Theorem 5, with  $a = 5/9$  and  $b = 1/2$ , and assuming the weights are generated by the function  $\phi(x)$  defined therein, the asymptotic variance of the MSLE can be written as a functional of  $\phi(x)$ . Specifically, we have  $\mathbf{w}^T \Sigma \mathbf{w} = \alpha^{1/2} n^{-2/9} S_0[\phi]$ , where

$$\begin{aligned} S_0[\phi] &= (s_1 + s_2) \int_c^1 \int_c^1 \phi(x) \phi(y) (x \vee y)^{1/2} \left( \frac{x \wedge y}{x \vee y} - \frac{s_1}{3(s_1 + s_2)} \left( \frac{x \wedge y}{x \vee y} \right)^2 \right) dx dy \\ &\quad + s_3 \int_c^1 \phi^2(x) x^{-3} dx - 2k \left( \int_c^1 \phi(x) dx - 1 \right). \end{aligned} \quad (5.21)$$

Here, the positive coefficients  $s_1$ ,  $s_2$  and  $s_3$  are defined as

$$s_1 = \frac{4}{\beta} \int_0^T \sigma_t^6 dt, \quad s_2 = \frac{2\beta T}{3} \int_0^T \sigma_t^2 d\langle \sigma^2, \sigma^2 \rangle_t, \quad s_3 = \frac{\Phi}{\alpha^{9/2} \beta^2 T^2}, \quad (5.22)$$

and  $k \in \mathbb{R}$  is a Lagrange multiplier that enforces the constraint that the weights sum to one. Defining  $\varphi(x) = x^{-3/2} \phi(x)$ ,  $\gamma = s_1/(3(s_1 + s_2)) > 0$  and  $\lambda = -(s_1 + s_2)/s_3 < 0$ , a scaled version of  $S_0[\phi]$  can be expressed as

$$S[\varphi] = s_3^{-1} S_0[\phi] = -\lambda \int_c^1 \int_c^1 \varphi(x) \varphi(y) K(x, y) dx dy + \int_0^1 \varphi(x) (\varphi(x) - 2kx^{3/2}) dx + \text{const.}, \quad (5.23)$$

where the kernel function is defined as

$$K(x, y) = x^{3/2} y^{3/2} (x \vee y)^{1/2} \left( \frac{x \wedge y}{x \vee y} - \gamma \left( \frac{x \wedge y}{x \vee y} \right)^2 \right). \quad (5.24)$$

A necessary condition for the extremum of the functional  $S[\varphi]$  is that  $\varphi(x)$  is a solution to the following Fredholm integral equation of the second kind (Lao and Zhao, 2021),

$$\varphi(x) = f(x) + \lambda \int_c^1 K(x, y) \varphi(y) dy, \quad (5.25)$$

where  $f(x) = kx^{3/2}$ , and  $\varphi(x)$  satisfies the constraint  $\int_c^1 \varphi(x) x^{3/2} dx = 1$ .

Although a closed-form solution to this integral equation is difficult to obtain, we can approximate the solution using discretization and the Hilbert-Schmidt theorem. For given parameters  $\gamma > 0$  and  $\lambda < 0$ , discretization allows us to approximate the integral equation as a linear system of equations. This enables us to solve the integral equation using a smaller value of  $M_n$  and then use the resulting solution to generate weights for a larger  $M_n$ . The Hilbert-Schmidt theorem, on the other hand, can be employed to reduce computational complexity. These approaches enable us to approximate the optimal weights under noisy settings with a large  $M_n$  in a computational efficient manner.

As an example, with  $m_n = 0$ , we use a discretization level of  $\tilde{M}_n = 100$  to solve Equation (5.25) with  $c = 0$ ,  $\gamma = 1/6$ , and  $\lambda = -100$ . The number of eigenvalues used in the Hilbert-Schmidt solution is set to  $k^* = 20$ , and the normalized weighting function  $\phi(x) = x^{3/2}\varphi(x)$  is shown in Figure 4a. The approximate Hilbert-Schmidt solution exhibits high accuracy when compared to a direct discrete solution with  $M_n = 2000$ . Figure 4b presents the approximate solutions for different  $\lambda$  values. It can be observed that as the noise level decreases (and therefore  $|\lambda|$  increases), the weight function derived from the solution of Equation (5.25) tends to assign more weight to the smaller scales, while still retaining some weight on the largest scales.

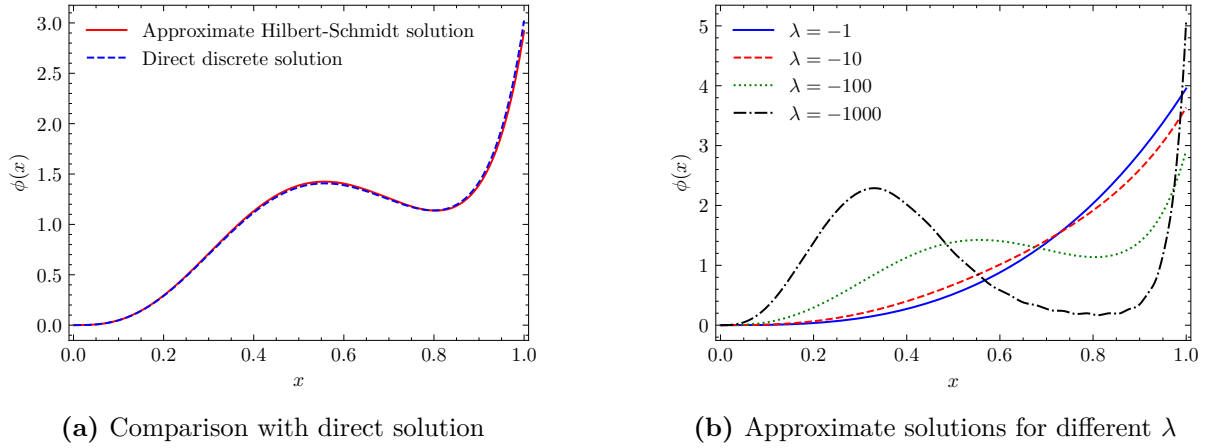


**Figure 4:** Approximate solutions of weight function  $\phi(x)$ .

Specifically, consider the case when the noise becomes excessively large, so that  $s_3 \rightarrow \infty$ . Equation (5.25) then simplifies to  $\varphi(x) = f(x)$ , and consequently, the optimal weight function is  $\phi(x) = 4x^3$ . Conversely, if the noise vanishes, such that  $s_3 \rightarrow 0$ , Equation (5.25) transforms into a Fredholm integral equation of the first kind, which is often regarded as an ill-posed problem. As a result, when  $s_3$  is sufficiently small, the approximate Hilbert-Schmidt method employed in this section is no longer effective.

### 5.3 Practical aspects

This section discusses practical considerations related to the weight optimization problem. First, we demonstrate the impact of the noise level on the optimal weights and their approximations. Second, we assess the accuracy of the results pertaining to the variance induced by noise. Third, we propose a simple weighting method based on improving the optimal SALE estimator using the approximation method presented in Section 5.1.

Figure 5 illustrates the impact of the noise level. For a given set of scales ranging from 21 to 200 (with  $n = 23400$ ,  $m_n = 20$ ,  $M_n = 180$  and  $M_n^* = 200$ ) and fixed values of  $s_1$  and  $s_2$ , as  $|\lambda|$  increases, the noise level  $s_3$  decreases, leading to significant changes in the asymptotic variances of the SALE estimators. The asymptotic forms of  $\Sigma_{p,q}^{(\text{disc})}$  and  $\Sigma_{p,q}^{(\text{noise})}$  given in Equation (5.3) and Equation (5.20) are used to determine the optimal weights for each scenario. When the noise level is high, as illustrated in the first four subfigures of Figure 5, the total variance is

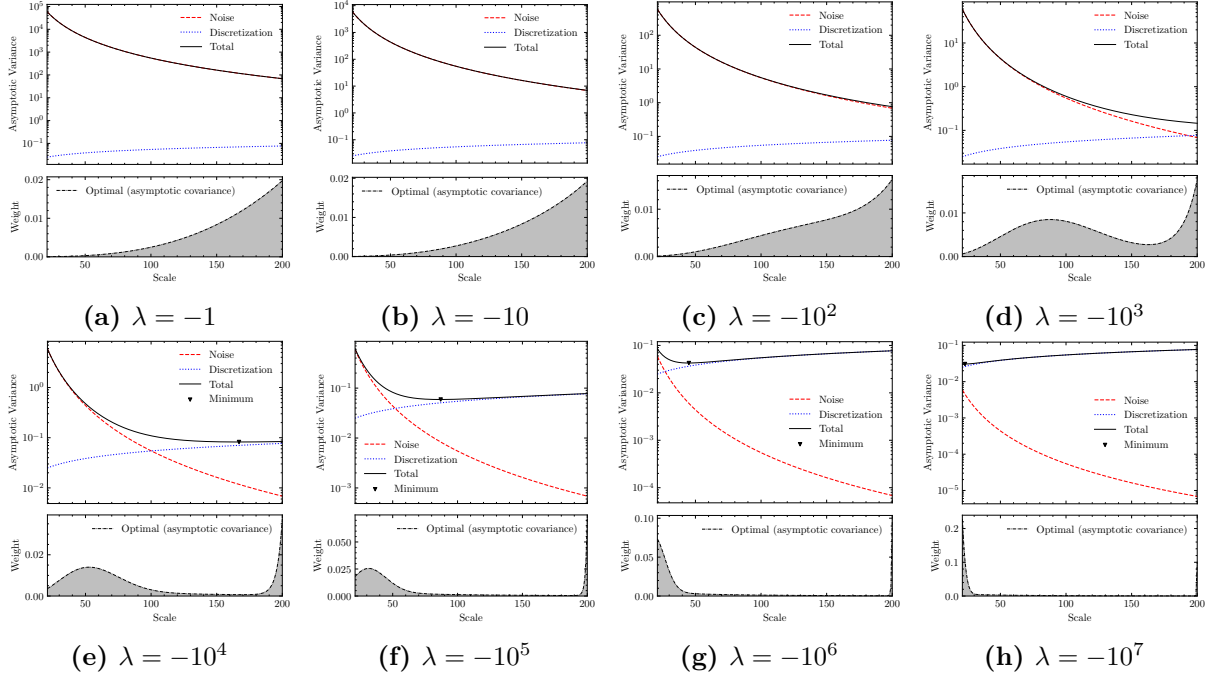


**Figure 5:** Sources of asymptotic variances of SALEs with different  $\lambda$  and corresponding optimal weights for MSLE. Note that the asymptotic variances are displayed on a logarithmic scale.  $n = 23400$ ,  $m_n = 20$ ,  $M_n = 180$ ,  $H_n^* = 200$ ,  $s_1 = 1/2$ ,  $s_2 = 1/2$ ,  $s_3 = (-\lambda)^{-1}$ .

dominated by noise, and the optimal weights can be approximated using the Hilbert-Schmidt method applied to the Fredholm integral equation of the second kind, as described in Section 5.2. Conversely, when the noise level is very low, as shown in the last subfigure of Figure 5, the total asymptotic variance is dominated by the discretization, and the optimal weights closely resemble the closed-form approximate weights derived in Section 5.1. However, in intermediate cases, both sources contribute significantly to the total variance, resulting in a minimum total variance at a specific scale within the given range. For these intermediate cases, approximating the optimal weights using the methods described in Section 5.1 or Section 5.2 is challenging. Therefore, we propose a simple weighting method. First, we find the optimal scale  $\tilde{H}_n$  that minimizes the total variance of SALE. This scale,  $\tilde{H}_n$ , is approximately  $6^{2/7} \approx 1.67$  times the minimum scale at which the noise contribution is less than that of the discretization. Second, we use the approximate weights for the noise-free setting, as described in Section 5.1, to generate weights for the remaining scales starting from  $\tilde{H}_n$ . This is justified because the noise contributes only about  $1/7$  of the total variance at  $\tilde{H}_n$  and even less at larger scales.

It may appear too conservative to discard all scales smaller than  $\tilde{H}_n$ . There are two primary reasons for this approach. First, the preceding arguments rely on the asymptotic forms of  $\Sigma_{p,q}^{(\text{disc})}$  and  $\Sigma_{p,q}^{(\text{noise})}$  because they are mathematically tractable and yield more stable optimal weights. Therefore, employing a conservative method can provide a buffer against approximation errors. This is particularly important for the variance induced by noise, because the derivation of Proposition 1 implicitly assumes that the noise level is not excessively small, an assumption that may be violated as  $|\lambda| \rightarrow \infty$ . Consequently, the more precise version of the variance due to noise provided in Appendix A should be used in practice. Figure 6 and Figure 7 provide a detailed explanation of this point. Second, discarding these scales allows us to utilize the approximate weights for the noise-free setting, which are more accurate and stable. The simulation study presented in Section 6 demonstrates that the loss of this approach is minimal.



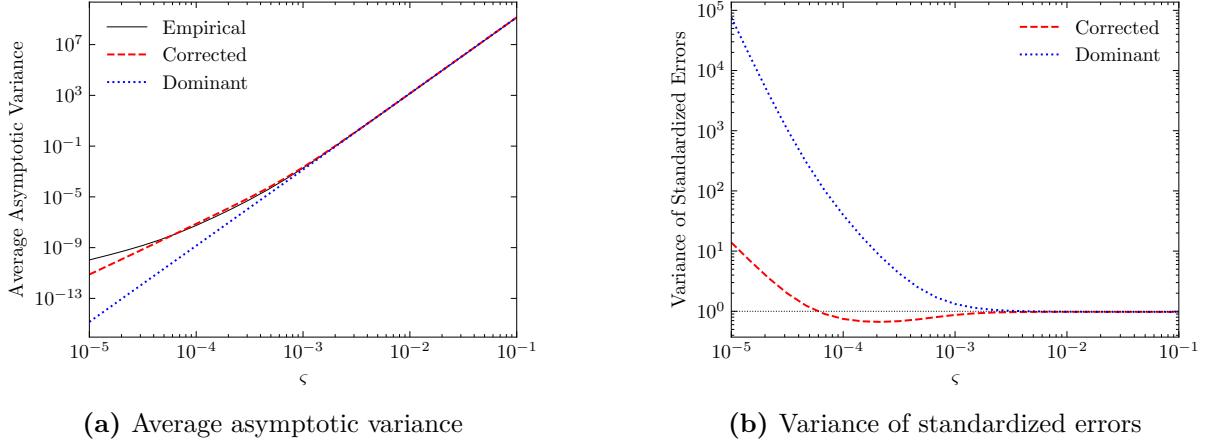


**Figure 6:** Asymptotic variance of all-observation estimators due to noise with different noise levels. A total of  $N = 5000$  paths are simulated with the same model and parameters as in Section 6, and iid normal noise of standard error  $\zeta$  is used to contaminate the data. For each path  $j$ , the error due to noise  $e_j$  is defined as the difference between the noisy and noise-free version of all-observation LE estimator, and the asymptotic variance due to noise is calculated with Equation (3.8) as  $V_j$  (the dominant) and Equation (A.98) as  $V'_j$  (the corrected). Denote  $\mathbb{E}_N[X] = N^{-1} \sum_{j=1}^N X_j$  as the average of random variable  $X$  over  $N$  paths. The figure shows (a) the average asymptotic variance due to noise:  $\mathbb{E}_N[e^2]$  for “Empirical”,  $\mathbb{E}_N[V']$  for “Corrected” and  $\mathbb{E}_N[V]$  for “Dominant”, and (b) the variance of standardized errors of the optimal weights:  $\mathbb{E}_N[e^2/V']$  for “Corrected” and  $\mathbb{E}_N[e^2/V]$  for “Dominant”. The figure demonstrates that the corrected version of the variance due to noise, presented in Appendix A, is more accurate than the dominant terms given in Proposition 1, particularly when  $\zeta < 10^{-3}$ .

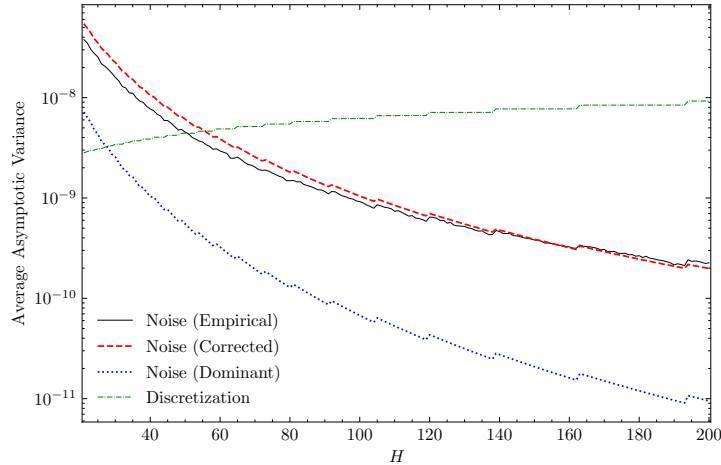


**Figure 7:** Asymptotic variance of SALE estimators due to noise. The same simulated paths are used as Figure 6, and the noise level is  $\zeta = 6 \times 10^{-4}$ . The figure demonstrates that the corrected variance due to noise should be used to determine the optimal scale  $\tilde{H}_n$  for the SALE estimator.

## 6 Simulation study

The asymptotic properties of the proposed SALE and MSLE estimators are validated for three circumstances: the noise-free situation, the iid noise situation, and the dependent noise situation. Both infeasible and feasible CLTs are considered. Furthermore, the finite sample performance of the MSLE estimator is compared with other methods: the all-observation estimator in the noise-free setting, and the pre-averaging estimator in the noisy setting.

### 6.1 Validation of the asymptotic properties

#### 6.1.1 Data generating processes

The Heston model (Heston, 1993) is used to generate the discrete values of the underlying continuous processes. The model is defined as

$$\begin{aligned} dX_t &= \left( \mu - \frac{\sigma_t^2}{2} \right) dt + \sigma_t dW_t, \\ d\sigma_t^2 &= \kappa(\theta - \sigma_t^2)dt + \gamma\sigma_t \left( \rho dW_t + \sqrt{1 - \rho^2} dB_t \right). \end{aligned} \quad (6.1)$$

Here,  $X_t$  represents the log-price process, and  $V_t = \sigma_t^2$  represents the volatility process. The model is driven by independent Brownian motions  $W_t$  and  $B_t$ . The leverage effect in this model is  $\langle X, V \rangle_T = \gamma\rho \int_0^T V_t dt$ . The parameters are set as follows:  $\mu = 0.02, \kappa = 5, \theta = 0.04, \gamma = 0.5, \rho = -0.7$ . The initial values are set as  $X_0 = 0, V_0 = 0.02$ . Furthermore, we set  $T = 1/252$  and  $n = 23400$ , and simulate 5000 paths for each case.

In the *noise-free* situation, the discrete values of log-price process  $\{X_i\}_{i=0}^n$  can be directly observed. In the noisy situations, the observations are contaminated by noise  $\{\varepsilon_i\}_{i=0}^n$  with zero mean and a variance of  $\varsigma^2$ .

For the *iid noise* situation, we consider the following distributions for  $\{\varepsilon_i\}_{i=0}^n$ .

1. Normal:  $\varepsilon_i \sim \mathcal{N}(0, \varsigma^2)$ ;
2. Uniform:  $\varepsilon_i \sim \text{Unif}(-\sqrt{3}\varsigma, \sqrt{3}\varsigma)$ ;
3. Skew normal: the pdf of  $\varepsilon_i$  is  $f(x) = 2\omega^{-1}\phi_{\mathcal{N}}(\omega^{-1}(x - \xi))\Phi_{\mathcal{N}}(\alpha\omega^{-1}(x - \xi))$ , where  $\phi_{\mathcal{N}}$  and  $\Phi_{\mathcal{N}}$  are pdf and cdf of the standard normal distribution, respectively. The parameters are  $\xi = -\omega\delta\sqrt{2/\pi}$ ,  $\omega = \varsigma(1 - 2\delta^2/\pi)^{-1/2}$ , where  $\delta = \alpha(1 + \alpha^2)^{-1/2}$ . The shape parameter  $\alpha$  is set as 1.

For the *dependent noise* situation, both MA(2) and AR(1) processes driven by Gaussian white noise are considered. Note that MA(2) process satisfies our assumption of the dependent noise with  $q = 2$ , whereas AR(1) process does not satisfy this assumption with any non-negative integer  $q$ . However, given the difficulty in determining the dependence level accurately for real-world noisy data, the AR(1) noise can be used to assess the robustness of the proposed estimators under a truncated dependence level  $q$ .

1. For the MA(2) process, we set

$$\varepsilon_i = e_i + \theta_1 e_{i-1} + \theta_2 e_{i-2}, \quad e_i \stackrel{\text{iid}}{\sim} \mathcal{N}(0, \varsigma^2(1 + \theta_1^2 + \theta_2^2)^{-1}). \quad (6.2)$$

The second and fourth moments of the process are

$$\nu_2 = \varsigma^2, \quad \nu_4 = 2\varsigma^4(1 + 2\theta_1^2 + 2\theta_2^2 + \theta_1^4 + \theta_2^4 + 2\theta_1^2\theta_2^2), \quad (6.3)$$

and the generalized acfs defined in Equation (3.14) are

$$\begin{aligned}
\rho_2(l) &= 1_{\{l=0\}} + \frac{\theta_1 + \theta_1\theta_2}{1 + \theta_1^2 + \theta_2^2} 1_{\{|l|=1\}} + \frac{\theta_2}{1 + \theta_1^2 + \theta_2^2} 1_{\{|l|=2\}}, \\
\rho_3(l) &= 0, \\
\rho_4(l) &= 1_{\{l=0\}} + \frac{\theta_1^2\theta_2^2 + \theta_1^2 + 2\theta_1^2\theta_2}{1 + 2\theta_1^2 + 2\theta_2^2 + \theta_1^4 + \theta_2^4 + 2\theta_1^2\theta_2^2} 1_{\{|l|=1\}} \\
&\quad + \frac{\theta_2^2}{1 + 2\theta_1^2 + 2\theta_2^2 + \theta_1^4 + \theta_2^4 + 2\theta_1^2\theta_2^2} 1_{\{|l|=2\}}.
\end{aligned} \tag{6.4}$$

The parameters  $(\theta_1, \theta_2)$  are set to  $(0.7, 0.5)$  and  $(-0.7, 0.5)$ .

2. For the AR(1) process, we set

$$\varepsilon_i = \phi\varepsilon_{i-1} + e_i, \quad e_i \stackrel{\text{iid}}{\sim} \mathcal{N}(0, \varsigma^2\sqrt{1-\phi^2}), \tag{6.5}$$

where  $\phi \in (-1, 1)$  denotes the autoregressive coefficient. This is a common setting for modeling the stationary component of dependent noise (see Jacod et al., 2017; Li and Linton, 2022). The moments of the process are

$$\nu_2 = \varsigma^2, \quad \nu_4 = 3\varsigma^4, \tag{6.6}$$

and the generalized acfs are

$$\rho_2(l) = \phi^{|l|}, \quad \rho_3(l) = 0, \quad \rho_4(l) = \phi^{2|l|}. \tag{6.7}$$

The parameter is set to  $\phi = 0.7$ .

### 6.1.2 Standardized estimation errors

**Table 4:** Scales and weights for SALE and MSLE.

Noise	SALE	MSLE	
	Scale	Scales	Weights
Noise-free	1, 15	1, 2, ..., 15	$w_H \propto H^{-3/2}$
IID	1, 15	1, 2, ..., 15	$w_H \propto H^3$
Dependent	15	11, 12, ..., 15	$w_H \propto H^3$

In this section, we validate the CLTs for the SALE and MSLE estimators. The estimators are applied to the simulated data, and both infeasible and feasible asymptotic variances are calculated to construct the standardized estimation errors for each path:

$$Z_j = \frac{\text{Estimate}_j - \text{True}_j}{\sqrt{\text{AsymptoticVariance}_j}}, \quad j = 1, \dots, n_{\text{path}}. \tag{6.8}$$

Thus,  $\{Z_j\}_{j=1}^{n_{\text{path}}}$  is supposed to be a random sample from the standard normal distribution, which can be used to validate the CLTs. Throughout this section, the standard deviation of the noise is set to  $\varsigma = 0.005$ . Moreover, for the length of spot volatility window, we set  $k_n = \lfloor \beta n^b \rfloor$  for SALE and  $k_p = \lfloor \beta \lfloor n/H_p \rfloor^b \rfloor$  for the scale  $H_p$  in MSLE, with  $\beta = 1/2$  and  $b = 1/2$ . The selection of scales and weights in SALE or MSLE estimators is summarized in Table 4. The standardized estimation errors calculated with both infeasible and feasible asymptotic variances are reported in Table 5 as well as Figure 9 and Figure 8. The simulation results indicate that the standardized errors are well-behaved and approximate the standard normal distribution, supporting the validity of the CLTs for both the SALE and MSLE estimators.

**Table 5:** Standardized estimation errors of the estimators calculated with both infeasible and feasible asymptotic variances under different noise settings. The mean, standard deviation and the 25th, 50th and 75th percentiles are reported for each estimator and each noise setting. The LE estimator in the table represents the all-observation estimator, *i.e.* SALE with  $H = 1$ .

Type	Noise Setting	Estimator	Mean	Std	$Q_1$	$Q_2$	$Q_3$	
Infeasible	Noise-free	LE	-0.016	1.013	-0.693	-0.013	0.683	
		SALE	0.012	0.990	-0.650	0.012	0.685	
		MSLE	-0.012	1.013	-0.694	0.005	0.678	
	IID	Normal	LE	-0.022	1.004	-0.693	-0.030	0.650
			SALE	-0.008	1.003	-0.693	-0.007	0.673
			MSLE	-0.005	1.047	-0.718	0.000	0.702
		Uniform	LE	0.008	1.009	-0.653	0.019	0.680
			SALE	0.002	0.998	-0.679	-0.009	0.673
			MSLE	0.004	1.023	-0.707	0.008	0.689
		Skew-normal	LE	0.010	1.004	-0.662	0.018	0.685
			SALE	0.008	1.010	-0.681	0.015	0.691
			MSLE	0.010	1.048	-0.699	0.001	0.716
	Dependent	MA(2) ( $\theta_1 = 0.7$ )	SALE	-0.013	1.012	-0.706	-0.024	0.676
			MSLE	-0.008	1.032	-0.727	-0.007	0.696
		MA(2) ( $\theta_1 = -0.7$ )	SALE	0.001	1.022	-0.682	0.008	0.680
			MSLE	-0.001	1.073	-0.717	0.004	0.727
		AR(1)	SALE	-0.011	1.006	-0.693	-0.015	0.666
			MSLE	-0.005	1.040	-0.705	-0.008	0.685
Feasible	Noise-free	LE	-0.014	1.013	-0.693	-0.013	0.684	
		SALE	0.013	0.996	-0.652	0.012	0.687	
		MSLE	-0.010	1.014	-0.696	0.005	0.676	
	IID	Normal	LE	-0.022	0.998	-0.691	-0.030	0.643
			SALE	-0.007	0.991	-0.684	-0.007	0.666
			MSLE	-0.005	1.019	-0.699	0.000	0.685
		Uniform	LE	0.008	1.002	-0.651	0.019	0.676
			SALE	0.002	0.983	-0.667	-0.009	0.663
			MSLE	0.004	0.989	-0.683	0.007	0.668
		Skew-normal	LE	0.010	0.999	-0.655	0.018	0.678
			SALE	0.008	0.999	-0.676	0.014	0.686
			MSLE	0.010	1.021	-0.680	0.001	0.696
	Dependent	MA(2) ( $\theta_1 = 0.7$ )	SALE	-0.012	1.004	-0.698	-0.024	0.671
			MSLE	-0.008	1.022	-0.721	-0.007	0.689
		MA(2) ( $\theta_1 = -0.7$ )	SALE	0.001	1.015	-0.677	0.008	0.678
			MSLE	-0.001	1.063	-0.709	0.004	0.723
		AR(1)	SALE	-0.010	0.996	-0.690	-0.015	0.657
			MSLE	-0.003	1.028	-0.695	-0.008	0.680
Asymptotic Value (Standard Normal)			0.000	1.000	-0.674	0.000	0.674	

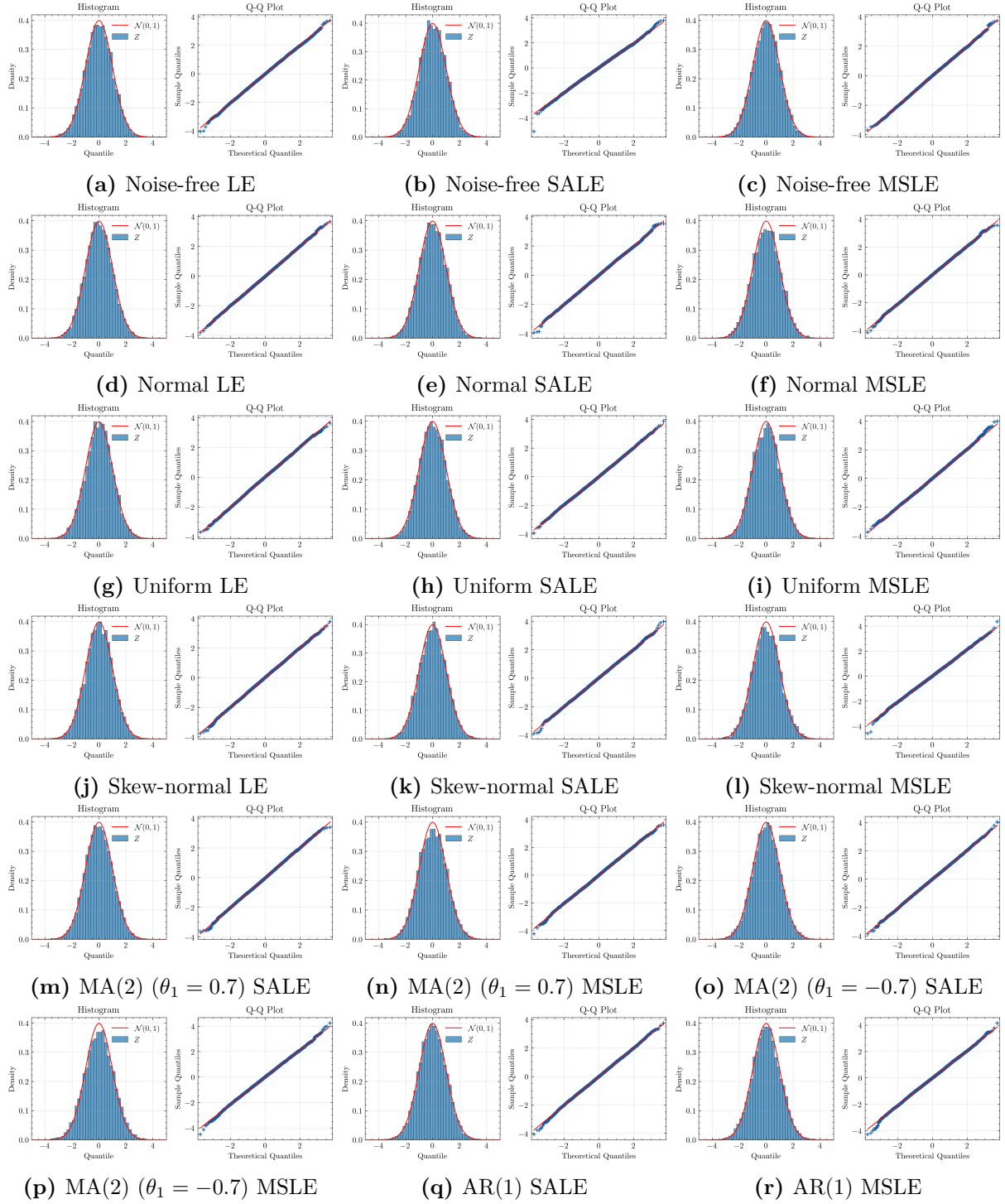


**Figure 8:** Histograms and Q-Q plots of standardized estimation errors calculated with infeasible asymptotic variances across noise settings and estimators. Blue bars and points represent empirical standardized errors; red curves and lines represent the standard normal distribution.

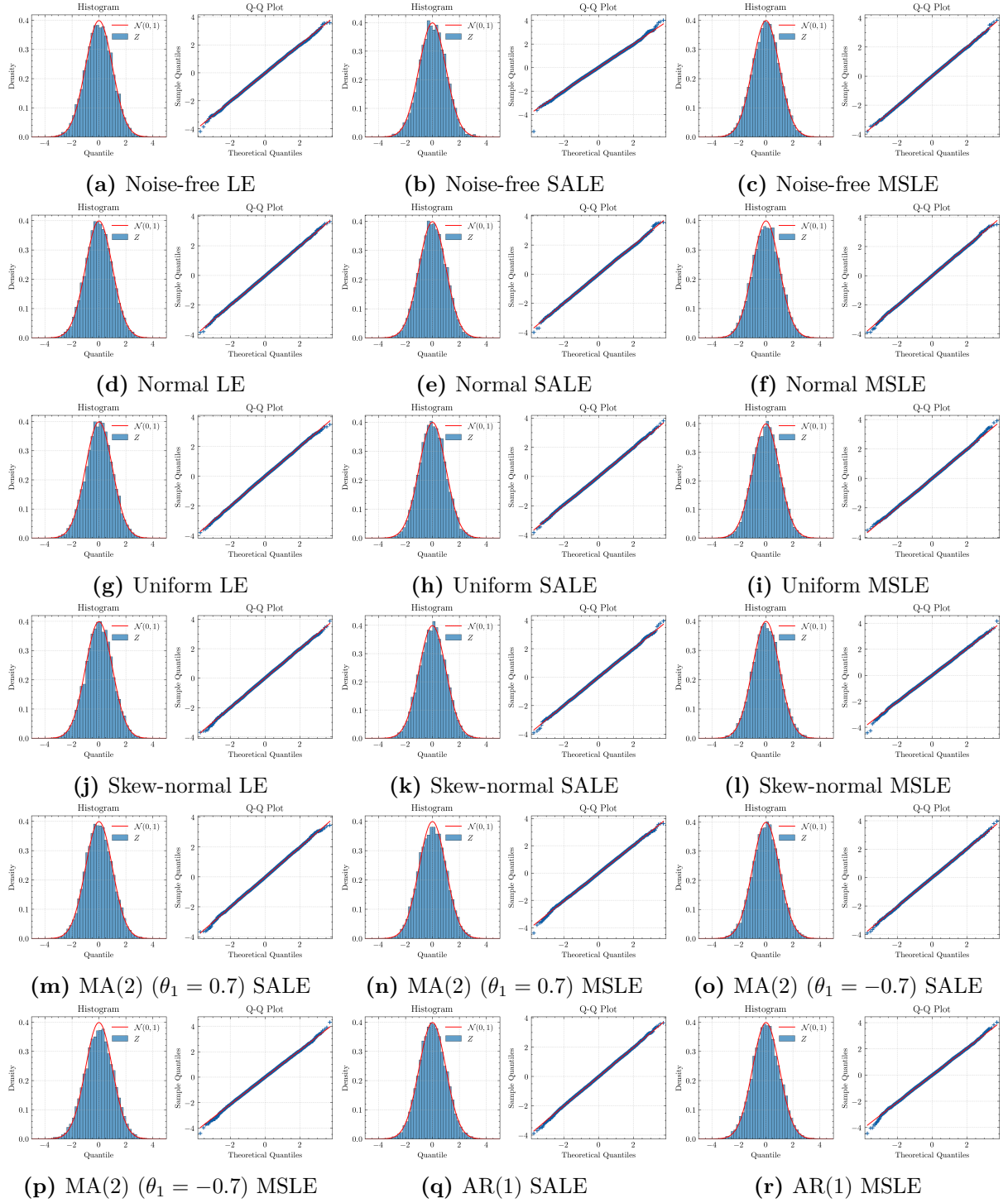


**Figure 9:** Histograms and Q-Q plots of standardized estimation errors calculated with feasible asymptotic variances across noise settings and estimators. Blue bars and points represent empirical standardized errors; red curves and lines represent the standard normal distribution.

## 6.2 Performance of the MSLE estimator

This section illustrates the performance of the MSLE estimator. The MSLE estimator offers two advantages compared with the existing methods. First, for noise-free data, the MSLE estimator outperforms the all-observation LE estimator in terms of asymptotic variance and finite sample RMSE. Second, for noisy data, particularly when the noise magnitude is small, the MSLE estimator exhibits superior performance compared to the pre-averaging LE estimator in terms of finite sample RMSE and robustness to dependent noise.

### 6.2.1 Noise-free setting

The performances of the MSLE estimator with optimal and approximate weights are compared to that of the all-observation LE estimator. Four settings of time horizon  $T$  are considered: one day ( $T = 1/252$ ), one week ( $T = 5/252$ ), two weeks ( $T = 10/252$ ) and one month ( $T = 22/252$ ). Each day consists of 23400 observations, corresponding to sampling every second for 6.5 hours of trading. A total of  $N = 5000$  paths are generated for each value of  $T$ , using the same parameters as in Section 6.1. The scales in MSLE are determined by  $m_n = 0$  and  $H_n^* = \lfloor \alpha n^a \rfloor$ , where  $\alpha = 0.5$  and  $a = 0.5$ ; that is,  $H_p = 1, 2, \dots, \lfloor 0.5n^{0.5} \rfloor$ , where  $n = 23400 \times 252T$ . The optimal weights of MSLE are calculated using the non-asymptotic form of the asymptotic covariance defined in Equation (4.22), while the approximate weights of MSLE are calculated using Equation (5.15).

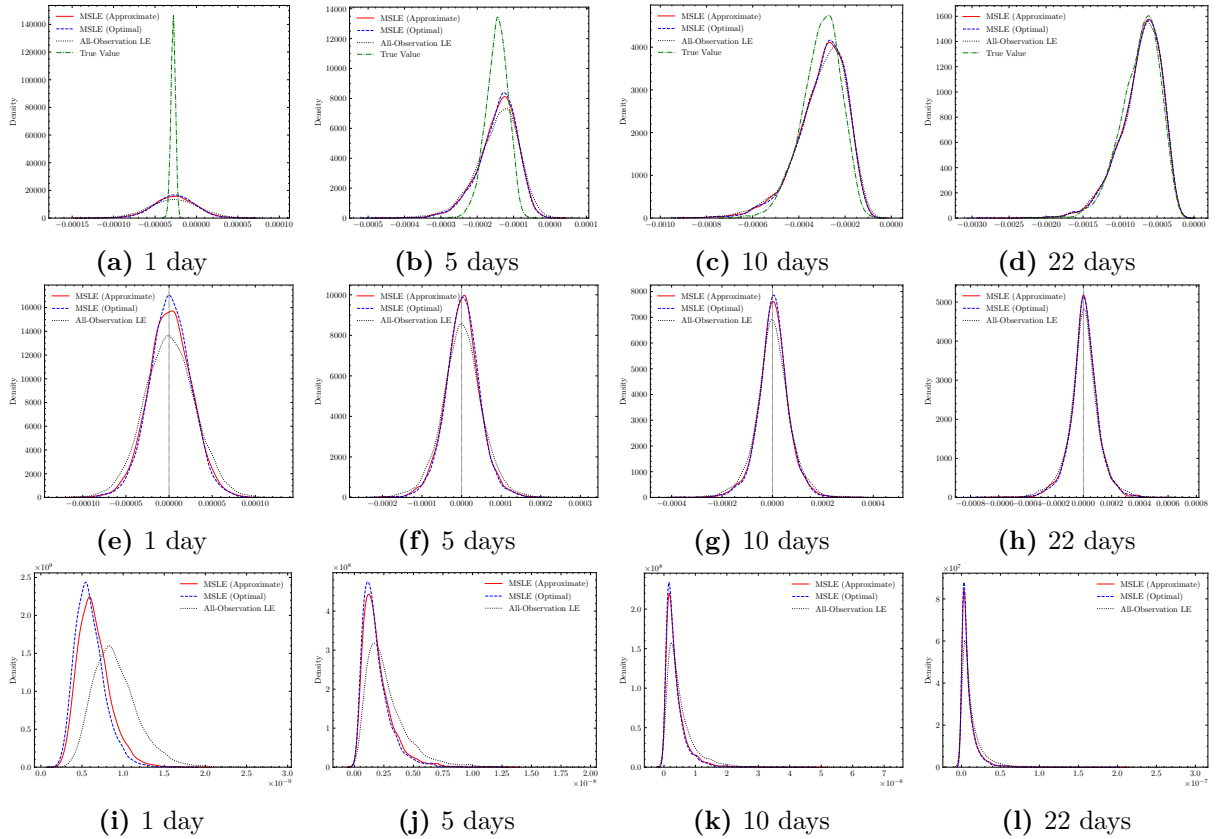


**Figure 10:** The performances of the MSLE and pre-averaging LE estimators for each setting of  $T$  in the noise-free setting. The first row shows the true and estimated values of leverage effect, the second row shows the estimation errors, and the third row shows the asymptotic variances.

Figure 10 compares the estimated values, estimation errors, and asymptotic variances of the MSLE and all-observation LE estimators for each setting of  $T$ . Table 6 reports the RMSE of the MSLE and all-observation LE estimators. The results indicate that the MSLE estimator



**Table 6:** RMSE of the MSLE and all-observation LE estimators in the noise-free setting. The “RMSE-Std Ratio” is the ratio of the RMSE to the standard deviation of the true value, which makes the results comparable across different  $T$ .

Days	True Value		RMSE			RMSE-Std Ratio		
	Mean	Std	Approximate	Optimal	LE	Approximate	Optimal	LE
1	$-2.810 \times 10^{-5}$	$2.811 \times 10^{-6}$	$2.520 \times 10^{-5}$	$2.420 \times 10^{-5}$	$2.961 \times 10^{-5}$	8.96	8.61	10.53
5	$-1.464 \times 10^{-4}$	$3.074 \times 10^{-5}$	$4.490 \times 10^{-5}$	$4.401 \times 10^{-5}$	$5.178 \times 10^{-5}$	1.46	1.43	1.68
10	$-3.049 \times 10^{-4}$	$8.597 \times 10^{-5}$	$6.298 \times 10^{-5}$	$6.204 \times 10^{-5}$	$7.111 \times 10^{-5}$	0.73	0.72	0.83
22	$-7.296 \times 10^{-4}$	$2.621 \times 10^{-4}$	$1.035 \times 10^{-4}$	$1.039 \times 10^{-4}$	$1.130 \times 10^{-4}$	0.40	0.40	0.43

outperforms the all-observation LE estimator in terms of both asymptotic variance and finite sample RMSE. Furthermore, the performance of MSLE with approximate weights is very close to that with optimal weights.

### 6.2.2 IID noise setting

The performances of the MSLE estimator with optimal and approximate weights are compared to that of the pre-averaging LE estimator. As in the noise-free setting, four settings of  $T$  are considered, corresponding to 1, 5, 10, and 22 trading days, with 23,400 observations each day. IID normal noise with three noise levels are considered:  $\varsigma = 10^{-4}, 10^{-3.5}, 10^{-3}$ , corresponding to small, medium and large noise levels (see Christensen et al., 2014; Li and Linton, 2022). The scales in MSLE are determined by  $m_n = 0$  and  $H_n^* = \lfloor \alpha n^a \rfloor$ , where  $\alpha = 1$  and  $a = 5/9$ ; that is,  $H_p = 1, 2, \dots, \lfloor n^{5/9} \rfloor$ . A total of  $N = 1000$  paths are generated for each combination of  $T$  and  $\varsigma$ .

**Table 7:** Settings of the MSLE estimator with approximate weights and pre-averaging LE with optimal pre-averaging window in the iid noise setting.

$\varsigma$	1 day		5 days		10 days		22 days	
	$\tilde{H}_n$	$A_n$	$\tilde{H}_n$	$A_n$	$\tilde{H}_n$	$A_n$	$\tilde{H}_n$	$A_n$
$10^{-4}$	7	8	7	7	6	7	5	6
$10^{-3.5}$	43	25	35	23	32	21	26	19
$10^{-3}$	190	79	171	73	152	67	128	59

Two versions of the MSLE and pre-averaging LE estimators are considered. The approximate MSLE uses the approximate weights described in Section 5.3, where  $\tilde{H}_n$  is derived by minimizing the asymptotic variance of SALE. The optimal MSLE uses the optimal weights that minimize the total asymptotic variance. The covariance due to discretization is calculated using Equation (4.22), and the covariance due to noise is calculated using the corrected formula in Equation (A.98) in Appendix A.2. The *ex-post* selected pre-averaging LE is the one with the smallest RMSE among those with pre-averaging windows of 5, 10, 30, 60, and 120, selected for each combination of parameters. The optimal pre-averaging LE use the optimal pre-averaging window  $A_n$ , which is determined by minimizing the asymptotic variance as provided by Aït-Sahalia et al. (2017). For simplicity, for each combination of  $T$  and  $\varsigma$ , the same  $\tilde{H}_n$  and  $A_n$  are used for each path. These values are calculated using the average asymptotic variance across all simulated paths. These settings are summarized in Table 7.

Figure 11 shows the estimated values and estimation errors of the MSLE and pre-averaging LE estimators for each setting of  $T$  with  $\varsigma = 10^{-4}$ . Table 8 reports the RMSE of the MSLE and pre-averaging LE estimators. The results indicate that the MSLE estimator with approximate weights outperforms the pre-averaging LE estimator in terms of finite sample RMSE, particularly for small and medium noise levels. Moreover, the performance of MSLE with approximate

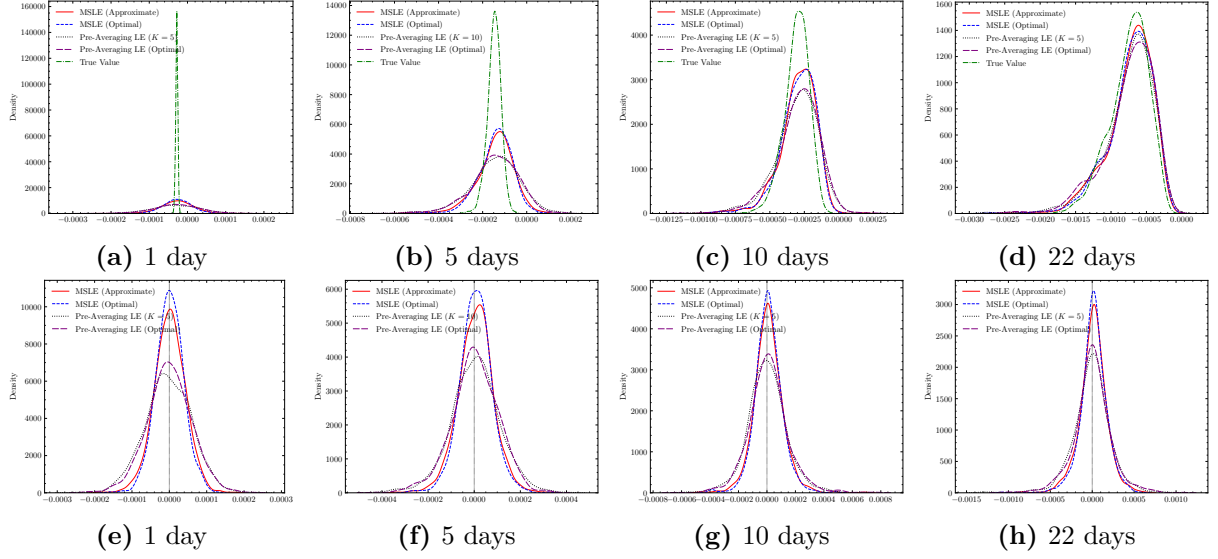


**Figure 11:** The performances of the MSLE and pre-averaging LE estimators for each setting of  $T$  in the iid noise setting ( $\varsigma = 10^{-4}$ ). The first row shows the true and estimated values of leverage effect, and the second row shows the estimation error.

**Table 8:** RMSE of the MSLE and pre-averaging LE estimators in the iid noise setting. The “RMSE-Std Ratio” is the ratio of the RMSE to the standard deviation of the true value, which makes the results comparable across different  $T$ .

$\varsigma$	Days	True Value		RMSE				RMSE-Std Ratio			
				MSLE		Pre-Averaging LE		MSLE		Pre-Averaging LE	
		Mean	Std	Approximate	Optimal	Selected	Optimal	Approximate	Optimal	Selected	Optimal
$10^{-4}$	1	$-2.804 \times 10^{-5}$	$2.767 \times 10^{-6}$	$4.197 \times 10^{-5}$	$3.707 \times 10^{-5}$	$5.925 \times 10^{-5}$	$6.165 \times 10^{-5}$	15.17	13.39	21.41	22.28
	5	$-1.476 \times 10^{-4}$	$3.097 \times 10^{-5}$	$7.638 \times 10^{-5}$	$6.982 \times 10^{-5}$	$1.018 \times 10^{-4}$	$1.067 \times 10^{-4}$	2.47	2.25	3.29	3.45
	10	$-3.062 \times 10^{-4}$	$8.978 \times 10^{-5}$	$1.037 \times 10^{-4}$	$9.613 \times 10^{-5}$	$1.416 \times 10^{-4}$	$1.364 \times 10^{-4}$	1.16	1.07	1.58	1.52
$10^{-3.5}$	22	$-7.437 \times 10^{-4}$	$2.720 \times 10^{-4}$	$1.638 \times 10^{-4}$	$1.585 \times 10^{-4}$	$2.217 \times 10^{-4}$	$2.253 \times 10^{-4}$	0.60	0.58	0.82	0.83
	1	$-2.804 \times 10^{-5}$	$2.767 \times 10^{-6}$	$5.861 \times 10^{-5}$	$6.038 \times 10^{-5}$	$7.786 \times 10^{-5}$	$7.937 \times 10^{-5}$	21.18	21.82	28.13	28.68
	5	$-1.476 \times 10^{-4}$	$3.097 \times 10^{-5}$	$1.045 \times 10^{-4}$	$1.066 \times 10^{-4}$	$1.320 \times 10^{-4}$	$1.354 \times 10^{-4}$	3.37	3.44	4.26	4.37
$10^{-3}$	10	$-3.062 \times 10^{-4}$	$8.978 \times 10^{-5}$	$1.429 \times 10^{-4}$	$1.399 \times 10^{-4}$	$1.766 \times 10^{-4}$	$1.808 \times 10^{-4}$	1.59	1.56	1.97	2.01
	22	$-7.437 \times 10^{-4}$	$2.720 \times 10^{-4}$	$2.304 \times 10^{-4}$	$2.190 \times 10^{-4}$	$2.920 \times 10^{-4}$	$3.126 \times 10^{-4}$	0.85	0.81	1.07	1.15
	1	$-2.804 \times 10^{-5}$	$2.767 \times 10^{-6}$	$8.604 \times 10^{-5}$	$1.118 \times 10^{-4}$	$9.852 \times 10^{-5}$	$1.005 \times 10^{-4}$	31.09	40.39	35.60	36.32
	5	$-1.476 \times 10^{-4}$	$3.097 \times 10^{-5}$	$1.622 \times 10^{-4}$	$1.863 \times 10^{-4}$	$1.795 \times 10^{-4}$	$1.719 \times 10^{-4}$	5.24	6.02	5.80	5.55
	10	$-3.062 \times 10^{-4}$	$8.978 \times 10^{-5}$	$2.264 \times 10^{-4}$	$2.531 \times 10^{-4}$	$2.431 \times 10^{-4}$	$2.387 \times 10^{-4}$	2.52	2.82	2.71	2.66
	22	$-7.437 \times 10^{-4}$	$2.720 \times 10^{-4}$	$3.453 \times 10^{-4}$	$3.903 \times 10^{-4}$	$4.077 \times 10^{-4}$	$4.040 \times 10^{-4}$	1.27	1.44	1.50	1.49

weights is very close to that with optimal weights for small and medium noise levels, and even surpasses it for large noise levels.

### 6.2.3 Dependent noise setting

**Table 9:** The setting of the MSLE estimator with approximate weights in the dependent noise setting.

$\varsigma$	$\bar{H}_n$			
	1 day	5 days	10 days	22 days
$10^{-4}$	10	9	8	6
$10^{-3.5}$	57	47	44	37
$10^{-3}$	230	219	201	169

In the dependent noise case, AR(1) model defined in Equation (6.5) with  $\phi = 0.7$  is used

to generate the noise. The settings of  $T$ ,  $\varsigma$  and  $N$  are the same as in the iid noise case. To calculate the asymptotic variance of the MSLE estimator,  $q = 3$  is used to truncate the generalized autocovariance functions (ACFs) of the noise, and the covariance due to noise is calculated using the corrected formula in Equation (A.114) in Appendix A.2. Therefore,  $m_n$  is set to 6, as Proposition 2 requires that the scale  $H$  satisfies  $H > 2q$ . Also,  $H_n^* = \lfloor \alpha n^a \rfloor$ , where  $\alpha = 1$  and  $a = 5/9$ . Specifically,  $H_p = 7, 8, \dots, \lfloor n^{5/9} \rfloor$ . The performances of the approximate MSLE and the *ex-post* selected pre-averaging LE are compared. The setting of  $\bar{H}_n$  for MSLE is listed in Table 9, where  $\bar{H}_n$  is calculated by minimizing the average asymptotic variance of SALE. The pre-averaging LE is selected *ex-post* based on RMSE from pre-averaging windows of 5, 10, 30, 60, 90, 120, 180, 240, and 300 for each combination of parameters.

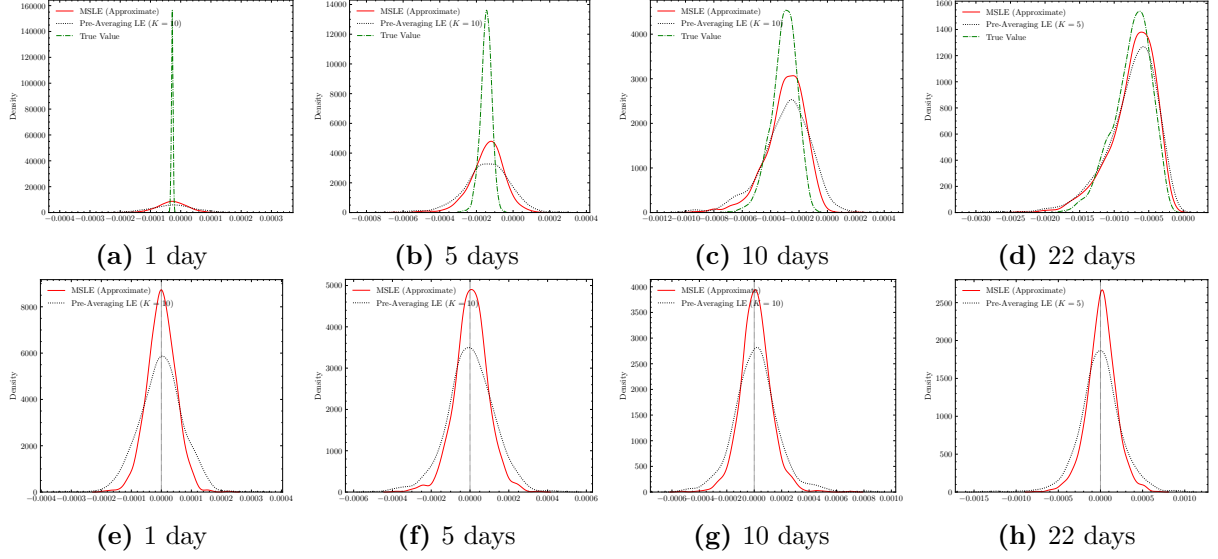


**Figure 12:** The performances of the MSLE and pre-averaging LE estimators for each setting of  $T$  in the dependent noise setting ( $\varsigma = 10^{-4}$ ). The first row shows the true and estimated values of leverage effect, and the second row shows the estimation error.

**Table 10:** RMSE of the MSLE and pre-averaging LE estimators in the dependent noise setting. The “RMSE-Std Ratio” is the ratio of the RMSE to the standard deviation of the true value, which makes the results comparable across different  $T$ .

$\varsigma$	Days	True Value		RMSE		RMSE-Std Ratio	
		Mean	Std	MSLE	Pre-Averaging LE	MSLE	Pre-Averaging LE
$10^{-4}$	1	$-2.804 \times 10^{-5}$	$2.767 \times 10^{-6}$	$4.777 \times 10^{-5}$	$7.108 \times 10^{-5}$	17.26	25.69
	5	$-1.476 \times 10^{-4}$	$3.097 \times 10^{-5}$	$8.671 \times 10^{-5}$	$1.209 \times 10^{-4}$	2.80	3.91
	10	$-3.062 \times 10^{-4}$	$8.978 \times 10^{-5}$	$1.142 \times 10^{-4}$	$1.615 \times 10^{-4}$	1.27	1.80
	22	$-7.437 \times 10^{-4}$	$2.720 \times 10^{-4}$	$1.744 \times 10^{-4}$	$2.498 \times 10^{-4}$	0.64	0.92
$10^{-3.5}$	1	$-2.804 \times 10^{-5}$	$2.767 \times 10^{-6}$	$6.652 \times 10^{-5}$	$9.283 \times 10^{-5}$	24.04	33.55
	5	$-1.476 \times 10^{-4}$	$3.097 \times 10^{-5}$	$1.184 \times 10^{-4}$	$1.616 \times 10^{-4}$	3.82	5.22
	10	$-3.062 \times 10^{-4}$	$8.978 \times 10^{-5}$	$1.633 \times 10^{-4}$	$2.196 \times 10^{-4}$	1.82	2.45
	22	$-7.437 \times 10^{-4}$	$2.720 \times 10^{-4}$	$2.670 \times 10^{-4}$	$3.651 \times 10^{-4}$	0.98	1.34
$10^{-3}$	1	$-2.804 \times 10^{-5}$	$2.767 \times 10^{-6}$	$9.628 \times 10^{-5}$	$1.179 \times 10^{-4}$	34.79	42.62
	5	$-1.476 \times 10^{-4}$	$3.097 \times 10^{-5}$	$1.819 \times 10^{-4}$	$2.274 \times 10^{-4}$	5.88	7.34
	10	$-3.062 \times 10^{-4}$	$8.978 \times 10^{-5}$	$2.528 \times 10^{-4}$	$3.074 \times 10^{-4}$	2.82	3.42
	22	$-7.437 \times 10^{-4}$	$2.720 \times 10^{-4}$	$3.821 \times 10^{-4}$	$4.864 \times 10^{-4}$	1.40	1.79

Figure 12 shows the estimated values and estimation errors of the MSLE and pre-averaging LE estimators for each setting of  $T$  with  $\varsigma = 10^{-4}$ . Table 10 reports the RMSE of the MSLE and pre-averaging LE estimators. The results indicate that the MSLE estimator with approximate

weights outperforms the pre-averaging LE estimator in terms of finite sample RMSE. Moreover, it is important to note that selecting the best pre-averaging LE is not feasible in practice, whereas our MSLE estimator with approximate weights can be easily implemented.

### 6.3 Why does multi-scale excel pre-averaging?

This section provides an intuitive explanation for the superior finite-sample performance of the MSLE estimator compared to the pre-averaging LE estimator. We begin by comparing the asymptotic variances of the SALE and pre-averaging LE estimators in the noise-free setting. With both subsampling scale and pre-averaging window length being  $H_n$ , their asymptotic variances are

$$\text{AVAR of SALE} = \frac{8}{3k_n} \int_0^T \sigma_t^6 dt + \frac{2T}{3} k_n H_n \Delta_n \int_0^T \sigma_t^2 d\langle \sigma^2, \sigma^2 \rangle_t, \quad (6.9)$$

$$\text{AVAR of Pre-Averaging LE} = \frac{4}{k_n} \int_0^T \sigma_t^6 dt + \frac{2T}{3} k_n H_n \Delta_n \int_0^T \sigma_t^2 d\langle \sigma^2, \sigma^2 \rangle_t. \quad (6.10)$$

Thus, SALE consistently outperforms pre-averaging LE for any  $H_n$  in the asymptotic sense, provided that the pre-averaging window length is not excessively large (*e.g.*,  $b \leq 1/2$ ). Furthermore, MSLE can easily outperform SALE with appropriate weight assignment.

When noise is present, their asymptotic variances arise from two sources: discretization and noise. This is illustrated for SALE estimators in Figure 5. The asymptotic variances due to discretization, as described by Equations (6.9) and (6.10), increase with  $H_n$ , while those due to noise decrease and eventually diminish as  $H_n$  increases. Therefore, the total asymptotic variances typically decrease and then increase, with the minimum corresponding to the optimal choice of scales or pre-averaging window lengths.

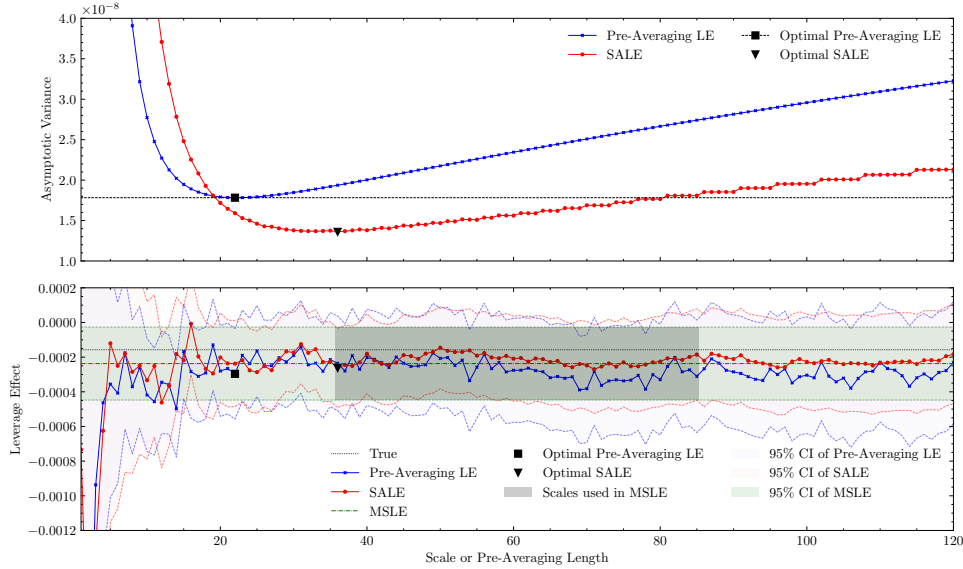


**Figure 13:** Signature plot of estimators for a simulated path with time horizon  $T = 5/252$  (one week) and noise scale  $\varsigma = 3 \times 10^{-4}$ . The figure above compares the asymptotic variances of SALE and pre-averaging LE estimators. The figure below shows the estimated values of SALE, MSLE and pre-averaging LE and their confidence intervals. In this case, the optimal SALE outperforms the optimal pre-averaging LE estimator, while the former is further improved by MSLE.

However, as the noise level increases, the asymptotic variance of SALE increases much more rapidly than that of pre-averaging LE. While MSLE mitigates this large asymptotic variance

due to noise, it still exhibits an inferior convergence rate for  $O_p(1)$  noise. However, the fact that the noise is relatively small in real-world scenarios brings good news for SALEs and MSLEs, as shown in Figure 13. The impact of noise on SALE is greater than on the pre-averaging LE estimator. This results in a larger total asymptotic variance for SALE compared to pre-averaging LE for smaller values of  $H_n$ , and a larger optimal scale for SALE compared to the optimal pre-averaging window length for pre-averaging LE. Nevertheless, for sufficiently large  $H_n$ , the impact of noise diminishes, and SALE eventually outperforms pre-averaging LE with the same  $H_n$ . More importantly, the optimal total asymptotic variance of SALE can be smaller than that of the pre-averaging LE estimator, as illustrated in the figure. This is the key reason why MSLE and SALE estimators can outperform pre-averaging LE estimators.

## 7 Empirical study

In the empirical study, the high-frequency trading data for a selection of assets from 2014 to 2023, encompassing 10 years (2,516 trading days), are collected from the TAQ database. The data is cleaned before analysis, retaining regular trades executed between 9:30 AM and 4:00 PM and removing erroneous entries.<sup>1</sup> The dataset consists of 15 ETFs and 15 individual stocks, as listed in Table 11. The ETFs track the performance of the S&P 500, NASDAQ 100, Dow Jones Industrial Average, Russell 2000 indices, as well as the 11 sectors of the S&P 500. The individual stocks are selected to represent a range of liquidity and volatility levels, covering various sectors such as technology, consumer goods, healthcare, and entertainment, thus providing a diverse set of assets for the empirical study. Among the 30 assets, XLC and XLRE were issued partway through the sample period. Therefore, our analysis for them begins at the start of their second year, in 2017 and 2019, respectively. After data cleaning, we resample the data to obtain 1-second and 5-second returns.

We apply the jump test proposed by Aït-Sahalia et al. (2012) to identify and remove trading days with the presence of jumps for each stock. This test is a robustified version of the test introduced by Aït-Sahalia and Jacod (2009), incorporating the pre-averaging method to deal with the MMS noise. After computing the standardized statistics with 5-second intraday data, we apply the universal threshold technique proposed by Bajgrowicz et al. (2016) to eliminate spurious jump detections. This method is more stringent than the FDR procedure and is designed to asymptotically remove all spurious detections, thereby minimizing data loss. As a result, 909 asset-days, comprising 1.2% of the entire dataset of 73,910 asset-days, are identified as containing jumps and excluded from further analysis. The numbers of days with jumps for each asset are listed in Table 11.

We estimate the leverage effects over both week (defined as every five trading days) and month (defined as natural months) periods using both 1-second and 5-second data for each stock. This is done in several steps.

1. The ReMeDI estimator proposed by Li and Linton (2022) is used to estimate the moments  $\nu_2$ ,  $\nu_4$  and the generalized acfs  $\rho_2(l)$ ,  $\rho_3(l)$ , and  $\rho_4(l)$  of the MMS noise in each period. The existence and the dependence level of noise are determined by its autocovariances.<sup>2</sup> The

<sup>1</sup>A practical and detailed guideline on high-frequency data cleaning is offered by Barndorff-Nielsen et al. (2009). While we follow most of the steps therein, some are omitted. For example, the entries with *Sale Conditions* ‘I’ (odd lot trade) and ‘C’ (cash trade) are retained because of their significant contribution to our dataset. We also remove the “bounceback” outliers described by Aït-Sahalia et al. (2011).

<sup>2</sup>For the ReMeDI estimator, we consider the first five dependence levels of the noise ( $|l| \leq 5$ ). To avoid underestimating the noise, conservative procedures are adopted. These include: (i) using 90% confidence intervals of autocovariances for testing, (ii) handling unreasonable ReMeDI estimates as detailed below, and (iii) applying a noisy procedure for noise with insignificant yet relatively non-negligible estimates ( $\hat{\nu}_2 \geq 10^{-4}$ ). Situations with unreasonable ReMeDI estimates include: (i)  $\hat{\nu}_2 \leq 0$ , which is treated as a noise-free situation; (ii)  $\hat{\nu}_2 > 0$  but  $\hat{\nu}_4 \leq 0$ , where the fourth-order moments are corrected by  $\hat{\mathbb{E}}[\varepsilon_i^2 \varepsilon_{i+l}^2] = \hat{\nu}_2^2 (\hat{\mathbb{E}}[\varepsilon_i \varepsilon_{i+l}])^2$ ; and (iii)  $\hat{\mathbb{E}}[\varepsilon_i^2 \varepsilon_{i+l}^2] < (\hat{\mathbb{E}}[\varepsilon_i \varepsilon_{i+l}])^2$ , where the fourth-order moments are corrected such that  $\hat{\mathbb{E}}[\varepsilon_i^2 \varepsilon_{i+l}^2] \geq (\hat{\mathbb{E}}[\varepsilon_i \varepsilon_{i+l}])^2$ .

results show that the noise in the dataset is small, while the dependencies are common. For example, the analysis of noise in monthly 5-second frequency data shows that: (i) for the ETFs, 33.9% of asset-months exhibit significant noise, among which 71.5% are dependent and the average noise scale is  $\varsigma = 9.6 \times 10^{-5}$ ; while (ii) for the stocks, 63.5% of the asset-months exhibit significant noise, among which 60.8% are dependent and the average noise scale is  $\varsigma = 2.0 \times 10^{-4}$ .

2. The scale parameter  $\tilde{H}_n$  in the approximate weights of the MSLE estimator is determined by minimizing the total asymptotic variances of SALE estimators, where the asymptotic variances are estimated using 1-minute average return data.<sup>3</sup> With the existence of noise, additional lower bounds for  $\tilde{H}_n$  are applied, such that: (i)  $\tilde{H}_n$  satisfies  $\tilde{H}_n \geq 2\hat{q} + 1$ , where  $\hat{q}$  is the estimated dependence level; and (ii) the minimum values of  $\tilde{H}_n$  are 20 for 1-second data (corresponding to 20 seconds) and 12 for 5-second data (corresponding to 60 seconds). The first bound is a condition for the proposed SALE and MSLE estimators, while the second is a rather conservative manual intervention, which mitigates numerical instability at the cost of larger asymptotic variance.
3. The leverage effect and its asymptotic variance are estimated using the MSLE estimator with approximate weights, where the number of scales is set to  $M_n = 50$  for computational efficiency.<sup>4</sup>

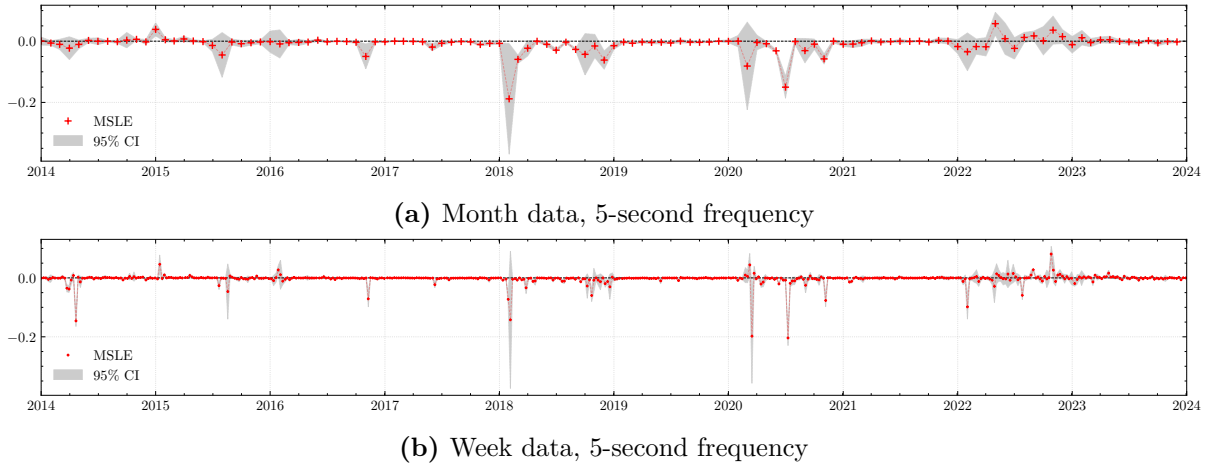


**Figure 14:** Leverage effect estimation for AMZN (Amazon.com, Inc.) with month and week data in 5-second frequency.

Figure 14 gives an example of leverage effect estimation with month and week data in 5-second frequency. The proportions of the signs for each asset are presented in Table 11. For most ETFs and stocks included in the study, negative leverage effects are more prevalent than positive ones, with the notable exceptions of AMC and GME. Figure 15 provides a comprehensive visualization of the stocks included in this empirical study, including information on trading volumes, volatilities, daily observations, and leverage effects.

<sup>3</sup>As explained in Figure 7, the corrected version of asymptotic variance due to noise of SALE in Equation (A.98) is used to decide the scale parameter.

<sup>4</sup>For MSLE in the noisy situation, although its asymptotic variance is given by Theorem 5, the asymptotic variance due to noise might be inaccurate as the magnitudes of the noise are relatively small in this dataset. As a workaround, the corrected version of the asymptotic variance due to noise of SALEs is calculated using Equation (A.98), and the inequality  $\text{Var}(\mathbf{w}^T \boldsymbol{\xi}) \leq (\mathbf{w}^T \boldsymbol{\sigma})^2$  with  $\boldsymbol{\sigma} = \text{diag}(\text{Cov}(\boldsymbol{\xi}))$  is used to derive an upper bound for the asymptotic variance due to noise of MSLE. Given the minor contribution of noise to the total asymptotic variance, this provides a reasonable approximation.



**Table 11:** Data descriptions and results of empirical study.

Type	Ticker	Name	Average Daily Observations	Average Daily Volume	Annualized Volatility	Trading Days	Days with Jumps	Signs of Leverage Effects (%)							
								M, 1-sec	M, 5-sec	W, 1-sec	W, 5-sec	M, 1-sec	M, 5-sec	W, 1-sec	W, 5-sec
								-	+	-	+	-	+	-	+
ETF	SPY	SPDR S&P 500 ETF Trust	428321	$9.27 \times 10^7$	0.175	2516	5	89.2	10.8	93.3	6.7	83.3	16.7	86.7	13.3
	QQQ	Invesco QQQ Trust	219580	$4.14 \times 10^7$	0.215	2516	3	88.3	11.7	90.8	9.2	84.9	15.1	86.7	13.3
	DIA	SPDR Dow Jones Industrial Average ETF Trust	35501	$4.53 \times 10^6$	0.174	2516	11	86.7	13.3	90.0	10.0	77.4	22.6	82.1	17.9
	IWM	iShares Russell 2000 ETF	153098	$2.98 \times 10^7$	0.221	2516	5	86.7	13.3	89.2	10.8	77.0	23.0	80.4	19.6
	XLC	The Communication Services Select Sector SPDR ETF Fund	27626	$4.65 \times 10^6$	0.242	1393	6	88.3	11.7	86.7	13.3	75.1	24.9	76.3	23.7
	XLY	The Consumer Discretionary Select Sector SPDR Fund	49127	$5.63 \times 10^6$	0.208	2516	12	88.3	11.7	90.0	10.0	74.2	25.8	79.8	20.2
	XLP	The Consumer Staples Select Sector SPDR Fund	45530	$1.19 \times 10^7$	0.146	2516	21	70.8	29.2	75.8	24.2	62.5	37.5	61.9	38.1
	XLE	The Energy Select Sector SPDR Fund	112759	$2.10 \times 10^7$	0.298	2516	24	71.7	28.3	75.8	24.2	62.5	37.5	64.9	35.1
	XLF	The Financial Select Sector SPDR Fund	72205	$5.54 \times 10^7$	0.221	2516	15	81.7	18.3	87.5	12.5	71.2	28.8	71.6	28.4
	XLV	The Health Care Select Sector SPDR Fund	63047	$9.89 \times 10^6$	0.170	2516	19	82.5	17.5	88.3	11.7	69.0	31.0	68.8	31.2
	XLI	The Industrial Select Sector SPDR Fund	65217	$1.15 \times 10^7$	0.196	2516	13	80.8	19.2	90.8	9.2	71.4	28.6	73.8	26.2
	XLB	The Materials Select Sector SPDR Fund	38370	$6.33 \times 10^6$	0.206	2516	20	73.3	26.7	77.5	22.5	69.0	31.0	68.8	31.2
	XLRE	The Real Estate Select Sector SPDR Fund	15748	$4.21 \times 10^6$	0.214	2069	30	73.8	26.2	75.0	25.0	59.8	40.2	63.5	36.5
	XLK	The Technology Select Sector SPDR Fund	60643	$1.04 \times 10^7$	0.226	2516	7	89.2	10.8	91.7	8.3	83.3	16.7	83.7	16.3
	XLU	The Utilities Select Sector SPDR Fund	66683	$1.48 \times 10^7$	0.191	2516	48	64.2	35.8	65.0	35.0	55.4	44.6	57.1	42.9
Stock	AAPL	Apple Inc.	368263	$1.37 \times 10^8$	0.284	2516	22	76.7	23.3	75.8	24.2	70.2	29.8	73.6	26.4
	AMC	AMC Entertainment Holdings, Inc.	104278	$2.77 \times 10^6$	1.352	2516	56	50.8	49.2	48.3	51.7	47.8	52.2	49.6	50.4
	AMZN	Amazon.com, Inc.	164947	$8.02 \times 10^7$	0.332	2516	21	78.3	21.7	76.7	23.3	68.7	31.3	68.8	31.2
	CLX	The Clorox Company	16352	$1.18 \times 10^6$	0.227	2516	70	52.5	47.5	55.8	44.2	49.6	50.4	51.2	48.8
	CPB	The Campbell's Company	18902	$2.32 \times 10^6$	0.236	2516	66	51.7	48.3	49.2	50.8	54.8	45.2	53.6	46.4
	GME	GameStop Corp.	51874	$1.82 \times 10^7$	1.080	2516	52	43.3	56.7	49.2	50.8	47.2	52.8	48.2	51.8
	KO	The Coca-Cola Company	78632	$1.42 \times 10^7$	0.180	2516	44	65.8	34.2	67.5	32.5	55.4	44.6	59.1	40.9
	MRK	Merck & Co., Inc.	68200	$1.08 \times 10^7$	0.214	2516	52	64.2	35.8	56.7	43.3	56.0	44.0	50.8	49.2
	MSFT	Microsoft Corporation	231381	$3.02 \times 10^7$	0.271	2516	16	72.5	27.5	73.3	26.7	65.5	34.5	66.3	33.7
	NVDA	VIDIA Corporation	204440	$4.58 \times 10^8$	0.464	2516	30	71.7	28.3	76.7	23.3	68.1	31.9	68.7	31.3
	PEP	PepsiCo, Inc.	44764	$4.69 \times 10^6$	0.184	2516	44	66.7	33.3	68.3	31.7	52.0	48.0	54.6	45.4
	PFE	Pfizer Inc.	113288	$2.79 \times 10^7$	0.226	2516	40	65.8	34.2	61.7	38.3	57.3	42.7	57.1	42.9
	PG	The Procter & Gamble Company	61423	$8.27 \times 10^6$	0.182	2516	61	69.2	30.8	65.8	34.2	59.1	40.9	61.5	38.5
	TAP	Molson Coors Beverage Company	16751	$1.83 \times 10^6$	0.282	2516	67	60.0	40.0	59.2	40.8	52.0	48.0	52.6	47.4
	TSLA	Tesla, Inc.	368486	$1.13 \times 10^8$	0.557	2516	29	75.8	24.2	74.2	25.8	63.7	36.3	63.7	36.3

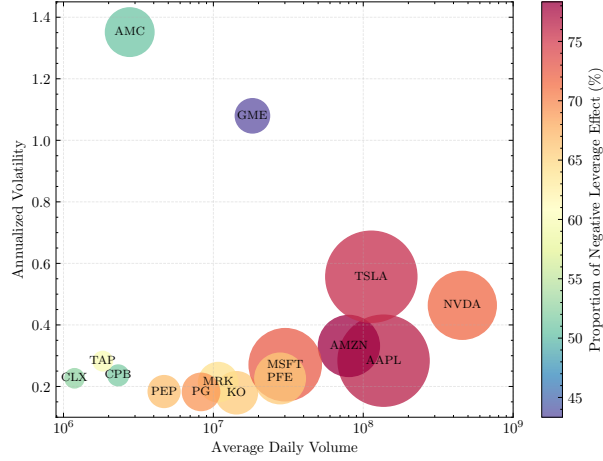


**Figure 15:** Individual stocks included in the empirical study. The sizes of the circles represent the average number of daily observations in our dataset, while the colors represent the proportion of negative leverage effect detected using monthly data sampled at 1-second frequency.

## References

- Yacine Aït-Sahalia and Jean Jacod. Testing for jumps in a discretely observed process. *The Annals of Statistics*, 37(1), February 2009. ISSN 0090-5364. doi: 10.1214/07-AOS568.
- Yacine Aït-Sahalia and Jean Jacod. *High-Frequency Financial Econometrics*. Princeton University Press, July 2014. ISBN 978-1-4008-5032-7. doi: 10.1515/9781400850327.
- Yacine Aït-Sahalia and Dacheng Xiu. A Hausman test for the presence of market microstructure noise in high frequency data. *Journal of Econometrics*, 211(1):176–205, July 2019. ISSN 03044076. doi: 10.1016/j.jeconom.2018.12.013.
- Yacine Aït-Sahalia, Per A. Mykland, and Lan Zhang. How Often to Sample a Continuous-Time Process in the Presence of Market Microstructure Noise. *Review of Financial Studies*, 18(2): 351–416, 2005. ISSN 0893-9454, 1465-7368. doi: 10.1093/rfs/hhi016.



- Yacine Aït-Sahalia, Per A. Mykland, and Lan Zhang. Ultra high frequency volatility estimation with dependent microstructure noise. *Journal of Econometrics*, 160(1):160–175, January 2011. ISSN 03044076. doi: 10.1016/j.jeconom.2010.03.028.
- Yacine Aït-Sahalia, Jean Jacod, and Jia Li. Testing for jumps in noisy high frequency data. *Journal of Econometrics*, 168(2):207–222, June 2012. ISSN 03044076. doi: 10.1016/j.jeconom.2011.12.004.
- Yacine Aït-Sahalia, Jianqing Fan, Roger J. A. Laeven, Christina Dan Wang, and Xiye Yang. Estimation of the Continuous and Discontinuous Leverage Effects. *Journal of the American Statistical Association*, 112(520):1744–1758, October 2017. ISSN 0162-1459, 1537-274X. doi: 10.1080/01621459.2016.1240082.
- Torben G. Andersen, Tim Bollerslev, Francis X. Diebold, and Paul Labys. Great realizations. *Risk*, 13:105–108, 2000.
- Pierre Bajgrowicz, Olivier Scaillet, and Adrien Treccani. Jumps in High-Frequency Data: Spurious Detections, Dynamics, and News. *Management Science*, 62(8):2198–2217, August 2016. ISSN 0025-1909, 1526-5501. doi: 10.1287/mnsc.2015.2234.
- Federico M. Bandi and Roberto Renò. Time-varying leverage effects. *Journal of Econometrics*, 169(1):94–113, July 2012. ISSN 03044076. doi: 10.1016/j.jeconom.2012.01.010.
- O. E. Barndorff-Nielsen, P. Reinhard Hansen, A. Lunde, and N. Shephard. Realized kernels in practice: Trades and quotes. *The Econometrics Journal*, 12(3):C1–C32, November 2009. ISSN 1368-4221, 1368-423X. doi: 10.1111/j.1368-423X.2008.00275.x.
- Fischer Black. Studies of stock price volatility changes. In *Proceedings of the 1976 Meeting of the Business and Economic Statistics Section, American Statistical Association*, pages 177–181. American Statistical Association, 1976.
- Carsten H. Chong and Viktor Todorov. Volatility of volatility and leverage effect from options. *Journal of Econometrics*, 240(1):105669, March 2024. ISSN 03044076. doi: 10.1016/j.jeconom.2024.105669.
- Carsten H. Chong, Thomas Delerue, and Guoying Li. When Frictions Are Fractional: Rough Noise in High-Frequency Data. *Journal of the American Statistical Association*, pages 1–14, January 2025. ISSN 0162-1459, 1537-274X. doi: 10.1080/01621459.2024.2428466.
- Kim Christensen, Roel C.A. Oomen, and Mark Podolskij. Fact or friction: Jumps at ultra high frequency. *Journal of Financial Economics*, 114(3):576–599, December 2014. ISSN 0304405X. doi: 10.1016/j.jfineco.2014.07.007.
- A Christie. The stochastic behavior of common stock variances Value, leverage and interest rate effects. *Journal of Financial Economics*, 10(4):407–432, December 1982. ISSN 0304405X. doi: 10.1016/0304-405X(82)90018-6.
- Imma Valentina Curato and Simona Sanfelici. Stochastic leverage effect in high-frequency data: A Fourier based analysis. *Econometrics and Statistics*, 23:53–82, July 2022. ISSN 24523062. doi: 10.1016/j.ecosta.2021.03.001.
- Rui Da and Dacheng Xiu. When Moving-Average Models Meet High-Frequency Data: Uniform Inference on Volatility. *Econometrica*, 89(6):2787–2825, 2021. ISSN 0012-9682. doi: 10.3982/ECTA15593.

- Steven L. Heston. A Closed-Form Solution for Options with Stochastic Volatility with Applications to Bond and Currency Options. *Review of Financial Studies*, 6(2):327–343, April 1993. ISSN 0893-9454, 1465-7368. doi: 10.1093/rfs/6.2.327.
- Jean Jacod. On continuous conditional Gaussian martingales and stable convergence in law. In Jacques Azéma, Marc Yor, and Michel Emery, editors, *Séminaire de Probabilités XXXI*, volume 1655, pages 232–246. Springer Berlin Heidelberg, Berlin, Heidelberg, 1997. ISBN 978-3-540-62634-3 978-3-540-68352-0. doi: 10.1007/BFb0119308.
- Jean Jacod and Philip E. Protter. *Discretization of Processes*. Number 67 in Stochastic Modelling and Applied Probability. Springer-Verlag Berlin Heidelberg, Berlin, Heidelberg, 2012. ISBN 978-3-642-24126-0 978-3-642-24127-7 978-1-283-45152-9. doi: 10.1007/978-3-642-24127-7.
- Jean Jacod, Yingying Li, Per A. Mykland, Mark Podolskij, and Mathias Vetter. Microstructure noise in the continuous case: The pre-averaging approach. *Stochastic Processes and their Applications*, 119(7):2249–2276, July 2009. ISSN 03044149. doi: 10.1016/j.spa.2008.11.004.
- Jean Jacod, Yingying Li, and Xinghua Zheng. Statistical Properties of Microstructure Noise. *Econometrica*, 85(4):1133–1174, 2017. ISSN 0012-9682. doi: 10.3982/ECTA13085.
- Ilze Kalnina and Oliver Linton. Estimating quadratic variation consistently in the presence of endogenous and diurnal measurement error. *Journal of Econometrics*, 147(1):47–59, November 2008. ISSN 03044076. doi: 10.1016/j.jeconom.2008.09.016.
- Ilze Kalnina and Dacheng Xiu. Nonparametric Estimation of the Leverage Effect: A Trade-Off Between Robustness and Efficiency. *Journal of the American Statistical Association*, 112(517):384–396, January 2017. ISSN 0162-1459, 1537-274X. doi: 10.1080/01621459.2016.1141687.
- Dazhong Lao and Shanshan Zhao. *Fundamental Theories and Their Applications of the Calculus of Variations*. Springer Singapore, Singapore, 1st ed. 2021 edition, 2021. ISBN 978-981-15-6069-9 978-981-15-6070-5. doi: 10.1007/978-981-15-6070-5.
- E. L. Lehmann. *Elements of Large-Sample Theory*. Springer Texts in Statistics. Springer, New York, 1999. ISBN 978-0-387-98595-4.
- Yingying Li, Shangyu Xie, and Xinghua Zheng. Efficient estimation of integrated volatility incorporating trading information. *Journal of Econometrics*, 195(1):33–50, November 2016. ISSN 03044076. doi: 10.1016/j.jeconom.2016.05.017.
- Z. Merrick Li and Oliver Linton. A ReMeDI for Microstructure Noise. *Econometrica*, 90(1):367–389, 2022. ISSN 0012-9682. doi: 10.3982/ECTA17505.
- Z. Merrick Li, Roger J.A. Laeven, and Michel H. Vellekoop. Dependent microstructure noise and integrated volatility estimation from high-frequency data. *Journal of Econometrics*, 215(2):536–558, April 2020. ISSN 03044076. doi: 10.1016/j.jeconom.2019.10.004.
- Per Mykland and Lan Zhang. Inference for Continuous Semimartingales Observed at High Frequency. *Econometrica*, 77(5):1403–1445, 2009. ISSN 0012-9682. doi: 10.3982/ECTA7417.
- Per A. Mykland and Lan Zhang. Between data cleaning and inference: Pre-averaging and robust estimators of the efficient price. *Journal of Econometrics*, 194(2):242–262, October 2016. ISSN 03044076. doi: 10.1016/j.jeconom.2016.05.005.
- Andrew J. Patton. Data-based ranking of realised volatility estimators. *Journal of Econometrics*, 161(2):284–303, April 2011. ISSN 03044076. doi: 10.1016/j.jeconom.2010.12.010.

- Mark Podolskij and Mathias Vetter. Bipower-type estimation in a noisy diffusion setting. *Stochastic Processes and their Applications*, 119(9):2803–2831, September 2009. ISSN 03044149. doi: 10.1016/j.spa.2009.02.006.
- Mark Podolskij and Mathias Vetter. Understanding limit theorems for semimartingales: A short survey. *Statistica Neerlandica*, 64(3):329–351, August 2010. ISSN 0039-0402, 1467-9574. doi: 10.1111/j.1467-9574.2010.00460.x.
- Mathias Vetter. Estimation of integrated volatility of volatility with applications to goodness-of-fit testing. *Bernoulli*, 21(4), November 2015. ISSN 1350-7265. doi: 10.3150/14-BEJ648.
- Christina D. Wang and Per A. Mykland. The Estimation of Leverage Effect With High-Frequency Data. *Journal of the American Statistical Association*, 109(505):197–215, January 2014. ISSN 0162-1459, 1537-274X. doi: 10.1080/01621459.2013.864189.
- Xiye Yang. Estimation of Leverage Effect: Kernel Function and Efficiency. *Journal of Business & Economic Statistics*, 41(3):939–956, July 2023. ISSN 0735-0015, 1537-2707. doi: 10.1080/07350015.2022.2097910.
- Huiling Yuan, Yan Mu, and Yong Zhou. Leverage effect in high-frequency data with market microstructure. *Statistics and Its Interface*, 13(1):91–101, 2020. ISSN 19387989, 19387997. doi: 10.4310/SII.2020.v13.n1.a8.
- Lan Zhang. Efficient estimation of stochastic volatility using noisy observations: A multi-scale approach. *Bernoulli*, 12(6), December 2006. ISSN 1350-7265. doi: 10.3150/bj/1165269149.
- Lan Zhang, Per A Mykland, and Yacine Aït-Sahalia. A Tale of Two Time Scales: Determining Integrated Volatility With Noisy High-Frequency Data. *Journal of the American Statistical Association*, 100(472):1394–1411, December 2005. ISSN 0162-1459, 1537-274X. doi: 10.1198/016214505000000169.
- Bin Zhou. High-Frequency Data and Volatility in Foreign-Exchange Rates. *Journal of Business & Economic Statistics*, 14(1):45–52, January 1996. ISSN 0735-0015, 1537-2707. doi: 10.1080/07350015.1996.10524628.

## A Proofs of propositions on variance due to noise

### A.1 Proof of Proposition 1

#### A.1.1 Notations

First, we make the following conventions in this section. We first rewrite the noisy all-observation estimator as

$$\widehat{[X, \sigma^2]}_T^{(\text{all})} = \frac{1}{k_n \Delta_n} \sum_{i \in I} u_i, \quad (\text{A.1})$$

where  $u_i$  is the  $i$ th summand in the estimator, defined as

$$u_i = (\Delta Y_i) \left( \sum_{j \in I^+(i)} (\Delta Y_j)^2 - \sum_{j \in I^-(i)} (\Delta Y_j)^2 \right). \quad (\text{A.2})$$

We further decompose  $u_i$  as

$$u_i = (a_i + A_i) (b_i + B_i), \quad (\text{A.3})$$

by defining

$$\begin{aligned} a_i + \textcolor{red}{A}_i &= (\Delta Y_i) = (\textcolor{blue}{\Delta X}_i) + \langle \theta_{\textcolor{red}{A}_i}, \varepsilon \rangle, \\ b_i + \textcolor{red}{B}_i &= \left( \sum_{j \in I^+(i)} (\Delta Y_j)^2 - \sum_{j \in I^-(i)} (\Delta Y_j)^2 \right) \\ &= \left( \sum_{j \in I^+(i)} (\textcolor{blue}{\Delta X}_j)^2 - \sum_{j \in I^-(i)} (\textcolor{blue}{\Delta X}_j)^2 \right) + \langle \theta_{\textcolor{red}{B}_i}, \varepsilon \rangle + \langle \phi_{\textcolor{red}{B}_i}, \varepsilon^2 \rangle + \langle \psi_{\textcolor{red}{B}_i}, \varepsilon \varepsilon_+ \rangle. \end{aligned} \quad (\text{A.4})$$

The lowercase letters  $a_i$  and  $b_i$  represent process-related terms in  $u_i$ , while the capital letters  $A_i$  and  $B_i$  represent noise-related terms in  $u_i$ .

The noise-related terms include three types:  $\varepsilon_j$ ,  $\varepsilon_j^2$ , and  $\varepsilon_j \varepsilon_{j+1}$  for valid  $j$  values. For simplicity, we denote the corresponding noise vectors as  $\varepsilon$ ,  $\varepsilon^2$ , and  $\varepsilon \varepsilon_+$ . These vectors are defined by

$$(\varepsilon)_j = \varepsilon_j, \quad (\varepsilon^2)_j = \varepsilon_j^2, \quad (\varepsilon \varepsilon_+)_j = \varepsilon_j \varepsilon_{j+1} I(j \neq n), \quad (\text{A.5})$$

for  $j \in \{0, 1, \dots, n\}$ . The non-zero values of the coefficient vectors  $\theta_{A_i}$ ,  $\theta_{B_i}$ ,  $\phi_{B_i}$ , and  $\psi_{B_i}$  are listed in Table 12. We also adopt the convention that the index of coefficient vectors is written as a superscript, so we have, for instance,  $\langle \psi_{B_i}, \varepsilon \varepsilon_+ \rangle = \sum_{j=0}^n \psi_{B_i}^j \varepsilon_j \varepsilon_{j+1}$ .

**Table 12:** Values of coefficient vectors in all-observation estimator

	$i - k_n - 1$	$i - k_n$	$\dots$	$i - 2$	$i - 1$	$i$	$i + 1$	$i + 2$	$i + 3$	$\dots$	$i + k_n + 1$	$i + k_n + 2$
$\theta_{A_i}$	0	0	$\dots$	0	0	-1	+1	0	0	$\dots$	0	0
$\theta_{B_i}$	$+2\Delta X_{i-k_n-1}$	$+2\Delta^2 X_{i-k_n-1}$	$\dots$	$+2\Delta^2 X_{i-3}$	$-2\Delta X_{i-2}$	0	0	$-2\Delta X_{i+2}$	$-2\Delta^2 X_{i+2}$	$\dots$	$-2\Delta^2 X_{i+k_n}$	$+2\Delta X_{i+k_n+1}$
$\phi_{B_i}$	-1	-2	$\dots$	-2	-1	0	0	+1	+2	$\dots$	+2	+1
$\psi_{B_i}$	+2	+2	$\dots$	+2	0	0	0	-2	-2	$\dots$	-2	0

#### A.1.2 Bias due to noise

Notice that the noise-free estimator can be written as

$$[X, \sigma^2]_T^{(\text{all})} = \frac{1}{k_n \Delta_n} \sum_{i \in I} v_i, \quad (\text{A.6})$$

where

$$v_i = (\Delta X_i) \left( \sum_{j \in I^+(i)} (\Delta X_j)^2 - \sum_{j \in I^-(i)} (\Delta X_j)^2 \right) = a_i b_i. \quad (\text{A.7})$$

We can conclude from Table 12 that  $A_i \perp B_i | \mathcal{F}$ . We can also conclude that  $\mathbb{E}A_i = \mathbb{E}B_i = 0$ , because  $\mathbb{E}[\varepsilon_j] = \mathbb{E}[\varepsilon_j \varepsilon_{j+1}] = 0$ , so that

$$\mathbb{E}[\langle \theta_{A_i}, \varepsilon \rangle | \mathcal{F}] = \mathbb{E}[\langle \theta_{B_i}, \varepsilon \rangle | \mathcal{F}] = \mathbb{E}[\langle \psi_{B_i}, \varepsilon \varepsilon_+ \rangle | \mathcal{F}] = 0; \quad (\text{A.8})$$

and  $\sum_j \phi_{B_i}^j = 0$  so that

$$\mathbb{E}[\langle \phi_{B_i}, \varepsilon^2 \rangle | \mathcal{F}] = 0. \quad (\text{A.9})$$

Therefore, each summand of the noisy estimator is unbiased due to noise:

$$\mathbb{E}[u_i | \mathcal{F}] = \mathbb{E}[(a_i + A_i)(b_i + B_i) | \mathcal{F}] = \mathbb{E}[a_i b_i | \mathcal{F}] = v_i, \quad (\text{A.10})$$

so that the unbiasedness of the all-observation estimator follows:

$$\mathbb{E} \left( \widehat{[X, \sigma^2]}_T^{(\text{all})} \middle| \mathcal{F} \right) = [X, \sigma^2]_T^{(\text{all})}. \quad (\text{A.11})$$

### A.1.3 Variance due to noise

Our goal is to derive the variance of the noisy all-observation estimator due to noise, which is given by

$$\begin{aligned} \text{Var} \left( \widehat{[X, \sigma^2]}_T^{(\text{all})} \middle| \mathcal{F} \right) &= \mathbb{E} \left( \left( \widehat{[X, \sigma^2]}_T^{(\text{all})} \right)^2 \middle| \mathcal{F} \right) - \left[ \mathbb{E} \left( \widehat{[X, \sigma^2]}_T^{(\text{all})} \middle| \mathcal{F} \right) \right]^2 \\ &= \mathbb{E} \left( \left( \widehat{[X, \sigma^2]}_T^{(\text{all})} \right)^2 \middle| \mathcal{F} \right) - ([X, \sigma^2]_T^{(\text{all})})^2 \\ &= \frac{1}{k_n^2 \Delta_n^2} \mathbb{E} \left( \sum_{k \in I} \sum_{l \in I} (u_k u_l - v_k v_l) \middle| \mathcal{F} \right). \end{aligned} \quad (\text{A.12})$$

At this stage, we obtain the main decomposition in this proof:

$$\begin{aligned} &k_n^2 \Delta_n^2 \text{Var} \left( \widehat{[X, \sigma^2]}_T^{(\text{all})} \middle| \mathcal{F} \right) \\ &= \sum_{k \in I} \sum_{l \in I} \mathbb{E} \left[ (a_k + A_k)(b_k + B_k)(a_l + A_l)(b_l + B_l) - a_k b_k a_l b_l \middle| \mathcal{F} \right] \\ &= \sum_{k \in I} \sum_{l \in I} \mathbb{E} \left[ N_1(k, l) + N_2(k, l) + N_3(k, l) + N_4(k, l) \middle| \mathcal{F} \right]. \end{aligned} \quad (\text{A.13})$$

Notice that in the above equation, the pure process-related term  $a_k b_k a_l b_l$  vanishes after simplification, while the remaining terms may contain one, two, three, or four noise-related terms. For simplicity, we omit the subscript  $k$  in  $(a_k, b_k, A_k, B_k)$  and denote  $(a_l, b_l, A_l, B_l)$  as  $(c, d, C, D)$  when these terms appear inside  $\sum_{k, l}$ . Thus, we can write

$$N_1(k, l) = \sum_{\text{comb}} Abcd = Abcd + aBcd + abCd + abcd, \quad (\text{A.14})$$

$$N_2(k, l) = \sum_{\text{comb}} ABcd = ABcd + AbCd + AbcD + aBCd + aBcD + abCD, \quad (\text{A.15})$$

$$N_3(k, l) = \sum_{\text{comb}} ABCd = ABCd + ABcD + AbCD + aBCD, \quad (\text{A.16})$$

$$N_4(k, l) = ABCD, \quad (\text{A.17})$$

where  $\sum_{\text{comb}}$  means all possible combinations of the four terms. We further adopt the conventions that, in Section A.1.3, noise terms in  $A, B, C, D$  are indexed by  $i, \alpha, j, \beta$  respectively, for example,  $A = \langle \theta_A, \varepsilon \rangle = \sum_{i=0}^n \theta_A^i \varepsilon_i$ .

To summarize, the variance due to noise can be calculated by

$$\text{Var} \left( \widehat{[X, \sigma^2]}_T^{(\text{all})} \middle| \mathcal{F} \right) = \sum_{m=1}^4 \frac{1}{k_n^2 \Delta_n^2} \sum_{k \in I} \sum_{l \in I} \mathbb{E} \left( N_m(k, l) \middle| \mathcal{F} \right). \quad (\text{A.18})$$

In the following part, we will calculate the summation by looking at the contribution of  $m = 1, 2, 3, 4$  respectively.

The following lemma, though trivial, will be used in the following calculations.

**Lemma 2.** *For mean zero, independent and identically distributed random variables  $\{X_i\}_{i=1}^l$ , we denote  $\nu_k = \mathbb{E}[X^k]$ . It is clear that the expectation of products*

$$\mathbb{E}[X_1^{k_1} X_2^{k_2} \cdots X_l^{k_l}] = \nu_{k_1} \nu_{k_2} \cdots \nu_{k_l}, \quad (\text{A.19})$$

where  $k_i \geq 1$  for all  $i = 1, \dots, l$  and the total times of power is  $n = \sum_{i=1}^l k_i$ . In order to make sure that the result is non-zero, an additional condition is that

$$k_i \geq 2, \quad \forall i = 1, \dots, l. \quad (\text{A.20})$$

It also follows that  $n \geq 2l$ .

**Contribution of  $N_1$**  With the same argument in Section A.1.2, we can conclude that

$$\mathbb{E}[Abcd|\mathcal{F}] = bcd\mathbb{E}[A|\mathcal{F}] = 0. \quad (\text{A.21})$$

Similarly,

$$\mathbb{E}[aBcd|\mathcal{F}] = \mathbb{E}[abCd|\mathcal{F}] = \mathbb{E}[abcD|\mathcal{F}] = 0. \quad (\text{A.22})$$

Therefore,  $N_1$  contributes nothing to the variance due to noise.

**Contribution of  $N_2$**  First, we have the following lemma concerning the noise-related terms in  $N_2$ .

**Lemma 3.** *For  $P, Q \in \{A, B, C, D\}$ ,  $P \neq Q$ , we have*

$$\begin{aligned} \mathbb{E}[PQ|\mathcal{F}] &= \nu_2 \langle \theta_P, \theta_Q \rangle + \nu_4 \langle \phi_P, \phi_Q \rangle \\ &+ \nu_2^2 [-\langle \phi_P, \phi_Q \rangle + \langle \psi_P, \psi_Q \rangle] + \nu_3 [\langle \theta_P, \phi_Q \rangle + \langle \phi_P, \theta_Q \rangle]. \end{aligned} \quad (\text{A.23})$$

*Proof.* Suppose the error terms are  $\varepsilon_\alpha, \varepsilon_\alpha^2, \varepsilon_\alpha \varepsilon_{\alpha+1}$  in  $P$ , and  $\varepsilon_\beta, \varepsilon_\beta^2, \varepsilon_\beta \varepsilon_{\beta+1}$  in  $Q$ . For all nine possible combination in  $PQ$ , by Lemma 2, the non-zero terms are

$$\begin{aligned} \mathbb{E}[\varepsilon_\alpha \varepsilon_\beta] &= \nu_2 \delta_{\alpha\beta}, \\ \mathbb{E}[\varepsilon_\alpha^2 \varepsilon_\beta^2] &= \nu_4 \delta_{\alpha\beta} + \nu_2^2 (1 - \delta_{\alpha\beta}), \\ \mathbb{E}[\varepsilon_\alpha \varepsilon_{\alpha+1} \varepsilon_\beta \varepsilon_{\beta+1}] &= \nu_2^2 \delta_{\alpha\beta}, \\ \mathbb{E}[\varepsilon_\alpha \varepsilon_\beta^2] &= \nu_3 \delta_{\alpha\beta}, \\ \mathbb{E}[\varepsilon_\alpha^2 \varepsilon_\beta] &= \nu_3 \delta_{\alpha\beta}. \end{aligned} \quad (\text{A.24})$$

Take the coefficients into considerations and notice that

$$\sum_{\alpha, \beta} \phi_P^\alpha \phi_Q^\beta = \sum_\alpha \phi_P^\alpha \sum_\beta \phi_Q^\beta = 0, \quad (\text{A.25})$$

so we have

$$\begin{aligned}
\mathbb{E}[PQ|\mathcal{F}] &= \nu_2 \sum_{\alpha,\beta} \theta_P^\alpha \theta_Q^\beta \delta_{\alpha\beta} + \nu_4 \sum_{\alpha,\beta} \phi_P^\alpha \phi_Q^\beta \delta_{\alpha\beta} \\
&\quad + \nu_2^2 \sum_{\alpha,\beta} \left( \phi_P^\alpha \phi_Q^\beta (1 - \delta_{\alpha\beta}) + \psi_P^\alpha \psi_Q^\beta \delta_{\alpha\beta} \right) \\
&\quad + \nu_3 \sum_{\alpha,\beta} \left( \theta_P^\alpha \phi_Q^\beta \delta_{\alpha\beta} + \phi_P^\alpha \theta_Q^\beta \delta_{\alpha\beta} \right) \\
&= \nu_2 \langle \theta_P, \theta_Q \rangle + \nu_4 \langle \phi_P, \phi_Q \rangle \\
&\quad + \nu_2^2 [-\langle \phi_P, \phi_Q \rangle + \langle \psi_P, \psi_Q \rangle] + \nu_3 [\langle \theta_P, \phi_Q \rangle + \langle \phi_P, \theta_Q \rangle].
\end{aligned} \tag{A.26}$$

The proof is thus completed.  $\square$

There are six terms to consider in the contribution of  $N_2$ . It is obvious that

$$\mathbb{E}[AB|\mathcal{F}] = \mathbb{E}[CD|\mathcal{F}] = 0, \tag{A.27}$$

so we only need to calculate

$$\frac{1}{k_n^2 \Delta_n^2} \sum_{k \in I} \sum_{l \in I} \mathbb{E} \left( bdAC + bcAD + adBC + acBD \middle| \mathcal{F} \right). \tag{A.28}$$

Notice that

$$\mathbb{E}[AC|\mathcal{F}] = \nu_2 \left( 2I(k=l) - I(|k-l|=1) \right), \tag{A.29}$$

so

$$\begin{aligned}
\sum_{k \in I} \sum_{l \in I} \mathbb{E}[bdAC|\mathcal{F}] &= \nu_2 \left( 2 \sum_{k=k_n+1}^{n-k_n-2} b_k^2 - \sum_{k=k_n+2}^{n-k_n-2} b_k b_{k-1} - \sum_{k=k_n+1}^{n-k_n-3} b_k b_{k+1} \right) \\
&= \nu_2 \left( \sum_{k=k_n+1}^{n-k_n-3} (\Delta b_k)^2 + b_{k_n+1}^2 + b_{n-k_n-2}^2 \right),
\end{aligned} \tag{A.30}$$

where

$$(\Delta b_k)^2 = \left( (\Delta X_{k+k_n+2})^2 - (\Delta X_{k+2})^2 - (\Delta X_{k-1})^2 + (\Delta X_{k-k_n-1})^2 \right)^2, \tag{A.31}$$

As [Mykland and Zhang \(2009\)](#) point out, the drift terms typically have no impact on the final result in the high-frequency setting, and locally constant approximations can be applied to simplify the analysis of asymptotic results. Therefore, by noticing that

$$\begin{aligned}
(\Delta b_k)^2 &\approx \left( \sigma_{k+k_n+2}^2 (\Delta W_{k+k_n+2})^2 - \sigma_{k+2}^2 (\Delta W_{k+2})^2 \right. \\
&\quad \left. - \sigma_{k-1}^2 (\Delta W_{k-1})^2 + \sigma_{k-k_n-1}^2 (\Delta W_{k-k_n-1})^2 \right)^2 \\
&\approx 8\sigma_k^4 \Delta_n^2,
\end{aligned} \tag{A.32}$$

we have

$$\Delta_n^{-1} \sum_{k \in I} \sum_{l \in I} \mathbb{E} \left( bdAC \middle| \mathcal{F} \right) \xrightarrow{p} 8\nu_2 \int_0^T \sigma_t^4 dt. \tag{A.33}$$

Notice that

$$\mathbb{E}[AD|\mathcal{F}] = \nu_2 \langle \theta_A, \theta_D \rangle + \nu_3 \langle \theta_A, \phi_D \rangle, \tag{A.34}$$

so

$$\sum_{k \in I} \sum_{l \in I} \mathbb{E}[bcAD|\mathcal{F}] = \nu_2 \sum_{k \in I} \sum_{l \in I} bc \langle \theta_A, \theta_D \rangle + \nu_3 \sum_{k \in I} \sum_{l \in I} bc \langle \theta_A, \phi_D \rangle. \tag{A.35}$$



When  $\langle \theta_A, \theta_D \rangle$  is not zero, it can be written as  $\sum_r \eta_r \Delta X_r$ , where up to four terms are present in this summation. The coefficient  $\eta_r$  satisfies  $|\eta_r| \leq 3$ , and  $\langle \theta_A, \theta_D \rangle$  is obviously mean zero as well as independent of  $bc$ , while  $bc$  only includes the linear and cubic terms of  $(\Delta X_r)$ . Therefore, we can ignore the impact of  $\sum_{k \in I} \sum_{l \in I} bc \langle \theta_A, \theta_D \rangle$  as its “standardized version” (divided by the order of its standard deviation) is asymptotically mean zero and therefore tight. As for  $\langle \theta_A, \phi_D \rangle$ , one can verify that

$$\langle \theta_A, \phi_D \rangle = I(|k - l| \in \{1, 2\}) - I(|k - l| \in \{k_n + 1, k_n + 2\}), \quad (\text{A.36})$$

so for a given  $k$ , there are up to eight non-zero  $\langle \theta_A, \phi_D \rangle$ , each with constant absolute value 1. When  $\langle \theta_A, \phi_D \rangle$  is non-zero,  $bc$  vanishes. Therefore, the “standardized version” of  $\sum_{k \in I} \sum_{l \in I} bc \langle \theta_A, \phi_D \rangle$  is tight as well. The order of variance can be estimated as  $O_p(k_n^2 \Delta_n)$  for  $\sum_{k \in I} \sum_{l \in I} bc \langle \theta_A, \phi_D \rangle$  and even smaller for  $\sum_{k \in I} \sum_{l \in I} bc \langle \theta_A, \theta_D \rangle$ . It follows that

$$k_n^{-1} \Delta_n^{-1/2} \sum_{k \in I} \sum_{l \in I} \mathbb{E}(bcAD | \mathcal{F}) = O_p(1). \quad (\text{A.37})$$

Moreover, because

$$\sum_{k \in I} \sum_{l \in I} adBC = \sum_{k \in I} \sum_{l \in I} a_k b_l B_k A_l = \sum_{k \in I} \sum_{l \in I} a_l b_k B_l A_k = \sum_{k \in I} \sum_{l \in I} bcAD, \quad (\text{A.38})$$

we also have

$$k_n^{-1} \Delta_n^{-1/2} \sum_{k \in I} \sum_{l \in I} \mathbb{E}(adBC | \mathcal{F}) = O_p(1). \quad (\text{A.39})$$

Lastly, notice that

$$\begin{aligned} \mathbb{E}[BD | \mathcal{F}] &= \nu_2 \langle \theta_B, \theta_D \rangle + \nu_4 \langle \phi_B, \phi_D \rangle \\ &\quad + \nu_2^2 [-\langle \phi_B, \phi_D \rangle + \langle \psi_B, \psi_D \rangle] + \nu_3 [\langle \theta_B, \phi_D \rangle + \langle \phi_B, \theta_D \rangle]. \end{aligned} \quad (\text{A.40})$$

Because  $ac \approx \sigma_k^2 \Delta_n I(k = l)$ , and

$$\|\phi_B\|^2 = 8k_n - 4, \quad \|\psi_B\|^2 = 8k_n, \quad (\text{A.41})$$

we can know that, as  $n \rightarrow \infty$ ,

$$\begin{aligned} &\sum_{k \in I} \sum_{l \in I} ac \left( \nu_4 \langle \phi_B, \phi_D \rangle + \nu_2^2 [-\langle \phi_B, \phi_D \rangle + \langle \psi_B, \psi_D \rangle] \right) \\ &\approx \sum_{k \in I} \sigma_k^2 \Delta_n \left[ \nu_4 \|\phi_B\|^2 + \nu_2^2 (-\|\phi_B\|^2 + \|\psi_B\|^2) \right] \\ &= \sum_{k \in I} \sigma_k^2 \Delta_n \left[ (8k_n - 4)(\nu_4 - \nu_2^2) + 8k_n \nu_2^2 \right] \\ &\approx \left[ (8k_n - 4)(\nu_4 - \nu_2^2) + 8k_n \nu_2^2 \right] \int_0^T \sigma_t^2 dt \\ &\approx 8k_n \nu_4 \int_0^T \sigma_t^2 dt. \end{aligned} \quad (\text{A.42})$$

For the  $ac \langle \theta_B, \theta_D \rangle$  term, when  $k \neq l$ , only  $(a, D)$  and  $(c, B)$  can overlap, so  $ac \langle \theta_B, \theta_D \rangle$  only contains the cubic terms of  $(\Delta X_r)$ , and thus vanishes. Therefore, the corresponding summation can be roughly estimated as

$$\begin{aligned} \sum_{k \in I} \sum_{l \in I} ac \left( \nu_2 \langle \theta_B, \theta_D \rangle \right) &\approx \nu_2 \sum_{k \in I} a^2 \|\theta_B\|^2 \approx \nu_2 \sum_{k \in I} \sigma_k^2 \Delta_n \|\theta_B\|^2 \\ &= \nu_2 \left( \int_0^T \sigma_t^2 dt \right) O_p(k_n \Delta_n) = O_p(k_n \Delta_n). \end{aligned} \quad (\text{A.43})$$

As for the  $ac\langle\theta_B, \phi_D\rangle$  term, notice that

$$\sum_{k \in I} \sum_{l \in I} ac\langle\theta_B, \phi_D\rangle = \sum_{k \in I} a^2\langle\theta_B, \phi_B\rangle + \sum_{k \in I} \sum_{l \in I} ac\langle\theta_B, \phi_D\rangle I(k \neq l). \quad (\text{A.44})$$

The first term vanishes because  $\langle\theta_B, \phi_B\rangle$  only contains linear terms of  $(\Delta X_r)$  and does not overlap with  $a^2$ . The second term vanishes because  $a$  only contains the linear terms of  $(\Delta X_r)$  and does not overlap with  $c$  or  $\langle\theta_B, \phi_D\rangle$ . As a result, the “standardized version” of  $\sum_{k \in I} \sum_{l \in I} ac\langle\theta_B, \phi_D\rangle$  is tight, which is

$$k_n^{-1} \Delta_n^{-3/2} \sum_{k \in I} \sum_{l \in I} ac\langle\theta_B, \phi_D\rangle = O_p(1). \quad (\text{A.45})$$

The same argument can be applied to the  $ac\langle\phi_B, \theta_D\rangle$  term. Therefore, we have

$$k_n^{-1} \sum_{k \in I} \sum_{l \in I} \mathbb{E}(acBD|\mathcal{F}) \xrightarrow{p} 8\nu_4 \int_0^T \sigma_t^2 dt. \quad (\text{A.46})$$

Therefore, by combining Equation (A.33), (A.37), (A.39), and (A.46), we can conclude that the contribution of the  $N_2$  term to the variance due to noise is

$$k_n^{-1} \sum_{k \in I} \sum_{l \in I} \mathbb{E}(N_2(k, l)|\mathcal{F}) \xrightarrow{p} 8\nu_4 \int_0^T \sigma_t^2 dt. \quad (\text{A.47})$$

**Contribution of  $N_3$**  The contribution of  $N_3$  can be calculated in a similar way as  $N_2$ . We have the following lemma concerning the noise-related terms in  $N_3$ .

**Lemma 4.** *For ABC and ACD terms, we have*

$$\mathbb{E}[ABC|\mathcal{F}] = \mathbb{E}[ACD|\mathcal{F}] = 0. \quad (\text{A.48})$$

*For ABD and BCD terms, we have*

$$\begin{aligned} \mathbb{E}[ABD|\mathcal{F}] = \sum_{i, \alpha, \beta} \Big\{ & \nu_2^2 [\theta_A^i \theta_B^\alpha \psi_D^\beta] (\delta_{i\beta}^{(k+1)} \delta_{\alpha, \beta+1}^{(k+2)} + \delta_{\alpha\beta}^{(k)} \delta_{i, \beta+1}^{(k-1)}) \\ & + \nu_2 \nu_3 [\theta_A^i \phi_B^\alpha \psi_D^\beta] (\delta_{i\beta}^{(k+1)} \delta_{\alpha, \beta+1}^{(k+2)} + \delta_{\alpha\beta}^{(k)} \delta_{i, \beta+1}^{(k-1)}) \Big\}, \end{aligned} \quad (\text{A.49})$$

where  $\delta_{i\beta}^{(k+1)}$  is defined as  $I(i = \beta = k + 1)$ , and

$$\begin{aligned} \mathbb{E}[BCD|\mathcal{F}] = \sum_{j, \alpha, \beta} \Big\{ & \nu_2^2 [\theta_C^j \theta_D^\beta \psi_B^\alpha] (\delta_{j\alpha}^{(l+1)} \delta_{\beta, \alpha+1}^{(l+2)} + \delta_{\beta\alpha}^l \delta_{j, \alpha+1}^{(l-1)}) \\ & + \nu_2 \nu_3 [\theta_C^j \phi_D^\beta \psi_B^\alpha] (\delta_{j\alpha}^{(l+1)} \delta_{\beta, \alpha+1}^{(l+2)} + \delta_{\beta\alpha}^l \delta_{j, \alpha+1}^{(l-1)}) \Big\}. \end{aligned} \quad (\text{A.50})$$

*Proof.* Firstly, consider  $\mathbb{E}[ABC|X, \sigma]$ . Notice that

$$ABC = \sum_{i, j, \alpha} \theta_A^i \varepsilon_i \left( \theta_B^\alpha \varepsilon_\alpha + \phi_B^\alpha \varepsilon_\alpha^2 + \psi_B^\alpha \varepsilon_\alpha \varepsilon_{\alpha+1} \right) \theta_C^j \varepsilon_j. \quad (\text{A.51})$$

There are three types of possible combinations in  $ABC$ , the expectations of which are

$$\begin{aligned} \mathbb{E}[\varepsilon_i \varepsilon_\alpha \varepsilon_j] &= 0, \\ \mathbb{E}[\varepsilon_i \varepsilon_\alpha^2 \varepsilon_j] &= \nu_2^2 \delta_{ij}, \\ \mathbb{E}[\varepsilon_i \varepsilon_\alpha \varepsilon_{\alpha+1} \varepsilon_j] &= 0, \end{aligned} \quad (\text{A.52})$$

according to Lemma 2. This is because  $i \neq \alpha$  for all terms and  $i \neq \alpha + 1$  additionally for terms with  $\varepsilon_\alpha \varepsilon_{\alpha+1}$ . Taking their coefficients into consideration, and notice that

$$\sum_{\alpha} \phi_B^\alpha = 0, \quad (\text{A.53})$$

so we have

$$\mathbb{E}[ABC|X, \sigma] = \sum_{i,j,\alpha} \nu_2^2 [\theta_A^i \phi_B^\alpha \theta_C^j] (\delta_{ij}) = \sum_i \nu_2^2 [\theta_A^i \theta_C^i] \sum_{\alpha} \phi_B^\alpha = 0. \quad (\text{A.54})$$

For the same reason, we can conclude that

$$\mathbb{E}[ACD|X, \sigma] = 0. \quad (\text{A.55})$$

Next, consider  $\mathbb{E}[ABD|X, \sigma]$ . Notice that

$$ABD = \sum_{i,\alpha,\beta} \theta_A^i \varepsilon_i \left( \theta_B^\alpha \varepsilon_\alpha + \phi_B^\alpha \varepsilon_\alpha^2 + \psi_B^\alpha \varepsilon_\alpha \varepsilon_{\alpha+1} \right) \left( \theta_D^\beta \varepsilon_\beta + \phi_D^\beta \varepsilon_\beta^2 + \psi_D^\beta \varepsilon_\beta \varepsilon_{\beta+1} \right). \quad (\text{A.56})$$

There are nine types of possible combinations, among which four types have non-zero expectations, and they are

$$\begin{aligned} \mathbb{E}[\varepsilon_i \varepsilon_\alpha \varepsilon_\beta \varepsilon_{\beta+1}] &= \nu_2^2 (\delta_{i\beta} \delta_{\alpha,\beta+1} + \delta_{\alpha\beta} \delta_{i,\beta+1}), \\ \mathbb{E}[\varepsilon_i \varepsilon_\alpha^2 \varepsilon_\beta] &= \nu_2^2 \delta_{i\beta}, \\ \mathbb{E}[\varepsilon_i \varepsilon_\alpha^2 \varepsilon_\beta^2] &= \nu_2 \nu_3 \delta_{i\beta}, \\ \mathbb{E}[\varepsilon_i \varepsilon_\alpha^2 \varepsilon_\beta \varepsilon_{\beta+1}] &= \nu_2 \nu_3 (\delta_{i\beta} \delta_{\alpha,\beta+1} + \delta_{\alpha\beta} \delta_{i,\beta+1}). \end{aligned} \quad (\text{A.57})$$

Therefore, we have

$$\begin{aligned} \mathbb{E}[ABD|\mathcal{F}] &= \sum_{i,\alpha,\beta} \left\{ \nu_2^2 [\theta_A^i \theta_B^\alpha \psi_D^\beta] (\delta_{i\beta} \delta_{\alpha,\beta+1} + \delta_{\alpha\beta} \delta_{i,\beta+1}) \right. \\ &\quad + \nu_2^2 [\theta_A^i \phi_B^\alpha \theta_D^\beta] (\delta_{i\beta}) + \nu_2 \nu_3 [\theta_A^i \phi_B^\alpha \phi_D^\beta] (\delta_{i\beta}) \\ &\quad \left. + \nu_2 \nu_3 [\theta_A^i \phi_B^\alpha \psi_D^\beta] (\delta_{i\beta} \delta_{\alpha,\beta+1} + \delta_{\alpha\beta} \delta_{i,\beta+1}) \right\} \\ &= \sum_{i,\alpha,\beta} \left\{ \nu_2^2 [\theta_A^i \theta_B^\alpha \psi_D^\beta] (\delta_{i\beta}^{(k+1)} \delta_{\alpha,\beta+1}^{(k+2)} + \delta_{\alpha\beta}^{(k)} \delta_{i,\beta+1}^{(k-1)}) \right. \\ &\quad \left. + \nu_2 \nu_3 [\theta_A^i \phi_B^\alpha \psi_D^\beta] (\delta_{i\beta}^{(k+1)} \delta_{\alpha,\beta+1}^{(k+2)} + \delta_{\alpha\beta}^{(k)} \delta_{i,\beta+1}^{(k-1)}) \right\}, \end{aligned} \quad (\text{A.58})$$

and  $\mathbb{E}[BCD|\mathcal{F}]$  can be calculated in a similar way. Thus, the proof is completed.  $\square$

Lemma 4 implies that we need to calculate

$$\frac{1}{k_n^2 \Delta_n^2} \sum_{k \in I} \sum_{l \in I} \mathbb{E}(cABD + aBCD|\mathcal{F}) = \frac{2}{k_n^2 \Delta_n^2} \sum_{k \in I} \sum_{l \in I} \mathbb{E}(cABD|\mathcal{F}). \quad (\text{A.59})$$

First, notice that

$$\begin{aligned} &\sum_{i,\alpha,\beta} \nu_2^2 [\theta_A^i \theta_B^\alpha \psi_D^\beta] (\delta_{i\beta}^{(k+1)} \delta_{\alpha,\beta+1}^{(k+2)} + \delta_{\alpha\beta}^{(k)} \delta_{i,\beta+1}^{(k-1)}) \\ &= \nu_2^2 \left\{ \theta_A^{k+1} \theta_B^{k+2} \psi_D^{k+1} + \theta_A^k \theta_B^{k-1} \psi_D^{k-1} \right\} \\ &= \nu_2^2 \left\{ (+1)(-2\Delta X_{k+2}) \psi_D^{k+1} + (-1)(-2\Delta X_{k-2}) \psi_D^{k-1} \right\}, \end{aligned} \quad (\text{A.60})$$

and  $\psi_D^{k+1}$  as well as  $\psi_D^{k-1}$  can be written as

$$\begin{aligned}\psi_D^{k+1} &= +2I(k+3 \leq l \leq k+k_n+2) - 2I(k-k_n \leq l \leq k-1), \\ \psi_D^{k-1} &= +2I(k+1 \leq l \leq k+k_n) - 2I(k-k_n-2 \leq l \leq k-3),\end{aligned}\tag{A.61}$$

so

$$\begin{aligned}& \sum_{k \in I} \sum_{l \in I} c \sum_{i, \alpha, \beta} \nu_2^2 [\theta_A^i \theta_B^\alpha \psi_D^\beta] (\delta_{i\beta}^{(k+1)} \delta_{\alpha, \beta+1}^{(k+2)} + \delta_{\alpha\beta}^{(k)} \delta_{i, \beta+1}^{(k-1)}) \\&= 2\nu_2^2 \left\{ - \sum_{k \in I} \sum_{l \in I} (\Delta X_l) (\Delta X_{k+2}) \psi_D^{k+1} + \sum_{k \in I} \sum_{l \in I} (\Delta X_l) (\Delta X_{k-2}) \psi_D^{k-1} \right\} \\&= 4\nu_2^2 \left\{ - \sum_{k \in I} \sum_{l \in I} (\Delta X_l) (\Delta X_{k+2}) I(k+3 \leq l \leq k+k_n+2) \right. \\&\quad + \sum_{k \in I} \sum_{l \in I} (\Delta X_l) (\Delta X_{k+2}) I(k-k_n \leq l \leq k-1) \\&\quad + \sum_{k \in I} \sum_{l \in I} (\Delta X_l) (\Delta X_{k-2}) I(k+1 \leq l \leq k+k_n) \\&\quad \left. - \sum_{k \in I} \sum_{l \in I} (\Delta X_l) (\Delta X_{k-2}) I(k-k_n-2 \leq l \leq k-3) \right\} \\&= 4\nu_2^2 \sum_{k=k_n+2}^{n-k_n-3} \left\{ -(\Delta X_{k+2})(X_{k+k_n+3} - X_{k+3}) + (\Delta X_{k+2})(X_k - X_{k-k_n}) \right. \\&\quad \left. + (\Delta X_{k-2})(X_{k+k_n+1} - X_{k+1}) - (\Delta X_{k-2})(X_{k-2} - X_{k-k_n-2}) \right\} \\&\quad + (\text{edge terms}) \\&\approx 4\nu_2^2 \sum_{k=k_n+2}^{n-k_n-3} (\Delta X_k) (\Delta_2 X_{k+k_n+1} - \Delta_2 X_{k+1} + \Delta_2 X_{k-2} - \Delta_2 X_{k-k_n-2}).\end{aligned}\tag{A.62}$$

It is clear that the expectation of this term vanishes, for  $(\Delta X_k)$  does not overlap with  $(\Delta_2 X_{k+k_n+1} - \Delta_2 X_{k+1} + \Delta_2 X_{k-2} - \Delta_2 X_{k-k_n-2})$ . In fact, a CLT for  $\eta_n = \sum_{k=k_n+2}^{n-k_n-3} (\Delta X_k) (\Delta_2 X_{k+k_n+1} - \Delta_2 X_{k+1} + \Delta_2 X_{k-2} - \Delta_2 X_{k-k_n-2})$  is

$$\Delta_n^{1/2} \eta_n \xrightarrow{\text{st}} \int_0^T 4\sigma_t^2 dW_t^{(\eta)}, \quad \text{as } n \rightarrow \infty,\tag{A.63}$$

where  $(W_t^{(\eta)})_{t \geq 0}$  is a Wiener process independent of  $(W_t)_{t \geq 0}$ , and the convergence mode is stable convergence. As a result,

$$\Delta_n^{1/2} \sum_{k \in I} \sum_{l \in I} c \sum_{i, \alpha, \beta} \nu_2^2 [\theta_A^i \theta_B^\alpha \psi_D^\beta] (\delta_{i\beta}^{(k+1)} \delta_{\alpha, \beta+1}^{(k+2)} + \delta_{\alpha\beta}^{(k)} \delta_{i, \beta+1}^{(k-1)}) = O_p(1).\tag{A.64}$$

Next, notice that

$$\begin{aligned}& \sum_{i, \alpha, \beta} \nu_2 \nu_3 [\theta_A^i \phi_B^\alpha \psi_D^\beta] (\delta_{i\beta}^{(k+1)} \delta_{\alpha, \beta+1}^{(k+2)} + \delta_{\alpha\beta}^{(k)} \delta_{i, \beta+1}^{(k-1)}) \\&= \nu_2 \nu_3 \left\{ \theta_A^{k+1} \phi_B^{k+2} \psi_D^{k+1} + \theta_A^k \phi_B^{k-1} \psi_D^{k-1} \right\} \\&= \nu_2 \nu_3 \left\{ (+1)(+1) \psi_D^{k+1} + (-1)(-1) \psi_D^{k-1} \right\} \\&= 2\nu_2 \nu_3 \left\{ I(k+3 \leq l \leq k+k_n+2) - I(k-k_n \leq l \leq k-1) \right. \\&\quad \left. + I(k+1 \leq l \leq k+k_n) - I(k-k_n-2 \leq l \leq k-3) \right\},\end{aligned}\tag{A.65}$$

so

$$\begin{aligned}
& \sum_{k \in I} \sum_{l \in I} c \sum_{i, \alpha, \beta} \nu_2 \nu_3 \left[ \theta_A^i \phi_B^\alpha \psi_D^\beta \right] \left( \delta_{i\beta}^{(k+1)} \delta_{\alpha, \beta+1}^{(k+2)} + \delta_{\alpha\beta}^{(k)} \delta_{i, \beta+1}^{(k-1)} \right) \\
&= 2\nu_2 \nu_3 \left\{ \sum_{k \in I} \sum_{l \in I} (\Delta X_l) \left[ I(k+3 \leq l \leq k+k_n+2) - I(k-k_n \leq l \leq k-1) \right. \right. \\
&\quad \left. \left. + I(k+1 \leq l \leq k+k_n) - I(k-k_n-2 \leq l \leq k-3) \right] \right\} \quad (\text{A.66}) \\
&= 2\nu_2 \nu_3 \left\{ \sum_{l \in I} (\Delta X_k) \sum_{k \in I} \left[ I(k+3 \leq l \leq k+k_n+2) - I(k-k_n \leq l \leq k-1) \right. \right. \\
&\quad \left. \left. + I(k+1 \leq l \leq k+k_n) - I(k-k_n-2 \leq l \leq k-3) \right] \right\}.
\end{aligned}$$

Different from some other summations in this section, in this summation, the center terms vanishes, while the edge terms dominate the result. After some careful calculation, we have

$$\begin{aligned}
& \sum_{k \in I} \sum_{l \in I} c \sum_{i, \alpha, \beta} \nu_2 \nu_3 \left[ \theta_A^i \phi_B^\alpha \psi_D^\beta \right] \left( \delta_{i\beta}^{(k+1)} \delta_{\alpha, \beta+1}^{(k+2)} + \delta_{\alpha\beta}^{(k)} \delta_{i, \beta+1}^{(k-1)} \right) \\
&= 2\nu_2 \nu_3 \left\{ \left( (-2k_n) \Delta X_{k_n+1} + (-2k_n+1) \Delta X_{k_n+2} + \sum_{q=1}^{k_n-1} (-2k_n+2q) \Delta X_{k_n+2+q} \right. \right. \\
&\quad \left. \left. + (-1) \Delta X_{2k_n+2} \right) + \left( \Delta X_{n-2k_n-3} + \sum_{q=1}^{k_n-1} 2q \Delta X_{n-2k_n-3-q} \right. \right. \\
&\quad \left. \left. + (2k_n-1) \Delta X_{n-k_n-3} + 2k_n \Delta X_{n-k_n-2} \right) \right\}. \quad (\text{A.67})
\end{aligned}$$

Of course, the expression vanishes if we omit the drift terms. However, in this case, it is safer to check it more carefully because of the special structure, where the drift terms at the start and end of the day are compared. Let the term inside the large bracket be denoted as  $\xi_n$ . The asymptotic mean of  $\xi_n$  is given by  $(\mu_T - \mu_0)k_n^2 \Delta_n$ , and its asymptotic stochastic variance is  $4(\sigma_0^2 + \sigma_T^2)k_n^3 \Delta_n/3$ . Thus, we can conclude that the “standardized version” of  $\xi_n$  is tight. Specifically, we have

$$k_n^{-3/2} \Delta_n^{-1/2} \sum_{k \in I} \sum_{l \in I} c \sum_{i, \alpha, \beta} \nu_2 \nu_3 \left[ \theta_A^i \phi_B^\alpha \psi_D^\beta \right] \left( \delta_{i\beta}^{(k+1)} \delta_{\alpha, \beta+1}^{(k+2)} + \delta_{\alpha\beta}^{(k)} \delta_{i, \beta+1}^{(k-1)} \right) = O_p(1). \quad (\text{A.68})$$

Therefore, by combining Equation (A.64) and (A.68), we can conclude that the contribution of the  $N_3$  term to the variance due to noise satisfies

$$k_n^{-3/2} \Delta_n^{-1/2} \sum_{k \in I} \sum_{l \in I} \mathbb{E} \left( N_3(k, l) \middle| \mathcal{F} \right) = O_p(1). \quad (\text{A.69})$$

**Contribution of  $N_4$**  Similarly, we have the following lemma.

**Lemma 5.** For  $\mathbb{E}[ABCD|\mathcal{F}]$ , we have

$$\begin{aligned}
\mathbb{E}[ABCD|\mathcal{F}] = \sum_{i,j,\alpha,\beta} \Big\{ & \nu_2^2 [\theta_A^i \theta_B^\alpha \theta_C^j \theta_D^\beta] (\delta_{ij} \delta_{\alpha\beta} + \delta_{i\beta} \delta_{\alpha j}) \\
& + \nu_2 \nu_3 [\theta_A^i \phi_B^\alpha \theta_C^j \theta_D^\beta + \theta_A^i \theta_B^\alpha \theta_C^j \phi_D^\beta] (\delta_{ij} \delta_{\alpha\beta} + \delta_{i\beta} \delta_{\alpha j}) \\
& + \nu_2 \nu_4 [\theta_A^i \phi_B^\alpha \theta_C^j \phi_D^\beta] (\delta_{ij} \delta_{\alpha\beta}) \\
& + \nu_2^3 [\theta_A^i \phi_B^\alpha \theta_C^j \phi_D^\beta] (\delta_{ij} (1 - \delta_{\alpha\beta})) \\
& + \nu_3^2 [\theta_A^i \phi_B^\alpha \theta_C^j \phi_D^\beta] (\delta_{i\beta} \delta_{\alpha j}) \\
& + \nu_2^3 [\theta_A^i \psi_B^\alpha \theta_C^j \psi_D^\beta] \left( \delta_{ij} \delta_{\alpha\beta} + \delta_{i\beta}^{(k+1)} \delta_{\alpha,\beta+1}^{(k+2)} \delta_{\alpha+1,j}^{(k+3)} I(l = k+3) \right. \\
& \quad \left. + \delta_{\alpha j}^{(l+1)} \delta_{\alpha+1,\beta}^{(l+2)} \delta_{i,\beta+1}^{(l+3)} I(l = k-3) \right) \Big\}. \tag{A.70}
\end{aligned}$$

*Proof.* Notice that

$$ABCD = \sum_{i,j,\alpha,\beta} \theta_A^i \varepsilon_i \left( \theta_B^\alpha \varepsilon_\alpha + \phi_B^\alpha \varepsilon_\alpha^2 + \psi_B^\alpha \varepsilon_\alpha \varepsilon_{\alpha+1} \right) \theta_C^j \varepsilon_j \left( \theta_D^\beta \varepsilon_\beta + \phi_D^\beta \varepsilon_\beta^2 + \psi_D^\beta \varepsilon_\beta \varepsilon_{\beta+1} \right). \tag{A.71}$$

There are nine types of possible combinations of noise terms, among which five types have non-zero expectations, and they are

$$\begin{aligned}
\mathbb{E}[\varepsilon_i \varepsilon_\alpha \varepsilon_j \varepsilon_\beta] &= \nu_2^2 (\delta_{ij} \delta_{\alpha\beta} + \delta_{i\beta} \delta_{\alpha j}), \\
\mathbb{E}[\varepsilon_i \varepsilon_\alpha^2 \varepsilon_j \varepsilon_\beta] &= \nu_2 \nu_3 (\delta_{ij} \delta_{\alpha\beta} + \delta_{i\beta} \delta_{\alpha j}), \\
\mathbb{E}[\varepsilon_i \varepsilon_\alpha \varepsilon_j \varepsilon_\beta^2] &= \nu_2 \nu_3 (\delta_{ij} \delta_{\alpha\beta} + \delta_{i\beta} \delta_{\alpha j}), \\
\mathbb{E}[\varepsilon_i \varepsilon_\alpha^2 \varepsilon_j \varepsilon_\beta^2] &= \nu_2 \nu_4 (\delta_{ij} \delta_{\alpha\beta}) + \nu_2^3 (\delta_{ij} (1 - \delta_{\alpha\beta})) + \nu_3^2 (\delta_{i\beta} \delta_{\alpha j}), \\
\mathbb{E}[\varepsilon_i \varepsilon_\alpha \varepsilon_{\alpha+1} \varepsilon_j \varepsilon_\beta \varepsilon_{\beta+1}] &= \nu_2^3 (\delta_{ij} \delta_{\alpha\beta} + \delta_{i\beta} \delta_{\alpha,\beta+1} \delta_{\alpha+1,j} + \delta_{\alpha j} \delta_{\alpha+1,\beta} \delta_{i,\beta+1}).
\end{aligned} \tag{A.72}$$

The proof is completed by taking the coefficients into consideration.  $\square$

According to Lemma 5, we need to calculate

$$\frac{1}{k_n^2 \Delta_n^2} \sum_{k \in I} \sum_{l \in I} \mathbb{E}(ABCD|\mathcal{F}). \tag{A.73}$$

Before we proceed, it would be helpful to notice that there are two frequently present patterns of coefficients and Kronecker deltas, which imply some conditions on  $k$  and  $l$ , and can be used to help simplify the calculation. Notice that

$$\begin{aligned}
\sum_{i,j} \theta_A^i \theta_C^j \delta_{ij} &= \sum_{i=k}^{k+1} \sum_{j=l}^{l+1} \theta_A^i \theta_C^j \delta_{ij} I(|k-l| \leq 1) \\
&= (\theta_A^k \theta_C^k + \theta_A^{k+1} \theta_C^{k+1}) I(k=l) \\
&\quad + \theta_A^k \theta_C^k I(l = k-1) + \theta_A^{k+1} \theta_C^{k+1} I(l = k+1) \\
&= 2I(k=l) - I(k=l-1) - I(k=l+1),
\end{aligned} \tag{A.74}$$

so for any coefficient vectors  $\xi$  and  $\eta$ , we have the first typical pattern:

$$\begin{aligned}
& \sum_{k \in I} \sum_{l \in I} \sum_{i,j,\alpha,\beta} [\theta_A^i \xi_B^\alpha \theta_C^j \eta_D^\beta] (\delta_{ij} \delta_{\alpha\beta}) \\
&= \sum_{k \in I} \sum_{l \in I} \left\{ \sum_{\alpha} \xi_B^\alpha \eta_D^\alpha \sum_{i,j} \theta_A^i \theta_C^j \delta_{ij} \right\} \\
&= \sum_{k \in I} \left\{ 2\langle \xi_B, \eta_B \rangle - \langle \xi_{B_k}, \eta_{B_{k-1}} \rangle I((k-1) \in I) - \langle \xi_{B_k}, \eta_{B_{k+1}} \rangle I((k+1) \in I) \right\},
\end{aligned} \tag{A.75}$$

The second typical pattern is

$$\begin{aligned} \sum_{k \in I} \sum_{l \in I} \sum_{i,j,\alpha,\beta} \left[ \theta_A^i \xi_B^\alpha \theta_C^j \eta_D^\beta \right] (\delta_{i\beta} \delta_{\alpha j}) &= \sum_{k \in I} \sum_{l \in I} \left\{ \sum_i \theta_A^i \eta_D^i \sum_j \theta_C^j \xi_B^j \right\} \\ &= \sum_{k \in I} \sum_{l \in I} \langle \theta_A, \eta_D \rangle \langle \theta_C, \xi_B \rangle. \end{aligned} \quad (\text{A.76})$$

These two patterns can be used to simplify the calculation.

First, we analyze the terms without coefficients  $\theta_B$  and  $\theta_D$ , as these terms only include constant coefficients, and thus are easier to handle and there is no need to take the expectation with respect to processes. They are also likely to have larger order than the terms with  $\theta_B$  and  $\theta_D$ . Notice that

$$\|\phi_B\|^2 = 8k_n - 4, \quad \text{for all } k \in I, \quad (\text{A.77})$$

$$\langle \phi_{B_k}, \phi_{B_{k+1}} \rangle = 8k_n - 8, \quad \text{for all } k, k+1 \in I, \quad (\text{A.78})$$

so we have

$$\begin{aligned} &\sum_{k \in I} \sum_{l \in I} \sum_{i,j,\alpha,\beta} \nu_2 \nu_4 \left[ \theta_A^i \phi_B^\alpha \theta_C^j \phi_D^\beta \right] (\delta_{ij} \delta_{\alpha\beta}) \\ &= \nu_2 \nu_4 \sum_{k \in I} \left\{ 2\|\phi_B\|^2 - \langle \phi_{B_k}, \phi_{B_{k-1}} \rangle I((k-1) \in I) - \langle \phi_{B_k}, \phi_{B_{k+1}} \rangle I((k+1) \in I) \right\} \\ &= \nu_2 \nu_4 \sum_{k \in I} \left\{ 2(8k_n - 4) - (8k_n - 8) - (8k_n - 8) \right\} \\ &= \nu_2 \nu_4 \left( (n - 2k_n - 4) \times 8 + 2 \times 8k_n \right) \\ &= \nu_2 \nu_4 (8n - 32). \end{aligned} \quad (\text{A.79})$$

Recall that  $\sum_\alpha \phi_B^\alpha = 0$ , so we have

$$\begin{aligned} &\sum_{k \in I} \sum_{l \in I} \sum_{i,j,\alpha,\beta} \nu_2^3 \left[ \theta_A^i \phi_B^\alpha \theta_C^j \phi_D^\beta \right] (\delta_{ij} (1 - \delta_{\alpha\beta})) \\ &= \nu_2^3 \sum_{k \in I} \sum_{l \in I} \left\{ \left( \sum_\alpha \phi_B^\alpha \right) \left( \sum_\beta \phi_D^\beta \right) \sum_{i,j} \theta_A^i \theta_C^j \delta_{ij} - \sum_{i,j,\alpha,\beta} \left[ \theta_A^i \phi_B^\alpha \theta_C^j \phi_D^\beta \right] (\delta_{ij} \delta_{\alpha\beta}) \right\} \\ &= -\nu_2^3 \sum_{k \in I} \sum_{l \in I} \sum_{i,j,\alpha,\beta} \left[ \theta_A^i \phi_B^\alpha \theta_C^j \phi_D^\beta \right] (\delta_{ij} \delta_{\alpha\beta}) \\ &= -\nu_2^3 (8n - 32). \end{aligned} \quad (\text{A.80})$$

Recall Equation (A.36). Because

$$\langle \theta_A, \phi_D \rangle = \langle \theta_C, \phi_B \rangle = I(|k-l| \in \{1, 2\}) - I(|k-l| \in \{k_n+1, k_n+2\}), \quad (\text{A.81})$$

we can know that

$$\langle \theta_A, \phi_D \rangle \langle \theta_C, \phi_B \rangle = I(|k-l| \in \{1, 2, k_n+1, k_n+2\}). \quad (\text{A.82})$$

Therefore, we have

$$\begin{aligned} &\sum_{k \in I} \sum_{l \in I} \sum_{i,j,\alpha,\beta} \nu_3^2 \left[ \theta_A^i \phi_B^\alpha \theta_C^j \phi_D^\beta \right] (\delta_{i\beta} \delta_{\alpha j}) \\ &= \nu_3^2 \sum_{k \in I} \sum_{l \in I} \langle \theta_A, \phi_D \rangle \langle \theta_C, \phi_B \rangle \\ &= \nu_3^2 \sum_{k \in I} \sum_{l \in I} I(|k-l| \in \{1, 2, k_n+1, k_n+2\}) \\ &= 2\nu_3^2 \sum_{q \in \{1, 2, k_n+1, k_n+2\}} (n - 2k_n - 2 - q) \\ &= \nu_3^2 (8n - 20k_n - 28). \end{aligned} \quad (\text{A.83})$$



Moreover, notice that

$$\|\psi_B\|^2 = 8k_n, \quad \text{for all } k \in I, \quad (\text{A.84})$$

$$\langle \psi_{B_k}, \psi_{B_{k+1}} \rangle = 8k_n - 8, \quad \text{for all } k, k+1 \in I, \quad (\text{A.85})$$

so we have

$$\begin{aligned} & \sum_{k \in I} \sum_{l \in I} \sum_{i,j,\alpha,\beta} \nu_2^3 [\theta_A^i \psi_B^\alpha \theta_C^j \psi_D^\beta] (\delta_{ij} \delta_{\alpha\beta}) \\ &= \nu_2^3 \sum_{k \in I} \left\{ 2\|\psi_B\|^2 - \langle \psi_{B_k}, \psi_{B_{k-1}} \rangle I((k-1) \in I) - \langle \psi_{B_k}, \psi_{B_{k+1}} \rangle I((k+1) \in I) \right\} \\ &= \nu_2^3 \sum_{k \in I} \left\{ 2 \times 8k_n - (8k_n - 8) - (8k_n - 8) \right\} \\ &= \nu_2^3 \left( (n - 2k_n - 4) \times 16 + 2 \times (8k_n + 8) \right) \\ &= \nu_2^3 (16n - 16k_n - 48). \end{aligned} \quad (\text{A.86})$$

The last term without coefficients  $\theta_B$  and  $\theta_D$  is

$$\begin{aligned} & \sum_{k \in I} \sum_{l \in I} \sum_{i,j,\alpha,\beta} \nu_2^3 [\theta_A^i \psi_B^\alpha \theta_C^j \psi_D^\beta] \left( \delta_{i\beta}^{(k+1)} \delta_{\alpha,\beta+1}^{(k+2)} \delta_{\alpha+1,j}^{(k+3)} I(l = k+3) \right. \\ & \quad \left. + \delta_{\alpha j}^{(l+1)} \delta_{\alpha+1,\beta}^{(l+2)} \delta_{i,\beta+1}^{(l+3)} I(l = k-3) \right) \\ &= \nu_2^3 \sum_{k \in I} \sum_{l \in I} \left\{ \theta_A^{k+1} \psi_B^{k+2} \theta_C^l \psi_D^{l-2} I(l = k+3) + \theta_A^k \psi_B^{k-2} \theta_C^{l+1} \psi_D^{l+2} I(l = k-3) \right\} \\ &= 4\nu_2^3 \sum_{k \in I} \sum_{l \in I} I(|k-l|=3) = \nu_2^3 (8n - 16k_n - 40). \end{aligned} \quad (\text{A.87})$$

Next, we consider terms with coefficients  $\theta_B$  and  $\theta_D$ . Notice that

$$\|\theta_B\|^2 \approx 16\sigma_k^2 k_n \Delta_n, \quad \text{for all } k \in I, \quad (\text{A.88})$$

$$\langle \theta_{B_k}, \theta_{B_{k+1}} \rangle \approx 16\sigma_k^2 (k_n - 1) \Delta_n, \quad \text{for all } k, k+1 \in I, \quad (\text{A.89})$$

so

$$\begin{aligned} & \sum_{k \in I} \sum_{l \in I} \sum_{i,j,\alpha,\beta} \nu_2^2 [\theta_A^i \theta_B^\alpha \theta_C^j \theta_D^\beta] (\delta_{ij} \delta_{\alpha\beta}) \\ &= \nu_2^2 \sum_{k \in I} \left\{ 2\|\theta_B\|^2 - \langle \theta_{B_k}, \theta_{B_{k-1}} \rangle I((k-1) \in I) - \langle \theta_{B_k}, \theta_{B_{k+1}} \rangle I((k+1) \in I) \right\} \\ &\approx \nu_2^2 \sum_{k \in I} \left\{ 2 \times 16\sigma_k^2 k_n \Delta_n - 16\sigma_k^2 (k_n - 1) \Delta_n I((k-1) \in I) \right. \\ & \quad \left. - 16\sigma_k^2 (k_n - 1) \Delta_n I((k+1) \in I) \right\} \\ &\approx \nu_2^2 \sum_{k \in I} 16\sigma_k^2 k_n \Delta_n \approx 16k_n \nu_2^2 \int_0^T \sigma_t^2 dt. \end{aligned} \quad (\text{A.90})$$

Notice that any of  $\langle \theta_A, \theta_D \rangle$  and  $\langle \theta_B, \theta_C \rangle$  is a linear combination of  $(\Delta X_r)$ 's, and the  $(\Delta X_r)$ 's in two terms never overlap, so the “standardized version” vanishes:

$$k_n^{-1/2} \Delta_n^{-1/2} \sum_{k \in I} \sum_{l \in I} \sum_{i,j,\alpha,\beta} \nu_2^2 [\theta_A^i \theta_B^\alpha \theta_C^j \theta_D^\beta] (\delta_{i\beta} \delta_{\alpha j}) \xrightarrow{p} 0. \quad (\text{A.91})$$

For similar reason, because  $\langle \phi_B, \theta_D \rangle$ ,  $\langle \theta_B, \phi_D \rangle$ ,  $\langle \theta_A, \phi_D \rangle$  and  $\langle \theta_C, \phi_B \rangle$  only contain linear combinations  $(\Delta X_r)$ 's, we have

$$k_n^{-1/2} \sum_{k \in I} \sum_{l \in I} \nu_2 \nu_3 [\theta_A^i \phi_B^\alpha \theta_C^j \theta_D^\beta + \theta_A^i \theta_B^\alpha \theta_C^j \phi_D^\beta] (\delta_{ij} \delta_{\alpha\beta} + \delta_{i\beta} \delta_{\alpha j}) \xrightarrow{p} 0. \quad (\text{A.92})$$

Therefore, by combining Equation (A.79), (A.80), (A.83), (A.86), (A.87), (A.90), (A.91) and (A.92), we can conclude that the contribution of the  $N_4$  term to the variance due to noise is

$$n^{-1} \sum_{k \in I} \sum_{l \in I} \mathbb{E} \left( N_4(k, l) \middle| \mathcal{F} \right) \xrightarrow{p} 8\nu_2\nu_4 + 16\nu_2^3 + 8\nu_3^2. \quad (\text{A.93})$$

**Total variance due to noise** Finally, by combining Equation (A.47), (A.69) and (A.93), we can see that  $N_4$  dominates the variance due to noise, so

$$n^{-1} \sum_{m=1}^4 \sum_{k \in I} \sum_{l \in I} \mathbb{E} \left( N_m(k, l) \middle| \mathcal{F} \right) \xrightarrow{p} 8\nu_2\nu_4 + 16\nu_2^3 + 8\nu_3^2. \quad (\text{A.94})$$

Therefore, according to Equation (A.18), the variance due to noise satisfies

$$\frac{\text{Var} \left( \widehat{[X, \sigma^2]}_T^{(\text{all})} \middle| \mathcal{F} \right)}{n^3 k_n^{-2}} \xrightarrow{p} \frac{8\nu_2\nu_4 + 16\nu_2^3 + 8\nu_3^2}{T^2}, \quad (\text{A.95})$$

as  $n \rightarrow \infty$ . Using the results above, one can also prove that

$$\frac{\mathbb{E} \left[ \text{Var} \left( \widehat{[X, \sigma^2]}_T^{(\text{all})} \middle| \mathcal{F} \right) \right]}{n^3 k_n^{-2}} \rightarrow \frac{8\nu_2\nu_4 + 16\nu_2^3 + 8\nu_3^2}{T^2}, \quad (\text{A.96})$$

as  $n \rightarrow \infty$ .

#### A.1.4 The central limit theorem

The detailed analysis above shows that, as  $n \rightarrow \infty$ , the process-related terms have no impact on the first and second order behavior of the estimator. Moreover, after ignoring the process-related terms in  $u_i$ , one can see that the resulting sequence  $\{u'_i\}$  is a stationary, mean-zero and  $(2k_n + 4)$ -dependent sequence. According to the central limit theorem for  $m$ -dependent sequence (Lehmann, 1999), we can prove the central limit theorem for the estimator which uses  $\Delta Y_i = \varepsilon_i$  as its observations. Then, with the continuous mapping theorem as well as the results above, we have the central limit theorem

$$\frac{\Delta_n^{3/2} k_n (\widehat{[X, \sigma^2]}_t^{(\text{all})} - [X, \sigma^2]_t^{(\text{all})})}{\sqrt{8\nu_2\nu_4 + 16\nu_2^3 + 8\nu_3^2}} \xrightarrow{d} \mathcal{N}(0, t), \quad \text{as } n \rightarrow \infty. \quad (\text{A.97})$$

Moreover, notice that the limiting process of the left hand side starts at zero and has independent increments. According to the unbiasedness due to noise, it is also uncorrelated with  $\mathcal{F}$ , so the limiting process is a Brownian motion independent of  $\mathcal{F}$ . This completes the proof of Proposition 1.

#### A.1.5 A more precise version

In fact, the above asymptotic analysis is based on two assumptions: the level of noise is not too small (for example,  $\nu_2 \gg 0, \nu_4 \gg 0$ ), and  $n \rightarrow \infty$ . When the noise is relatively small and the sample size is not large enough, it can be beneficial to use a more precise version of the variance due to noise, which is a by-product of the detailed analysis above. Combining Equation (A.33), Equation (A.46) and Equation (A.90), we have

$$\frac{\text{Var} \left( \widehat{[X, \sigma^2]}_T^{(\text{all})} \middle| \mathcal{F} \right)}{n^3 k_n^{-2}} \xrightarrow{p} T^{-2} \left[ (8\nu_2\nu_4 + 16\nu_2^3 + 8\nu_3^2) + \frac{k_n}{n^2} \cdot (8\nu_4 + 16\nu_2^2) \int_0^T \sigma_t^2 dt + \frac{1}{n^2} \cdot 8T\nu_2 \int_0^T \sigma_t^4 dt \right]. \quad (\text{A.98})$$

This can be helpful for finite sample analysis, especially when the scale of the noise is relatively small, as Figure 6 and Figure 7 illustrate.

## A.2 Proof of Proposition 2

### A.2.1 Proof

The unbiasedness of the subsample estimator and the SALE estimator can be directly derived from Proposition 1. The variance due to noise for the subsample estimator can also be derived similarly, which is

$$\frac{\text{Var} \left( \widehat{[X, \sigma^2]}_T^{(H_n, h)} \middle| \mathcal{F} \right)}{n^3 H_n^{-3} k_n^{-2}} \xrightarrow{p} \frac{8\nu_2\nu_4 + 16\nu_2^3 + 8\nu_3^2}{T^2}, \quad \text{as } n \rightarrow \infty. \quad (\text{A.99})$$

In order to derive the variance due to noise for the SALE estimator, we need to further consider the covariance between different subsample estimators:

$$\text{Var} \left( \widehat{[X, \sigma^2]}_T^{(H_n)} \middle| \mathcal{F} \right) = H_n^{-2} \sum_{h=1}^{H_n} \sum_{g=1}^{H_n} \text{Cov} \left( \widehat{[X, \sigma^2]}_T^{(H_n, h)}, \widehat{[X, \sigma^2]}_T^{(H_n, g)} \middle| \mathcal{F} \right). \quad (\text{A.100})$$

When  $\{\varepsilon_i\}_{i=0}^n$  is independent, it is easy to see that

$$\frac{\text{Var} \left( \widehat{[X, \sigma^2]}_T^{(H_n)} \middle| \mathcal{F} \right)}{n^3 H_n^{-4} k_n^{-2}} \xrightarrow{p} \frac{8\nu_2\nu_4 + 16\nu_2^3 + 8\nu_3^2}{T^2}, \quad \text{as } n \rightarrow \infty. \quad (\text{A.101})$$

When the noise is not independent, we can still derive the covariance between subsample  $(H_n, h)$  and  $(H_n, g)$ , and the assuming  $2q < H_n$  may simplify the calculation. This can be easily done by multiplying the moments of noise to the corresponding “generalized correlation” coefficients. In order to express it more explicitly, given a scale  $H_n$ , consider two subsamples indexed by  $h$  and  $g$  with  $|g - h| < q$ . Denoting  $I_{H_n} = \cap_{h=1}^{H_n} I_{H_n, h} = \{k_n + 1, \dots, n_{H_n} - k_n - 2\}$ , where  $n_{H_n} = \lfloor (n+1)/H_n \rfloor - 1$ , we can write the subsample estimators as

$$\widehat{[X, \sigma^2]}_T^{(H_n, h)} = \frac{1}{k_n H_n \Delta_n} \sum_{k \in I_{H_n}} u_{k, h}, \quad (\text{A.102})$$

$$\widehat{[X, \sigma^2]}_T^{(H_n, g)} = \frac{1}{k_n H_n \Delta_n} \sum_{l \in I_{H_n}} u_{l, g}, \quad (\text{A.103})$$

except for up to one end of the day term. The increment can be decomposed similarly as

$$\begin{aligned} u_{k, h} &= (\Delta_{H_n} Y_{k_h}) \left( \sum_{j \in I^+(k)} (\Delta_{H_n} Y_{j_h})^2 - \sum_{j \in I^-(k)} (\Delta_{H_n} Y_{j_h})^2 \right) \\ &= (a_{k, h} + A_{k, h}) (b_{k, h} + B_{k, h}), \end{aligned} \quad (\text{A.104})$$

where

$$\begin{aligned} a_{k, h} + A_{k, h} &= (\Delta_{H_n} Y_{k_h}) = (\Delta_{H_n} X_{k_h}) + \langle \theta_{A_{k, h}}, \varepsilon^{(h)} \rangle, \\ b_{k, h} + B_{k, h} &= \left( \sum_{j \in I^+(k)} (\Delta_{H_n} Y_{j_h})^2 - \sum_{j \in I^-(k)} (\Delta_{H_n} Y_{j_h})^2 \right) \\ &= \left( \sum_{j \in I^+(k)} (\Delta_{H_n} X_{j_h})^2 - \sum_{j \in I^-(k)} (\Delta_{H_n} X_{j_h})^2 \right) \\ &\quad + \langle \theta_{B_{k, h}}, \varepsilon^{(h)} \rangle + \langle \phi_{B_{k, h}}, \varepsilon^{(h)2} \rangle + \langle \psi_{B_{k, h}}, \varepsilon_{+}^{(h)} \rangle. \end{aligned} \quad (\text{A.105})$$

**Table 13:** Values of coefficient vectors in the subsample estimator

	$i - k_n - 1$	$i - k_n$	$\dots$	$i - 2$	$i - 1$	$i$	$i + 1$	$i + 2$	$i + 3$	$\dots$	$i + k_n + 1$	$i + k_n + 2$
$\theta_{A_{i,h}}$	0	0	$\dots$	0	0	-1	+1	0	0	$\dots$	0	0
$\theta_{B_{i,h}}$	$+2\Delta_{H_n} X_{i-k_n H_n - H_n}$	$+2\Delta_{H_n}^2 X_{i-k_n H_n - H_n}$	$\dots$	$+2\Delta_{H_n}^2 X_{i-3H_n}$	$-2\Delta_{H_n} X_{i-2H_n}$	0	0	$-2\Delta_{H_n} X_{i+2H_n}$	$-2\Delta_{H_n}^2 X_{i+2H_n}$	$\dots$	$-2\Delta_{H_n}^2 X_{i+k_n H_n}$	$+2\Delta_{H_n} X_{i+k_n H_n + H_n}$
$\phi_{B_{i,h}}$	-1	-2	$\dots$	-2	-1	0	0	+1	+2	$\dots$	+2	+1
$\psi_{B_{i,h}}$	+2	+2	$\dots$	+2	0	0	0	-2	-2	$\dots$	-2	0

Here, the noise vector is defined by

$$(\varepsilon^{(h)})_j = \varepsilon_{jh}, \quad (\varepsilon^{(h)2})_j = (\varepsilon_{jh})^2, \quad (\varepsilon \varepsilon_+^{(h)})_j = \varepsilon_{jh} \varepsilon_{(j+1)h} I(j \neq n_{H_n, h}), \quad (\text{A.106})$$

and the non-zero values of  $\theta_{A_{i,h}}$ ,  $\theta_{B_{i,h}}$ ,  $\phi_{B_{i,h}}$  and  $\psi_{B_{i,h}}$  are listed in Table 13, where the column represents the observation indices in subsample  $(H_n, h)$ .

Compared with the proof of Proposition 1, there are mainly two differences. First, the coefficient vectors  $\theta_{B_{i,h}}$  and  $\theta_{B_{i,g}}$  are different, but similar as in Appendix A.1, the corresponding terms are negligible in the final results. Second, for the noise terms in different subsamples, we have

$$\varepsilon_{ih} \perp \varepsilon_{jh}, \quad \text{if } i \neq j, \quad (\text{A.107})$$

and when  $i = j$ , the corresponding moments are corrected by the generalized correlation coefficients defined in Equation (3.14). For example,

$$\mathbb{E}[\varepsilon_{ih} \varepsilon_{jh}] = \nu_2 \rho_2(g - h) \delta_{ij}, \quad (\text{A.108})$$

$$\mathbb{E}[\varepsilon_{ih} \varepsilon_{jh}^2] = \sqrt{\nu_2 (\nu_4 - \nu_2^2)} \rho_3(g - h) \delta_{ij}, \quad (\text{A.109})$$

$$\mathbb{E}[\varepsilon_{ih}^2 \varepsilon_{jh}^2] = \nu_2^2 + (\nu_4 - \nu_2^2) \rho_4(g - h) \delta_{ij}. \quad (\text{A.110})$$

In this way, we can derive the covariance between different subsample estimators as

$$\begin{aligned} & n^{-3} H_n^3 k_n^2 \text{Cov} \left( \widehat{[X, \sigma^2]}_T^{(H_n, h)}, \widehat{[X, \sigma^2]}_T^{(H_n, g)} \middle| \mathcal{F} \right) \\ & \xrightarrow{p} 8\nu_2 (\nu_4 - \nu_2^2) \rho_2(g - h) \rho_4(g - h) + 24\nu_2^3 \rho_2^3(g - h) + 8\nu_2 (\nu_4 - \nu_2^2) \rho_3(g - h) \rho_3(h - g), \end{aligned} \quad (\text{A.111})$$

and therefore

$$\frac{\text{Var} \left( \widehat{[X, \sigma^2]}_T^{(H_n)} \middle| \mathcal{F} \right)}{n^3 H_n^{-4} k_n^{-2}} \xrightarrow{p} \frac{\Phi}{T^2}, \quad (\text{A.112})$$

where

$$\Phi = 8\nu_2 (\nu_4 - \nu_2^2) \sum_{l=-q}^q \left( \rho_2(l) \rho_4(l) + \rho_3(l) \rho_3(-l) \right) + 24\nu_2^3 \sum_{l=-q}^q \rho_2^3(l). \quad (\text{A.113})$$

The rest of the proof is similar. This completes the proof of Proposition 2.

### A.2.2 A more precise version

Similarly, a more precise version is given by

$$\frac{\text{Var} \left( \widehat{[X, \sigma^2]}_T^{(H_n)} \middle| \mathcal{F} \right)}{n^3 H_n^{-4} k_n^{-2}} \xrightarrow{p} \frac{\Phi'}{T^2}, \quad (\text{A.114})$$

where

$$\begin{aligned}
\Phi' = & 8\nu_2 (\nu_4 - \nu_2^2) \sum_{l=-q}^q \left( \rho_2(l)\rho_4(l) + \rho_3(l)\rho_3(-l) \right) + 24\nu_2^3 \sum_{l=-q}^q \rho_2^3(l) \\
& + \frac{k_n H_n}{n} \cdot \left[ 8(\nu_4 - \nu_2^2) \int_0^T \sigma_t^2 dt \sum_{l=-q}^q \left( 1 - \frac{|d|}{H_n} \right) \left( \rho_4(d) + \frac{\nu_2^2}{\nu_4 - \nu_2^2} (1 - \rho_2^2(d)) \right) \right] \\
& + \frac{k_n H_n}{n} \cdot \left[ 24\nu_2^2 \int_0^T \sigma_t^2 dt \sum_{l=-q}^q \left( 1 - \frac{|d|}{H_n} \right) \rho_2^2(d) \right] \\
& + \frac{H_n^2}{n^2} \cdot \left[ 8T\nu_2 \int_0^T \sigma_t^4 dt \sum_{l=-q}^q \left( 1 - \frac{|d|}{H_n} \right)^2 \rho_2(d) \right].
\end{aligned} \tag{A.115}$$

### A.3 On Proposition 3

#### A.3.1 The iid noise setting

When the noise is independent, the correlation between SALE at different scales are negligible except for a special case when one scale is exactly double the other. This can be established with the same way of calculating the contribution of noise terms as above. The calculation is tedious, so we will only explain the intuition instead of expanding the details. For example, consider the increment from two scales  $H_p \geq H_q$ .

$$\widehat{[X, \sigma^2]}_T^{(H_p)} = \frac{1}{k_p H_p^2 \Delta_n} \sum_{k=(k_p+1)H_p}^{n-(k_p+2)H_p} u_k^{(H_p)}, \tag{A.116}$$

$$\widehat{[X, \sigma^2]}_T^{(H_q)} = \frac{1}{k_q H_q^2 \Delta_n} \sum_{l=(k_q+1)H_q}^{n-(k_q+2)H_q} u_l^{(H_q)}, \tag{A.117}$$

where the increment can be decomposed similarly as before. For example, denote that we decompose  $u_k^{(H_p)}$  as  $(a_k + A_k)(b_k + B_k)$ , and  $u_l^{(H_q)}$  as  $(c_k + C_k)(d_k + D_k)$ . The dominant terms can be established similar as in Lemma 5, where we only consider terms without  $\theta_B$  and  $\theta_D$  as they become negligible as  $n \rightarrow \infty$ . However, for  $H_p > H_q$ , one can conclude after some tedious calculation that the only terms that remain after summation over  $l$  is

$$\sum_{l=(k_q+1)H_q}^{n-(k_q+2)H_q} \sum_{i,j,\alpha,\beta} \nu_2(\nu_4 - \nu_2^2) [\theta_A^i \phi_B^\alpha \theta_C^j \phi_B^\beta] (\delta_{ij} \delta_{\alpha\beta}) = 2\nu_2(\nu_4 - \nu_2^2) I(H_p = 2H_q), \tag{A.118}$$

so  $H_p = 2H_q$  is a very special situation. The contribution of elements from  $\phi_B$  and  $\phi_D$  at  $l-2, l-1, l+2$ , and  $l+3$  adds up to 2 in total, while the contribution at  $l-m$  and  $l+m+1$  for any  $m \geq 3$  cancels out. The former distinguishes  $H_p = 2H_q$  from any other cases.

For the same reason, shifting the spot volatility estimation window outward by one time interval (shown in Figure 1) can completely eliminate this distribution, so the correlation between different scales become really negligible.

#### A.3.2 The dependent noise setting

Although the closed-form expression of the covariance between different scales is difficult to derive, a multi-scale alternative of Lemma 5 (dropping terms with  $\theta_B$  and  $\theta_D$ ) can be used as an algorithm to explicitly calculate the covariance due to noise when the noise is dependent. The idea is very simple. First, for each given pair of  $k$  and  $l$ , the contribution can be calculated with this multi-scale and dependent alternative of Lemma 5. Second, suppose we have a fixed  $k$ , and

for the summation over  $l$ , we need to consider all  $l$ 's that may have potential contribution to the final result. That is, if the dependent level of noise is  $\tilde{q}$ , we need consider the following  $l$ 's:

$$l \in \{k - (k_p + 1)H_p - \tilde{q} - (k_q + 2)H_q, \dots, k + (k_p + 2)H_p + \tilde{q} + (k_q + 1)H_p\}. \quad (\text{A.119})$$

Third, the summation over  $k$  is substituted by simply multiplying  $n$ . Finally, the result is normalized by  $k_p H_p^2 \Delta_n$  and  $k_q H_q^2 \Delta_n$ . The code has been implemented and utilized in the simulation study.

## B Proof of the main results

### B.1 Preliminary results

We begin with some preliminary results that will be used in the proof of the main theorems. The following lemma concerns the error distribution of the “oracle” leverage effect estimator.

**Lemma 6.** *Suppose there is an interval  $[s, t]$  with  $t - s \rightarrow 0$ . We have*

$$\mathbb{E} \left[ \left( (X_t - X_s) (\sigma_t^2 - \sigma_s^2) - \int_s^t 2\sigma_r^2 f_r dr \right)^2 \middle| \mathcal{F}_s \right] = 4\sigma_s^4 (2f_s^2 + g_s^2) (t - s)^2 + O_p((t - s)^{5/2}). \quad (\text{B.1})$$

*Proof.* First, notice that  $d\langle X, \sigma^2 \rangle_r = 2\sigma_r^2 f_r$  and

$$(X_t - X_s) (\sigma_t^2 - \sigma_s^2) = \int_s^t (\sigma_r^2 - \sigma_s^2) dX_r + \int_s^t (X_r - X_s) d\sigma_r^2 + \int_s^t d\langle X, \sigma^2 \rangle_r. \quad (\text{B.2})$$

Therefore, according the Itô isometry, we have

$$\begin{aligned} & \mathbb{E} \left[ \left( (X_t - X_s) (\sigma_t^2 - \sigma_s^2) - \int_s^t 2\sigma_r^2 f_r dr \right)^2 \middle| \mathcal{F}_s \right] \\ &= \mathbb{E} \left[ \left( \int_s^t (\sigma_r^2 - \sigma_s^2) dX_r + \int_s^t (X_r - X_s) d\sigma_r^2 \right)^2 \middle| \mathcal{F}_s \right] \\ &= \mathbb{E} \left[ \int_s^t (\sigma_r^2 - \sigma_s^2)^2 d\langle X, X \rangle_r + \int_s^t (X_r - X_s)^2 d\langle \sigma^2, \sigma^2 \rangle_r \right. \\ & \quad \left. + 2 \int_s^t (\sigma_r^2 - \sigma_s^2)(X_r - X_s) d\langle X, \sigma^2 \rangle_r \middle| \mathcal{F}_s \right]. \end{aligned} \quad (\text{B.3})$$

For simplicity, denote  $\partial\langle A, B \rangle_t = \frac{d\langle A, B \rangle_r}{dr} \big|_{r=t}$  for processes  $A$  and  $B$ . Because

$$(X_r - X_s)^2 = \partial\langle X, X \rangle_s (r - s) + O_p((r - s)^{3/2}), \quad (\text{B.4})$$

$$(\sigma_r^2 - \sigma_s^2)^2 = \partial\langle \sigma^2, \sigma^2 \rangle_s (r - s) + O_p((r - s)^{3/2}), \quad (\text{B.5})$$

$$(\sigma_r^2 - \sigma_s^2)(X_r - X_s) = \partial\langle X, \sigma^2 \rangle_s (r - s) + O_p((r - s)^{3/2}), \quad (\text{B.6})$$

the target term can be simplified as

$$\begin{aligned} & \mathbb{E} \left[ \int_s^t \partial\langle \sigma^2, \sigma^2 \rangle_s \partial\langle X, X \rangle_s (r - s) dr + \int_s^t \partial\langle X, X \rangle_s \partial\langle \sigma^2, \sigma^2 \rangle_s (r - s) dr \right. \\ & \quad \left. + 2 \int_s^t \partial\langle X, \sigma^2 \rangle_s \partial\langle X, \sigma^2 \rangle_s (r - s) dr \middle| \mathcal{F}_s \right] + O_p((t - s)^{5/2}) \\ &= \left[ \partial\langle X, X \rangle_s \partial\langle \sigma^2, \sigma^2 \rangle_s + (\partial\langle X, \sigma^2 \rangle_s)^2 \right] (t - s)^2 + O_p((t - s)^{5/2}) \\ &= 4\sigma_s^4 (2f_s^2 + g_s^2) (t - s)^2 + O_p((t - s)^{5/2}). \end{aligned} \quad (\text{B.7})$$

This completes the proof of Lemma 6.  $\square$

The following lemma is about the expectation of the overlapping terms in the integrals of the increments of the process and the volatility. The specific form is induced by the decomposition  $(X_b - X_a)^2 = \int_a^b 2(X_r - X_a)dX_r + \sigma_r^2 dr$ .

**Lemma 7.** *Suppose there are two intervals  $[v, s]$  and  $[u, t]$ , where  $v < s$  and  $u < t$ , and  $d = (s - v) \vee (t - u) \rightarrow 0$ . In the following two situations, we have:*

(a) *If  $v \leq u < s \leq t$ , then the overlapping time interval is  $[s, u]$ , and*

$$\mathbb{E} \left[ \left( \int_v^s (X_r - X_v) dX_r \right) \left( \int_u^t (X_r - X_u) dX_r \right) \middle| \mathcal{F}_v \right] = \frac{1}{2} \sigma_v^4 (s - u)^2 + O_p(d^{5/2}), \quad (\text{B.8})$$

$$\mathbb{E} \left[ \left( \int_v^s (\sigma_r^2 - \sigma_v^2) dr \right) \left( \int_u^t (\sigma_r^2 - \sigma_u^2) dr \right) \middle| \mathcal{F}_v \right] = \frac{1}{3} \frac{d\langle \sigma^2, \sigma^2 \rangle_t}{dt} \bigg|_{t=v} (s - u)^3 + O_p(d^{7/2}). \quad (\text{B.9})$$

(b) *If  $v \leq u < t \leq s$ , then the overlapping time interval is  $[u, t]$ , and*

$$\mathbb{E} \left[ \left( \int_v^s (X_r - X_v) dX_r \right) \left( \int_u^t (X_r - X_u) dX_r \right) \middle| \mathcal{F}_v \right] = \frac{1}{2} \sigma_v^4 (t - u)^2 + O_p(d^{5/2}), \quad (\text{B.10})$$

$$\mathbb{E} \left[ \left( \int_v^s (\sigma_r^2 - \sigma_v^2) dr \right) \left( \int_u^t (\sigma_r^2 - \sigma_u^2) dr \right) \middle| \mathcal{F}_v \right] = \frac{1}{3} \frac{d\langle \sigma^2, \sigma^2 \rangle_t}{dt} \bigg|_{t=v} (t - u)^3 + O_p(d^{7/2}). \quad (\text{B.11})$$

*Proof.* For  $a < b$ , according to the Burkholder-Davis-Gundy inequality, there exists positive constant  $C_1$  such that

$$\mathbb{E} \left[ \sup_{a \leq r \leq b} |X_r - X_a| \middle| \mathcal{F}_a \right] \leq C_1 \mathbb{E} \left[ \left( \int_a^b \sigma_r^2 dr \right)^{1/2} \middle| \mathcal{F}_a \right] \leq C_1 \sigma_+(b - a)^{1/2}. \quad (\text{B.12})$$

Here the impact of drift term is  $O_p(b - a)$ , so it is ignored. Therefore, we have

$$\mathbb{E} \left[ \left| \int_a^b (X_r - X_a) \mu_r dr \right| \middle| \mathcal{F}_a \right] \leq C_1 \sigma_+ \mu_+ (b - a)^{3/2}, \quad (\text{B.13})$$

where  $\sigma_+$  and  $\mu_+$  are some local upper bounds of  $|\sigma_r|$  and  $|\mu_r|$ . Therefore,

$$\mathbb{E} \left[ \int_a^b (X_r - X_a) dX_r \middle| \mathcal{F}_a \right] = \mathbb{E} \left[ \int_a^b (X_r - X_a) \mu_r dr \middle| \mathcal{F}_a \right] = O_p((b - a)^{3/2}). \quad (\text{B.14})$$

Obviously,  $\mathbb{E}[X_b - X_a | \mathcal{F}_a] = O_p(b - a)$ . According to the Itô isometry, we also have

$$\mathbb{E} \left[ (X_b - X_a) \int_a^b (X_r - X_a) dX_r \middle| \mathcal{F}_a \right] = \mathbb{E} \left[ \int_a^b (X_r - X_a) \sigma_r^2 dr \middle| \mathcal{F}_a \right] = O_p((b - a)^{3/2}). \quad (\text{B.15})$$

For the first equality in (a), decompose the integral as

$$\int_v^s (X_r - X_v) dX_r = \int_v^s (X_r - X_v) dX_r + (X_u - X_v)(X_s - X_u) + \int_u^s (X_r - X_u) dX_r, \quad (\text{B.16})$$

$$\int_u^t (X_r - X_u) dX_r = \int_u^s (X_r - X_u) dX_r + (X_s - X_u)(X_t - X_s) + \int_s^t (X_r - X_s) dX_r. \quad (\text{B.17})$$



By utilizing the nested property  $\mathbb{E}[\cdot|\mathcal{F}_v] = \mathbb{E}[\mathbb{E}(\mathbb{E}(\cdot|\mathcal{F}_s)|\mathcal{F}_u)|\mathcal{F}_v]$  and applying the previous results, one can verify that the only dominant term turns out to be

$$\begin{aligned}\mathbb{E}\left[\left(\int_u^s (X_r - X_u) dX_r\right)^2 \middle| \mathcal{F}_v\right] &= \mathbb{E}\left[\int_u^s (X_r - X_u)^2 \sigma_r^2 dr \middle| \mathcal{F}_v\right] \\ &= \sigma_v^4 \int_u^s (r - u) dr + O_p((s - u)^{5/2}) \\ &= \frac{1}{2} \sigma_v^4 (s - u)^2 + O_p(d^{5/2}),\end{aligned}\tag{B.18}$$

and all other terms are  $O_p(d^{5/2})$ . The rest of the proof is similar after utilizing integral by parts:

$$\int_a^b (\sigma_r^2 - \sigma_a^2) dr = - \int_a^b (\sigma_r^2 - \sigma_b^2) d(b - r) = \int_a^b (b - r) d\sigma_r^2.\tag{B.19}$$

This completes the proof.  $\square$

The following lemma is induced by the structure of multi-scale grids. Without loss of generality, we consider grids of two scales, with intervals being 1 for the larger scale and  $l \in (0, 1)$  for the smaller one. For a given larger scale interval, the grids of smaller scale partition the interval into several subintervals, with their lengths denoted as  $(\alpha_1, \dots, \alpha_p)$ . Define  $\alpha_1$  as a uniformly distributed random variable on  $(0, l]$ , so that  $p$  is also a random variable related to  $\alpha_1$  and  $l$ . The parameter of interest is the summation of  $k$ th powers of  $\alpha_i$ 's as  $S_k = S_k(\alpha_1, l) = \sum_{i=1}^p \alpha_i^k$ , and its expectation with respect to  $\alpha_1 \sim \text{Unif}(0, l]$  is discussed in the following lemma.

**Lemma 8.** *For any integer  $k \geq 1$ , we have*

$$\mathbb{E}_{\alpha_1 \sim \text{Unif}(0, l]} [S_k(\alpha_1, l)] = l^{k-1} \left(1 - \frac{k-1}{k+1} l\right) = l^{k-1} - \frac{k-1}{k+1} l^k.\tag{B.20}$$

*Proof.* It is equivalent to prove that

$$I(l) = \int_0^l S_k(\alpha_1, l) d\alpha_1 = l^k - \frac{k-1}{k+1} l^{k+1}.\tag{B.21}$$

Denote  $(\alpha_1, \alpha_2, \dots, \alpha_p) = (x, a_1, \dots, a_m)$ , where  $m = \lceil (1-x)/l \rceil = p-1$ ,  $x = \alpha_1 \in (0, l]$ ,  $a_1 = \dots, a_{m-1} = l$ , and  $a_m = 1 - x - (m-1)l$ . The summation can be rewritten as

$$S_k(\alpha_1, l) = x^k + T_k(x, l), \quad \text{where } T_k(x, l) = \sum_{i=1}^m a_i^k,\tag{B.22}$$

and the target integral is

$$I(l) = \frac{1}{k+1} l^{k+1} + J(l), \quad \text{where } J(l) = \int_0^l T_k(x, l) dx.\tag{B.23}$$

Therefore, it is further equivalent to prove that

$$J(l) = \int_0^l T_k(x, l) dx = l^k - \frac{k}{k+1} l^{k+1}.\tag{B.24}$$

It is easy to see that  $\lim_{l \rightarrow 0^+} J(l) = 0$ , which is consistent with Equation (B.24). According to the Leibniz's rule, the derivative of  $J(l)$  is

$$\frac{d}{dl} J(l) = T_k(l, l) + \int_0^l \frac{\partial}{\partial l} T_k(x, l) dx,\tag{B.25}$$

so we only need to prove that for any  $l \in (0, 1)$ ,

$$\frac{d}{dl}J(l) = kl^{k-1} - kl^k. \quad (\text{B.26})$$

For the first term in Equation (B.25), we have

$$T_k(l, l) = (m-1)l^k + a_m^k. \quad (\text{B.27})$$

For the second term in Equation (B.25), we need to derive the detailed form of  $\frac{\partial}{\partial l}T_k(x, l)$ . For a given  $a_m \in (0, l]$ , consider an arbitrarily small  $\Delta l > 0$ , so that  $m$  remains unchanged. In this case,  $a_i = l \rightarrow l + \Delta l, \forall i = 1, \dots, m-1$ ; while  $a_m \rightarrow a_m - (m-1)l$ . Therefore, the corresponding change in  $T_k(x, l)$  is

$$\begin{aligned} \Delta T_k(x, l) &= T_k(x, l + \Delta l) - T_k(x, l) \\ &= (m-1) \left[ (l + \Delta l)^k - l^k \right] + \left[ (a_m - (m-1)\Delta l)^k - a_m^k \right] \\ &= (m-1)k(l^{k-1} - a_m^{k-1})\Delta l + o(\Delta l), \end{aligned} \quad (\text{B.28})$$

so we have

$$\frac{\partial}{\partial l}T_k(x, l) = (m-1)k(l^{k-1} - a_m^{k-1}). \quad (\text{B.29})$$

Next, we need to consider the specific value of  $a_m$  as  $x$  ranges from 0 to  $l$ . In fact, for a given  $l$ , there exists  $r = \lceil 1/l \rceil$  and  $x_0 = 1 - (r-1)l$ , such that for  $x \in (0, l]$ , we have

$$m = \begin{cases} r, & \text{if } 0 < x < x_0, \\ r-1, & \text{if } x_0 \leq x \leq l, \end{cases} \quad (\text{B.30})$$

$$a_m = \begin{cases} -x + x_0, & \text{if } 0 < x < x_0, \\ -x + x_0 + l, & \text{if } x_0 \leq x \leq l, \end{cases} \quad (\text{B.31})$$

$$\frac{\partial T_k}{\partial l} = \begin{cases} (r-1)k(l^{k-1} - (x_0 - x)^{k-1}), & \text{if } 0 < x < x_0, \\ (r-2)k(l^{k-1} - (x_0 + l - x)^{k-1}), & \text{if } x_0 \leq x \leq l. \end{cases} \quad (\text{B.32})$$

As a result, the first term in Equation (B.25) is

$$T_k(l, l) = (r-2)l^k + x_0^k, \quad (\text{B.33})$$

and the second term in Equation (B.25) is

$$\begin{aligned} \int_0^l \frac{\partial}{\partial l}T_k(x, l)dx &= \int_0^{x_0} \frac{\partial}{\partial l}T_k(x, l)dx + \int_{x_0}^l \frac{\partial}{\partial l}T_k(x, l)dx \\ &= (r-1)k \left[ x_0 l^{k-1} - \frac{1}{k} x_0^k \right] + (r-2)k \left[ (l - x_0)l^{k-1} - \frac{1}{k} l^k + \frac{1}{k} x_0^k \right] \\ &= (r-2)(k-1)l^k + kx_0 l^{k-1} - x_0^k. \end{aligned} \quad (\text{B.34})$$

Therefore, the derivative of  $J(l)$  is

$$\begin{aligned} \frac{d}{dl}J(l) &= T_k(l, l) + \int_0^l \frac{\partial}{\partial l}T_k(x, l)dx \\ &= (r-2)l^k + x_0^k + (r-2)(k-1)l^k + kx_0 l^{k-1} - x_0^k \\ &= (r-2)kl^k + k[1 - (r-1)l]l^{k-1} \\ &= kl^{k-1} - kl^k, \end{aligned} \quad (\text{B.35})$$

which is the same as Equation (B.26). This completes the proof of Lemma 8.  $\square$

## B.2 Proof of Theorem 1

We use Jacod's central limit theorem for semimartingales (Jacod, 1997) in the form of Theorem 2.6 in Podolskij and Vetter (2010).

Recall that the noise-free SALE estimator includes a double summation over subsamples and observation indices within each subsample. This can be reorganized into a single summation, where each increment term represents a local leverage effect estimator at scale  $H_n$ , and consecutive terms correspond to moving forward by a time step of  $\Delta_n$ . Specifically, we have

$$\begin{aligned}
[X, \sigma^2]_T^{(H_n)} &= \frac{1}{H_n} \sum_{h=1}^{H_n} [X, \sigma^2]_T^{(H_n, h)} \\
&= \frac{1}{H_n} \sum_{h=1}^{H_n} \frac{1}{k_n H_n \Delta_n} \sum_{i \in I_{H_n, h}} (\Delta_{H_n} X_{i_h}) \left[ \sum_{j \in I^+(i)} (\Delta_{H_n} X_{j_h})^2 - \sum_{j \in I^-(i)} (\Delta_{H_n} X_{j_h})^2 \right] \\
&= \frac{1}{H_n} \sum_{i=(k_n+1)H_n}^{n-(k_n+2)H_n} (\Delta_{H_n} X_i) (\hat{\sigma}_{H_n, i+}^2 - \hat{\sigma}_{H_n, i-}^2) \\
&= \frac{1}{H_n} \sum_{i=(k_n+1)H_n}^{n-(k_n+2)H_n} V_{H_n, i}.
\end{aligned} \tag{B.36}$$

Here, the increment term at time  $i\Delta$  at scale  $H_n$  is denoted as

$$V_{H_n, i} = (\Delta_{H_n} X_i) (\hat{\sigma}_{H_n, i+}^2 - \hat{\sigma}_{H_n, i-}^2), \tag{B.37}$$

where  $\hat{\sigma}_{H_n, i+}^2$  and  $\hat{\sigma}_{H_n, i-}^2$  are right-side and left-side spot volatility estimators respectively. Denote  $S^+ = \{j - i | j \in I^+(i)\} = \{2, \dots, k_n + 1\}$ ,  $S^- = \{j - i | j \in I^-(i)\} = \{-k_n - 1, \dots, -2\}$ , and the spot volatility estimators can be written as

$$\hat{\sigma}_{H_n, i+}^2 = \frac{1}{k_n H_n \Delta_n} \sum_{j \in S^+} (\Delta_{H_n} X_{i+jH_n})^2, \tag{B.38}$$

$$\hat{\sigma}_{H_n, i-}^2 = \frac{1}{k_n H_n \Delta_n} \sum_{j \in S^-} (\Delta_{H_n} X_{i+jH_n})^2. \tag{B.39}$$

In order to establish the central limit theorem, we need to study the behavior of its error process, which is defined by  $u_n([X, \sigma^2]_T^{(H_n)} - \langle X, \sigma^2 \rangle_T)$  with a normalizing positive number sequence  $\{u_n\}$ , for which we can take  $u_n = \sqrt{k_n \wedge (k_n H_n \Delta_n)^{-1}}$ . Since the estimator is composed of overlapping increment terms, we need to consider the covariance between increment terms within some predefined large blocks. Specifically, we divide the timeline into large blocks of size  $L = (K + 2k_n + 3)H_n \Delta_n$ . The time period for the  $\nu$ th block is  $[L\nu, L\nu + L)$ , where  $\nu = 0, 1, \dots, \lfloor T/L \rfloor - 1$ . Here,  $K$  is an appropriately selected integer that increases with  $n$ . The division of the  $\nu$ th large block is illustrated in Figure 16.

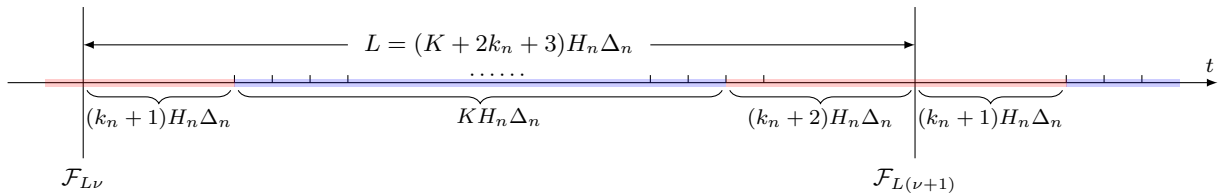


**Figure 16:** The block division in the  $\nu$ th large block

In the  $\nu$ th large block, the blue segment in the middle corresponds to the time period  $[L\nu + (k_n + 1)H_n\Delta_n, L\nu + (K + k_n + 1)H_n\Delta_n]$ , with a length of  $KH_n\Delta_n$ . The red segments on both sides are  $(k_n + 1)H_n\Delta_n$  and  $(k_n + 2)H_n\Delta_n$  long, respectively. Within this large block, we only consider the  $KH_n$  increment terms  $V_i$ 's for which the time points  $i\Delta_n$  lie within the left-closed, right-open interval shown by the blue segment, and their indices are  $J(\nu) = \{L\nu/\Delta_n + (k_n + 1)H_n, \dots, L\nu/\Delta_n + (K + k_n + 1)H_n - 1\}$ . The reason for this division is that all estimates contained in these  $V_i$ 's are within the time period  $[L\nu, L\nu + L)$  of the  $\nu$ th large block, meaning they are  $\mathcal{F}_{L(\nu+1)}$ -measurable. This measurability is crucial for applying the central limit theorem. Furthermore, to ensure the selection of large blocks is appropriate, we need to ensure that  $K$  satisfies two conditions. First,  $K/k_n \rightarrow \infty$  as  $n \rightarrow \infty$ , so that excluding the  $(2k_n + 3)H_n$  increment terms  $V_i$ 's corresponding to the red segments on both sides does not affect the results. Second,  $KH_n\Delta_n \rightarrow 0$  as  $n \rightarrow \infty$ , ensuring that the time span of each large block is sufficiently short, allowing the use of a local constant approximation for the parameters.

With the large block notations, the SALE estimator is now

$$[X, \sigma^2]_T^{(H_n)} = \frac{1}{H_n} \sum_{\nu=0}^{\lfloor T/L \rfloor - 1} \sum_{i \in J(\nu)} V_{H_n, i} + (\text{edge terms}), \quad (\text{B.40})$$

where edge terms include the increment terms corresponding to the red segments on both sides of the large block, and also include the increment terms beyond the last large block at the end of the day. Of course, in both cases, these edge terms do not affect the results. If we omit the edge terms, the normalized error process can be written as

$$u_n \left( [X, \sigma^2]_T^{(H_n)} - \langle X, \sigma^2 \rangle_T \right) = \sum_{\nu=0}^{\lfloor T/L \rfloor - 1} U_\nu, \quad (\text{B.41})$$

where the error term in the  $\nu$ th large block is

$$\begin{aligned} U_\nu &= u_n \left( \frac{1}{H_n} \sum_{i \in J(\nu)} V_{H_n, i} - \int_{L\nu}^{L(\nu+1)} d\langle X, \sigma^2 \rangle_t \right) - (\text{edge terms}) \\ &= \frac{u_n}{H_n} \sum_{i \in J(\nu)} \left( V_{H_n, i} - \int_{i\Delta_n}^{(i+H_n)\Delta_n} d\langle X, \sigma^2 \rangle_t \right) \\ &= U_{\nu,1} + U_{\nu,2}. \end{aligned} \quad (\text{B.42})$$

Here, the edge terms are ignored in the second line, and we define

$$U_{\nu,1} = \frac{u_n}{H_n} \sum_{i \in J(\nu)} \left( V_{H_n, i} - (\Delta_{H_n} X_i)(\Delta_{H_n} \sigma_i^2) \right), \quad (\text{B.43})$$

$$U_{\nu,2} = \frac{u_n}{H_n} \sum_{i \in J(\nu)} \left( (\Delta_{H_n} X_i)(\Delta_{H_n} \sigma_i^2) - \int_{i\Delta_n}^{(i+H_n)\Delta_n} d\langle X, \sigma^2 \rangle_t \right). \quad (\text{B.44})$$

Intuitively,  $U_{\nu,1}$  is the error due to spot volatility estimation, while  $U_{\nu,2}$  is the local error of “oracle” leverage estimation. For the error of spot volatility estimation, notice that

$$V_{H_n, i} - (\Delta_{H_n} X_i)(\Delta_{H_n} \sigma_i^2) = (\Delta_{H_n} X_i) \left( (\hat{\sigma}_{H_n, i+}^2 - \sigma_{i+H_n}^2) - (\hat{\sigma}_{H_n, i-}^2 - \sigma_i^2) \right), \quad (\text{B.45})$$

so we define the error terms of spot volatility estimation as

$$e_{H_n, i+} = \hat{\sigma}_{H_n, i+}^2 - \sigma_{i+H_n}^2, \quad e_{H_n, i-} = \hat{\sigma}_{H_n, i-}^2 - \sigma_i^2, \quad (\text{B.46})$$

for  $i \in J(\nu)$ , and we have

$$U_{\nu,1} = \frac{u_n}{H_n} \sum_{i \in J(\nu)} (\Delta_{H_n} X_i)(e_{H_n,i+} - e_{H_n,i-}). \quad (\text{B.47})$$

For these error terms, we have the following lemma.

**Lemma 9.** *Suppose that  $i, j \in J(\nu)$  and  $|i - j| < H_n$ . We have*

$$\begin{aligned} \mathbb{E}[e_{H_n,i\pm} e_{H_n,j\pm} | \mathcal{F}_{L\nu}] &= \left(\frac{1}{k_n}\right) \cdot 2 \left[ \left(\frac{|i-j|}{H_n}\right)^2 + \left(1 - \frac{|i-j|}{H_n}\right)^2 \right] \sigma_\nu^4 \\ &\quad + (k_n H_n \Delta_n) \cdot \frac{1}{3} \frac{d\langle \sigma^2, \sigma^2 \rangle_t}{dt} \Big|_{t=L\nu} + o_p(k_n^{-1} + k_n H_n \Delta_n), \quad (\text{B.48}) \\ \mathbb{E}[e_{H_n,i\pm} e_{H_n,j\mp} | \mathcal{F}_{L\nu}] &= o_p(k_n^{-1} + k_n H_n \Delta_n). \end{aligned}$$

Moreover, with  $u_n = \sqrt{k_n \wedge (k_n H_n \Delta_n)^{-1}}$ , we assert that, asymptotically and conditioned on  $\mathcal{F}_{L\nu}$ , the expressions  $u_n e_{H_n,i+}$  and  $u_n e_{H_n,i-}$  are independent of each other and  $\mathcal{F}$ , normally distributed, and have mean zero.

*Proof.* To begin with, denote

$$\begin{aligned} e_{H_n,i+} &= (\hat{\sigma}_{H_n,i+}^2 - \sigma_{i+2H_n}^2) + (\sigma_{i+2H_n}^2 - \sigma_{i+H_n}^2) = \tilde{e}_{H_n,i+} + \Delta_{H_n} \sigma_{i+H_n}^2, \\ e_{H_n,i-} &= (\hat{\sigma}_{H_n,i-}^2 - \sigma_{i-H_n}^2) + (\sigma_{i-H_n}^2 - \sigma_i^2) = \tilde{e}_{H_n,i-} + \Delta_{H_n} \sigma_{i-H_n}^2. \end{aligned} \quad (\text{B.49})$$

As we will see,  $\tilde{e}_{H_n,i\pm}$  are the dominant terms in the expressions. Notice that

$$\begin{aligned} \tilde{e}_{H_n,i+} &= \frac{1}{k_n H_n \Delta_n} \sum_{k \in S^+} \int_{(i+kH_n)\Delta_n}^{(i+(k+1)H_n)\Delta_n} 2(X_r - X_{i+kH_n}) dX_r + (\sigma_r^2 - \sigma_{i+2H_n}^2) dr \\ &= \frac{1}{k_n H_n \Delta_n} \left[ \left( \sum_{k \in S^+} \int_{(i+kH_n)\Delta_n}^{(i+(k+1)H_n)\Delta_n} 2(X_r - X_{i+kH_n}) dX_r \right) \right. \\ &\quad \left. + \int_{(i+2H_n)\Delta_n}^{(i+(k_n+2)H_n)\Delta_n} (\sigma_r^2 - \sigma_{i+2H_n}^2) dr \right] \\ &= \frac{1}{k_n H_n \Delta_n} \left[ \left( \sum_{k \in S^+} \xi_{i,k} \right) + \eta_i \right]. \end{aligned} \quad (\text{B.50})$$

Without loss of generality, we take  $0 \leq j < H_n$ , we have

$$\tilde{e}_{H_n,j+} = \frac{1}{k_n H_n \Delta_n} \left[ \left( \sum_{k \in S^+} \xi_{j,k} \right) + \eta_j \right]. \quad (\text{B.51})$$

According to Lemma 7, we can see that, for valid indices, the non-trivial terms are

$$\mathbb{E}[\xi_{i,k} \xi_{j,k} | \mathcal{F}_{(i+kH_n)\Delta_n}] = 2\sigma_{(i+kH_n)\Delta_n}^4 \left( \left(1 - \frac{j-i}{H_n}\right) H_n \Delta_n \right)^2 + o_p(H_n^2 \Delta_n^2), \quad (\text{B.52})$$

$$\mathbb{E}[\xi_{i,k+1} \xi_{j,k} | \mathcal{F}_{(j+kH_n)\Delta_n}] = 2\sigma_{(j+kH_n)\Delta_n}^4 \left( \left(\frac{j-i}{H_n}\right) H_n \Delta_n \right)^2 + o_p(H_n^2 \Delta_n^2), \quad (\text{B.53})$$

$$\mathbb{E}[\eta_i \eta_j | \mathcal{F}_{(i+2H_n)\Delta_n}] = \frac{1}{3} \frac{d\langle \sigma^2, \sigma^2 \rangle_t}{dt} \Big|_{t=(i+2H_n)\Delta_n} (k_n H_n \Delta_n)^3 + o_p(k_n^3 H_n^3 \Delta_n^3). \quad (\text{B.54})$$

As for the negligibility of cross terms such as  $\mathbb{E}[\xi_{j,k}\eta_i|\mathcal{F}_{(i+2H_n)\Delta_n}]$ , we have

$$\begin{aligned}
& \mathbb{E}\left[\xi_{j,k}\eta_i\middle|\mathcal{F}_{(i+2H_n)\Delta_n}\right] \\
&= \mathbb{E}\left[\left(\int_{(j+kH_n)\Delta_n}^{(j+(k+1)H_n)\Delta_n} 2(X_r - X_{j+kH_n})dX_r\right)\right. \\
&\quad \left.\left(\int_{(i+2H_n)\Delta_n}^{(i+(k_n+2)H_n)\Delta_n} [(i+(k_n+2)H_n)\Delta_n - r]d\sigma_r^2\right)\middle|\mathcal{F}_{(i+2H_n)\Delta_n}\right] \\
&\approx \left[(i+(k_n+2)H_n)\Delta_n - (j+kH_n)\Delta_n\right] \frac{d\langle X, \sigma^2 \rangle_t}{dt} \Big|_{t=(i+2H_n)\Delta_n} \\
&\quad \mathbb{E}\left[\int_{(j+kH_n)\Delta_n}^{(j+(k+1)H_n)\Delta_n \wedge (i+(k_n+2)H_n)\Delta_n} 2(X_r - X_{j+kH_n})dr \middle|\mathcal{F}_{(i+2H_n)\Delta_n}\right] \\
&= O_p(k_n H_n \Delta_n \cdot k_n H_n \Delta_n \cdot H_n \Delta_n) \\
&= O_p(k_n^2 H_n^3 \Delta_n^3).
\end{aligned} \tag{B.55}$$

Therefore, we have

$$\begin{aligned}
\mathbb{E}\left[\tilde{e}_{H_n,i+}\tilde{e}_{H_n,j+}\middle|\mathcal{F}_{L\nu}\right] &= \frac{1}{k_n^2 H_n^2 \Delta_n^2} \mathbb{E}\left[\left(\sum_{k \in S^+} \xi_{i,k} + \eta_i\right)\left(\sum_{l \in S^+} \xi_{j,l} + \eta_j\right)\middle|\mathcal{F}_{L\nu}\right] \\
&= \left(\frac{1}{k_n}\right) \cdot 2 \left[\left(\frac{j-i}{H_n}\right)^2 + \left(1 - \frac{j-i}{H_n}\right)^2\right] \sigma_\nu^4 \\
&\quad + (k_n H_n \Delta_n) \cdot \frac{1}{3} \frac{d\langle \sigma^2, \sigma^2 \rangle_t}{dt} \Big|_{t=L\nu} + o_p(k_n^{-1} + k_n H_n \Delta_n),
\end{aligned} \tag{B.56}$$

On the other hand, because  $\mathbb{E}[(\Delta_{H_n} \sigma_{i+H_n}^2)^2 | \mathcal{F}_{(i+H_n)\Delta_n}] = O_p(H_n \Delta_n)$ , we have

$$\begin{aligned}
\mathbb{E}\left[e_{H_n,i+}e_{H_n,j+}\middle|\mathcal{F}_{L\nu}\right] &= \left(\frac{1}{k_n}\right) \cdot 2 \left[\left(\frac{j-i}{H_n}\right)^2 + \left(1 - \frac{j-i}{H_n}\right)^2\right] \sigma_\nu^4 \\
&\quad + (k_n H_n \Delta_n) \cdot \frac{1}{3} \frac{d\langle \sigma^2, \sigma^2 \rangle_t}{dt} \Big|_{t=L\nu} + o_p(k_n^{-1} + k_n H_n \Delta_n),
\end{aligned} \tag{B.57}$$

and similar results can be proved for  $e_{H_n,i-}$  related terms. The remaining part of the lemma is easy to see under the local constant approximation.  $\square$

We need to verify some conditions on the error process to prove the central limit theorem.

**Ucp convergence** First, we need to prove

$$\sum_{\nu=0}^{\lfloor t/L \rfloor - 1} \mathbb{E}[U_\nu | \mathcal{F}_{L\nu}] \xrightarrow{\text{u.c.p.}} 0, \tag{B.58}$$

which is equivalent to

$$\sup_{t \in [0, T]} \left| \sum_{\nu=0}^{\lfloor t/L \rfloor - 1} \mathbb{E}[U_\nu | \mathcal{F}_{L\nu}] \right| \xrightarrow{p} 0, \tag{B.59}$$

while the left-hand side is bounded by

$$\sup_{t \in [0, T]} \left| \sum_{\nu=0}^{\lfloor t/L \rfloor - 1} \mathbb{E}[U_\nu | \mathcal{F}_{L\nu}] \right| \leq \sum_{\nu=0}^{\lfloor t/L \rfloor - 1} \left| \mathbb{E}[U_\nu | \mathcal{F}_{L\nu}] \right| \leq \sum_{\nu=0}^{\lfloor t/L \rfloor - 1} \left( \left| \mathbb{E}[U_{\nu,1} | \mathcal{F}_{L\nu}] \right| + \left| \mathbb{E}[U_{\nu,2} | \mathcal{F}_{L\nu}] \right| \right). \tag{B.60}$$

According to Lemma 9, we know that

$$\begin{aligned}
\mathbb{E}[U_{\nu,1}|\mathcal{F}_{L\nu}] &= \frac{u_n}{H_n} \sum_{i \in J(\nu)} \mathbb{E}[(\Delta_{H_n} X_i)(e_{H_n,i+} - e_{H_n,i-})|\mathcal{F}_{L\nu}] \\
&= \frac{1}{H_n} \sum_{i \in J(\nu)} \mathbb{E}[\Delta_{H_n} X_i|\mathcal{F}_{L\nu}] \mathbb{E}[u_n(e_{H_n,i+} - e_{H_n,i-})|\mathcal{F}_{L\nu}] \\
&= \frac{1}{H_n} \sum_{i \in J(\nu)} O_p(H_n \Delta_n) o_p(1) = o_p(K H_n \Delta_n).
\end{aligned} \tag{B.61}$$

On the other hand, by Lemma 6, we have

$$\begin{aligned}
|\mathbb{E}[U_{\nu,2}|\mathcal{F}_{L\nu}]| &\leq \frac{u_n}{H_n} \sum_{i \in J(\nu)} \mathbb{E} \left[ \left| (\Delta_{H_n} X_i)(\Delta_{H_n} \sigma_i^2) - \int_{i\Delta_n}^{(i+H_n)\Delta_n} d\langle X, \sigma^2 \rangle_t \right| \middle| \mathcal{F}_{L\nu} \right] \\
&\leq \frac{u_n}{H_n} \sum_{i \in J(\nu)} \sqrt{\mathbb{E} \left[ \left( (\Delta_{H_n} X_i)(\Delta_{H_n} \sigma_i^2) - \int_{i\Delta_n}^{(i+H_n)\Delta_n} d\langle X, \sigma^2 \rangle_t \right)^2 \middle| \mathcal{F}_{L\nu} \right]} \\
&= \frac{u_n}{H_n} \sum_{i \in J(\nu)} O_p(H_n \Delta_n) = o_p(u_n K H_n \Delta_n).
\end{aligned} \tag{B.62}$$

Therefore, we have

$$\sum_{\nu=0}^{\lfloor t/L \rfloor - 1} \left( |\mathbb{E}[U_{\nu,1}|\mathcal{F}_{L\nu}]| + |\mathbb{E}[U_{\nu,2}|\mathcal{F}_{L\nu}]| \right) = \sum_{\nu=0}^{\lfloor t/L \rfloor - 1} o_p(K H_n \Delta_n) + o_p(u_n K H_n \Delta_n) = o_p(t), \tag{B.63}$$

so the ucp convergence is verified.

**Quadratic variation** We need to prove

$$\sum_{\nu=0}^{\lfloor t/L \rfloor - 1} \left( \mathbb{E}[U_{\nu}^2|\mathcal{F}_{L\nu}] - \mathbb{E}[U_{\nu}|\mathcal{F}_{L\nu}]^2 \right) \xrightarrow{p} \int_0^t \zeta_s^2 ds, \tag{B.64}$$

for some predictable process  $(\zeta_s)_{s \geq 0}$ . According to previous results, the only non-trivial term in the summand is obviously  $\mathbb{E}[U_{\nu,1}^2|\mathcal{F}_{L\nu}]$  here. By Lemma 9, up to the highest order, we have

$$\begin{aligned}
\mathbb{E}[U_{\nu,1}^2|\mathcal{F}_{L\nu}] &= \frac{u_n^2}{H_n^2} \sum_{i \in J(\nu)} \sum_{j \in J(\nu)} \mathbb{E}[(\Delta_{H_n} X_i)(\Delta_{H_n} X_j)|\mathcal{F}_{L\nu}] \mathbb{E}[(e_{H_n,i+} - e_{H_n,i-})(e_{H_n,j+} - e_{H_n,j-})|\mathcal{F}_{L\nu}] \\
&= \frac{u_n^2}{H_n^2} \sum_{i \in J(\nu)} \sum_{j \in J(\nu), |i-j| < H_n} \sigma_\nu^2 \left( 1 - \frac{|i-j|}{H_n} \right) H_n \Delta_n \mathbb{E}[e_{H_n,i+} e_{H_n,j+} + e_{H_n,i-} e_{H_n,j-} | \mathcal{F}_{L\nu}] \\
&= \frac{u_n^2}{H_n^2} \sum_{i \in J(\nu)} \sum_{j \in J(\nu), |i-j| < H_n} \sigma_\nu^2 \left( 1 - \frac{|i-j|}{H_n} \right) H_n \Delta_n \\
&\quad \cdot 2 \left\{ \frac{1}{k_n} \cdot 2 \left[ \left( \frac{|i-j|}{H_n} \right)^2 + \left( 1 - \frac{|i-j|}{H_n} \right)^2 \right] \sigma_\nu^4 + k_n H_n \Delta_n \cdot \frac{1}{3} \frac{d\langle \sigma^2, \sigma^2 \rangle_t}{dt} \middle|_{t=L\nu} \right\} \\
&= u_n^2 \left( \frac{1}{k_n} \cdot \left( \frac{8}{3} + \frac{4}{3H_n^2} \right) \sigma_\nu^6 \cdot K H_n \Delta_n + k_n H_n \Delta_n \cdot \frac{2}{3} \sigma_\nu^2 \frac{d\langle \sigma^2, \sigma^2 \rangle_t}{dt} \middle|_{t=L\nu} \cdot K H_n \Delta_n \right).
\end{aligned} \tag{B.65}$$



Therefore, with  $u_n = \sqrt{k_n \wedge (k_n H_n \Delta_n)^{-1}}$ , we have

$$\begin{aligned}
& \sum_{\nu=0}^{\lfloor t/L \rfloor - 1} \left( \mathbb{E}[U_\nu^2 | \mathcal{F}_{L\nu}] - \mathbb{E}[U_\nu | \mathcal{F}_{L\nu}]^2 \right) \\
&= \frac{u_n^2}{k_n} \sum_{\nu=0}^{\lfloor t/L \rfloor - 1} \left( \frac{8}{3} + \frac{4}{3H_n^2} \right) \sigma_\nu^6 \cdot K H_n \Delta_n + u_n^2 k_n H_n \Delta_n \sum_{\nu=0}^{\lfloor t/L \rfloor - 1} \frac{2}{3} \sigma_\nu^2 \frac{d\langle \sigma^2, \sigma^2 \rangle_t}{dt} \Big|_{t=L\nu} \cdot K H_n \Delta_n \\
&\xrightarrow{p} \frac{u_n^2}{k_n} \int_0^t \left( \frac{8}{3} + \frac{4}{3H_n^2} \right) \sigma_s^6 ds + u_n^2 k_n H_n \Delta_n \int_0^t \frac{2}{3} \sigma_s^2 d\langle \sigma^2, \sigma^2 \rangle_s.
\end{aligned} \tag{B.66}$$

**Quadratic covariation** We need to prove

$$\sum_{\nu=0}^{\lfloor t/L \rfloor - 1} \mathbb{E} \left[ U_\nu (M_{L(\nu+1)} - M_{L\nu}) \Big| \mathcal{F}_{L\nu} \right] \xrightarrow{p} 0, \quad \forall M \in \{W, B, N\}, \tag{B.67}$$

where  $(N_s)_{s \geq 0}$  is an arbitrary bounded  $\mathcal{F}_t$ -martingale with  $N_0 = 0$  and  $\langle W, N \rangle = \langle B, N \rangle = 0$ . As before, we omit  $U_{\nu,2}$  for its minor contribution, while for  $U_{\nu,1}$ , we have

$$\begin{aligned}
& \sum_{\nu=0}^{\lfloor t/L \rfloor - 1} \mathbb{E} \left[ U_{\nu,1} (M_{L(\nu+1)} - M_{L\nu}) \Big| \mathcal{F}_{L\nu} \right] \\
&= \sum_{\nu=0}^{\lfloor t/L \rfloor - 1} \frac{1}{H_n} \sum_{i \in J(\nu)} \mathbb{E} \left[ (\Delta_{H_n} X_i) (M_{L(\nu+1)} - M_{L\nu}) \Big| \mathcal{F}_{L\nu} \right] \mathbb{E} \left[ u_n (e_{H_n, i+} - e_{H_n, i-}) \Big| \mathcal{F}_{L\nu} \right] \\
&= \sum_{\nu=0}^{\lfloor t/L \rfloor - 1} \frac{1}{H_n} \sum_{i \in J(\nu)} O_p(H_n \Delta_n) o_p(1) = o_p \left( \frac{t}{K H_n \Delta_n} \cdot \frac{1}{H_n} \cdot K H_n \cdot H_n \Delta_n \cdot 1 \right) \\
&= o_p(t).
\end{aligned} \tag{B.68}$$

This argument holds for any bounded  $\mathcal{F}_t$ -martingale.

**Lindeberg condition** We need to prove

$$\sum_{\nu=0}^{\lfloor t/L \rfloor - 1} \mathbb{E} \left[ U_\nu^2 1_{\{|U_\nu| > \epsilon\}} \Big| \mathcal{F}_{L\nu} \right] \xrightarrow{p} 0, \quad \forall \epsilon > 0. \tag{B.69}$$

It is well-known that a sufficient condition for Equation (B.69) is

$$\sum_{\nu=0}^{\lfloor t/L \rfloor - 1} \mathbb{E} \left[ |U_\nu|^{2+\delta} \Big| \mathcal{F}_{L\nu} \right] \xrightarrow{p} 0, \tag{B.70}$$

for any  $\delta > 0$ . We take  $\delta = 2$  for simplicity, and omit  $U_{\nu,2}$ . The resulting expression is

$$\begin{aligned}
& \sum_{\nu=0}^{\lfloor t/L \rfloor - 1} \mathbb{E}[U_{\nu,1}^4 | \mathcal{F}_{L\nu}] \\
&= \sum_{\nu=0}^{\lfloor t/L \rfloor - 1} \frac{1}{H_n^4} \mathbb{E} \left[ \prod_{k=1}^4 \sum_{i_k \in J(\nu)} (\Delta_{H_n} X_{i_k}) u_n(e_{H_n, i_k+} - e_{H_n, i_k-}) \middle| \mathcal{F}_{L\nu} \right] \\
&= \sum_{\nu=0}^{\lfloor t/L \rfloor - 1} \frac{1}{H_n^4} \sum_{i_1, i_2, i_3, i_4 \in J(\nu)} \mathbb{E} \left[ \prod_{k=1}^4 (\Delta_{H_n} X_{i_k}) \middle| \mathcal{F}_{L\nu} \right] \mathbb{E} \left[ \prod_{k=1}^4 u_n(e_{H_n, i_k+} - e_{H_n, i_k-}) \middle| \mathcal{F}_{L\nu} \right] \quad (\text{B.71}) \\
&= \sum_{\nu=0}^{\lfloor t/L \rfloor - 1} \frac{1}{H_n^4} O_p((KH_n)^2 H_n^2 \cdot H_n^2 \Delta_n^2 + (KH_n)^4 \cdot H_n^4 \Delta_n^4) \\
&= O_p(tKH_n \Delta_n) = o_p(t).
\end{aligned}$$

**Final result** Finally, combine Equation (B.58), Equation (B.64), Equation (B.67), and Equation (B.69), we can prove Theorem 1 with Jacod's semimartingale central limit theorem, and the result is

$$\begin{aligned}
& u_n \left( [X, \sigma^2]_t^{(H_n)} - \langle X, \sigma^2 \rangle_t \right) \\
& \xrightarrow{\text{st}} \int_0^t \sqrt{\frac{u_n^2}{k_n} \left( \frac{8}{3} + \frac{4}{3H_n^2} \right) \sigma_s^6 + u_n^2 k_n H_n \Delta_n \frac{2}{3} \sigma_s^2 \frac{d\langle \sigma^2, \sigma^2 \rangle_r}{dr} \bigg|_{r=s}} dW'_s, \quad (\text{B.72})
\end{aligned}$$

where  $(W'_s)_{s \geq 0}$  is a Brownian motion defined on an extension of the original probability space and independent of  $\mathcal{F}$ .

### B.3 Proof of Theorem 2

The proof follows directly from Proposition 2 and Theorem 1. First, according to Proposition 2, we have

$$\Delta_n^{3/2} H_n^2 k_n \left( \widehat{[X, \sigma^2]_t}^{(H_n)} - [X, \sigma^2]_t^{(H_n)} \right) \xrightarrow{d} \int_0^t \sqrt{\Phi} dB_t^{(H_n)}, \quad (\text{B.73})$$

where  $(B_t^{H_n})_{t \geq 0}$  is a Brownian motion independent of  $\mathcal{F}$ . Next, we apply Jacod's central limit theorem to the normalized error process of noise-free SALE estimator, which is  $u_n([X, \sigma^2]_t^{(H_n)} - \langle X, \sigma^2 \rangle_t)$ , again, but for Equation (B.67), we need to add that the convergence in probability holds for any bounded  $\sigma(B_t^{(H_n)})$ -martingale, which is trivial. Thus, we can prove that the stable convergence as shown in Equation (B.72) still holds, but the corresponding probability space is the product space of  $(\Omega, \mathcal{F}, \mathbb{P})$  and the space of the Brownian motion  $(B_t^{(H_n)})_{t \geq 0}$ . Thus, according to the property of stable convergence,  $\Delta_n^{3/2} H_n^2 k_n (\widehat{[X, \sigma^2]_t}^{(H_n)} - [X, \sigma^2]_t^{(H_n)})$  and  $u_n([X, \sigma^2]_t^{(H_n)} - \langle X, \sigma^2 \rangle_t)$  converges jointly to the corresponding limit processes, so their summation also stably converges to the summation of these limit processes. After that, adjust the convergence rate and corresponding constant coefficients, and we complete the proof of Theorem 2.

### B.4 Proof of Theorem 3

The theorem follows from a property of stable convergence. We explain the construction of  $G_n^{(1)}$  and  $G_n^{(2)}$  here. According to Theorem 3.4.1 of Jacod and Protter (2012), or Example 3.2

of Podolskij and Vetter (2010), it has been established that

$$\Delta_n \sum_{i=0}^{\lfloor t/\Delta_n \rfloor - 1} \left( \frac{\Delta X_i}{\sqrt{\Delta_n}} \right)^6 \xrightarrow{\text{u.c.p.}} 15 \int_0^t \sigma_s^6 ds, \quad (\text{B.74})$$

so we have

$$G_n^{(1)} = \frac{1}{15\Delta_n^2} \sum_{i=0}^{n-1} (\Delta X_i)^6 \xrightarrow{p} \int_0^T \sigma_t^6 dt. \quad (\text{B.75})$$

According to Theorem 8.11 of Aït-Sahalia and Jacod (2014), or Theorem 2.6 of Vetter (2015), It has been proved that

$$\frac{1}{k_n} \sum_{i \in I} \left( \frac{3}{2} (\hat{\sigma}_{j+}^2 - \hat{\sigma}_{j-}^2)^2 - \frac{1}{k_n^2 \Delta_n^2} \sum_{j \in I^{\pm(i)}} (\Delta X_j)^4 \right) \xrightarrow{p} \langle \sigma^2, \sigma^2 \rangle_T, \quad (\text{B.76})$$

so we have

$$G_n^{(2)} = \frac{1}{k_n \Delta_n} \sum_{i \in I} (\Delta X_i)^2 \left( \frac{3}{2} (\hat{\sigma}_{j+}^2 - \hat{\sigma}_{j-}^2)^2 - \frac{1}{k_n^2 \Delta_n^2} \sum_{j \in I^{\pm(i)}} (\Delta X_j)^4 \right) \xrightarrow{p} \int_0^T \sigma_t^2 d\langle \sigma^2, \sigma^2 \rangle_t. \quad (\text{B.77})$$

The construction of  $\widehat{G}_n^{(1)}$  and  $\widehat{G}_n^{(2)}$  is based on the pre-averaging correction on  $G_n^{(1)}$  and  $G_n^{(2)}$ .

## B.5 Proof of Proposition 4, Proposition 5, Theorem 4, and Theorem 5

The proof of Theorem 4 is similar as that of Theorem 1. We still use the large block techniques combined with local constant approximation, while we will only present the calculation of asymptotic variance, which is the essential part of the proof, and other tedious verification steps for conditions are omitted.

For each scale  $H \in \{H_1, \dots, H_{M_n}\}$ , the window length for spot volatility estimation (which is  $k_n$  in the SALE estimator) varies, so we denote the window length for scale  $H_p$  as  $k_p$ . We use the largest scale  $H_{M_n}$  to define the large block in a similar way as in Section B.2, so that  $L \asymp KH_{M_n}\Delta_n$  (here we write  $X_n \asymp Y_n$  if  $X_n/Y_n \rightarrow 1$  as  $n \rightarrow \infty$ ), and the  $\nu$ th large block corresponds to the time interval  $[L\nu, L\nu + L)$ . After that, we denote the increment term at scale  $H$  as  $V_{H,i}$ , and the index set for  $V_{H,i}$  in the  $\nu$ th large block as  $J_H(\nu)$ . Although one can observe that  $J_H(\nu)$  decreases as  $H$  increases, we still have  $|J_H(\nu)| \asymp KM_n$  for all  $H \in \{H_1, \dots, H_{M_n}\}$ . On the whole, it is tedious and meaningless to present the detailed operations of the edge terms and the differences of index sets between different scales, because it is only a way to construct some kind of conditional expectation and local approximation in the proof, so we will just stop here and focus on the important things.

With the large block notations, the MSLE estimator can be expressed as

$$[X, \sigma^2]_T^{(\text{MS})} = \sum_{p=1}^{M_n} w_p [X, \sigma^2]_T^{H_p} = \sum_{\nu=0}^{\lfloor T/L \rfloor - 1} \sum_{p=1}^{M_n} \frac{w_p}{H_p} \sum_{i \in J_{H_p}(\nu)} V_{H_p,i} + (\text{edge terms}). \quad (\text{B.78})$$

Here, the increment term is defined as

$$V_{H_p,i} = (\Delta_{H_p} X_i) \left( \hat{\sigma}_{H_p,i+}^2 - \hat{\sigma}_{H_p,i-}^2 \right), \quad (\text{B.79})$$

where the spot volatility estimators are

$$\hat{\sigma}_{H_p,i+}^2 = \frac{1}{k_n H_p \Delta_n} \sum_{j \in S_{H_p}^+} (\Delta_{H_p} X_{i+jH_p})^2, \quad (\text{B.80})$$

$$\hat{\sigma}_{H_p,i-}^2 = \frac{1}{k_n H_p \Delta_n} \sum_{j \in S_{H_p}^-} (\Delta_{H_p} X_{i+jH_p})^2, \quad (\text{B.81})$$

and the shifting index sets are  $S_{H_p}^+ = \{2, \dots, k_p + 1\}$  and  $S_{H_p}^- = \{-k_p - 1, \dots, -2\}$ . With a proper positive normalizing sequence  $u_n$  (which is different from that in Section B.2), omitting the edge terms, the normalized error process of the MSLE estimator is

$$u_n \left( [X, \sigma^2]_T^{(\text{MS})} - \langle X, \sigma^2 \rangle_T \right) = \sum_{\nu=0}^{\lfloor T/L \rfloor - 1} \sum_{p=1}^{M_n} w_p U_{H_p, \nu}, \quad (\text{B.82})$$

where the error term at scale  $H$  in the  $\nu$ th large block is

$$U_{H_p, \nu} = \frac{u_n}{H_p} \sum_{i \in J_{H_p}(\nu)} \left( V_{H_p, i} - \int_{i\Delta_n}^{(i+H_p)\Delta_n} d\langle X, \sigma^2 \rangle_t \right) = U_{H_p, \nu, 1} + U_{H_p, \nu, 2}. \quad (\text{B.83})$$

Here, we denote the error caused by spot volatility estimation and by the discretization of quadratic covariation as

$$U_{H_p, \nu, 1} = \frac{u_n}{H_p} \sum_{i \in J_{H_p}(\nu)} \left( V_{H_p, i} - (\Delta_{H_p} X_i)(\Delta_{H_p} \sigma_i^2) \right), \quad (\text{B.84})$$

$$U_{H_p, \nu, 2} = \frac{u_n}{H_p} \sum_{i \in J_{H_p}(\nu)} \left( (\Delta_{H_p} X_i)(\Delta_{H_p} \sigma_i^2) - \int_{i\Delta_n}^{(i+H_p)\Delta_n} d\langle X, \sigma^2 \rangle_t \right), \quad (\text{B.85})$$

respectively. Obviously,  $U_{H_p, \nu, 1}$  is the dominant term in the error process.

Before diving into the proof, we need to introduce some notations concerning the adjustment factors in Proposition 4. The definition naturally arises when considering the overlapping situation of the increment terms at different scales.

**Definition 1.** Suppose  $p, q, H_p, H_q, k_p, k_q$  are positive integers that satisfy  $p \geq q$  and  $H_p \geq H_q$ . Define the following discrete function  $\mathcal{K}_{p,q} : \mathbb{Z} \rightarrow \mathbb{R}$  as

$$\mathcal{K}_{p,q}(d) = \begin{cases} \frac{d+H_q}{H_p H_q}, & \text{if } -H_q < d < 0, \\ \frac{1}{H_p}, & \text{if } 0 \leq d \leq H_p - H_q, \\ \frac{-d+H_p}{H_p H_q}, & \text{if } H_p - H_q < d < H_p, \\ 0, & \text{otherwise.} \end{cases} \quad (\text{B.86})$$

One verify that  $\sum_{d \in \mathbb{Z}} \mathcal{K}_{p,q}(d) = 1$ . For any  $i, j \in \mathbb{Z}$ , define the following two sets of grid points

$$G_p(i) = \{i + kH_p : k \in \mathbb{Z}\} \quad \text{and} \quad G_q(j) = \{j + kH_q : k \in \mathbb{Z}\}, \quad (\text{B.87})$$

and two points  $L_{p,q}(i, j)$  and  $R_{p,q}(i, j)$  as

$$L_{p,q}(i, j) = (i + 2H_p) \vee (j + 2H_q) \quad \text{and} \quad R_{p,q}(i, j) = (i + (k_p + 2)H_p) \wedge (j + (k_q + 2)H_q). \quad (\text{B.88})$$

Next, define the *cubed overlapping length* (COL) and its normalized version as

$$\text{COL}_{p,q}(i, j) = [(R_{p,q}(i, j) - L_{p,q}(i, j))_+]^3 \quad \text{and} \quad \widetilde{\text{COL}}_{p,q}(i, j) = \frac{\text{COL}_{p,q}(i, j)}{k_q^3 H_q^3}. \quad (\text{B.89})$$

Moreover, consider the following steps. Denote a set of points

$$P_{p,q}(i, j) = (G_p(i) \cup G_q(j)) \cap [L_{p,q}(i, j), R_{p,q}(i, j)], \quad (\text{B.90})$$

and then sort the elements in  $P_{p,q}(i, j)$  in ascending order to get a sequence  $Q_{p,q}(i, j) = [x_1, \dots, x_m]$  with  $m \geq 0$ , and finally define the *sum of squares of overlapping segments* (SSOS) and its normalized version as

$$\text{SSOS}_{p,q}(i, j) = \sum_{k=1}^{m-1} (x_{k+1} - x_k)^2 \quad \text{and} \quad \widetilde{\text{SSOS}}_{p,q}(i, j) = \frac{\text{SSOS}_{p,q}(i, j)}{k_q H_q^2}. \quad (\text{B.91})$$

It is easy to see that both  $\text{COL}_{p,q}(i, j)$  and  $\text{SSOS}_{p,q}(i, j)$  depend on  $i, j$  only through  $j - i$ . Finally, we define the *adjustment factors*  $v_{p,q}^{(1)}$  and  $v_{p,q}^{(2)}$  as

$$v_{p,q}^{(1)} = \sum_{d \in \mathbb{Z}} \mathcal{K}_{p,q}(d) \widetilde{\text{SSOS}}_{p,q}(0, d), \quad (\text{B.92})$$

$$v_{p,q}^{(2)} = \sum_{d \in \mathbb{Z}} \mathcal{K}_{p,q}(d) \widetilde{\text{COL}}_{p,q}(0, d). \quad (\text{B.93})$$

This definition can also be used as an algorithm to calculate the adjustment factors.

Note that in the above definition, suppose  $k_p = \lfloor \beta \lfloor n/H_p \rfloor^b \rfloor$  holds for all  $p \in \{1, \dots, M_n\}$ , with some constant  $\beta > 0$  and  $b \in (0, 1)$ , we have  $v_{p,q}^{(1)}, v_{p,q}^{(2)} \in [0, 1]$ .

With the definition above, we first establish the following lemma concerning the covariance of  $U_{H_p, \nu, 1}$  and  $U_{H_q, \nu, 1}$  within a large block.

**Lemma 10.** *We have*

$$\begin{aligned} & \mathbb{E}(U_{H_p, \nu, 1} U_{H_q, \nu, 1} | \mathcal{F}_{L\nu}) \\ &= \frac{u_n^2}{k_p} \cdot 4v_{p,q}^{(1)} \frac{H_q}{H_p} \cdot \sigma_\nu^6 L + u_n^2 k_p H_p \Delta_n \cdot \frac{2}{3} v_{p,q}^{(2)} \left( \frac{k_q H_q}{k_p H_p} \right)^2 \cdot \sigma_\nu^2 \frac{d\langle \sigma^2, \sigma^2 \rangle_t}{dt} \Big|_{t=L\nu} L \\ & \quad + o_p(u_n^2 k_p^{-1} L + u_n^2 k_p H_p \Delta_n L). \end{aligned} \quad (\text{B.94})$$

*Proof.* We can rewrite  $U_{H_p, \nu, 1}$  as

$$U_{H_p, \nu, 1} = \frac{u_n}{H_p} \sum_{i \in J_{H_p}(\nu)} \left( V_{H_p, i} - (\Delta_{H_p} X_i)(\Delta_{H_p} \sigma_i^2) \right) = \frac{u_n}{H_p} \sum_{i \in J_{H_p}(\nu)} (\Delta_{H_p} X_i)(e_{H_p, i+} - e_{H_p, i-}), \quad (\text{B.95})$$

where  $e_{H_p, i+} = \hat{\sigma}_{H_p, i+}^2 - \sigma_{i+H_p}^2$ , and  $e_{H_p, i-} = \hat{\sigma}_{H_p, i-}^2 - \sigma_i^2$ , and repeat this similarly for  $U_{H_q, \nu, 1}$ . As a result, we have

$$\begin{aligned} \mathbb{E}(U_{H_p, \nu, 1} U_{H_q, \nu, 1} | \mathcal{F}_{L\nu}) &= \frac{u_n^2}{H_p H_q} \sum_{i \in J_{H_p}(\nu)} \left\{ \sum_{j \in J_{H_q}(\nu)} \mathbb{E}[(\Delta_{H_p} X_i)(\Delta_{H_q} X_j) | \mathcal{F}_{L\nu}] \right. \\ & \quad \left. \mathbb{E}[(e_{H_p, i+} - e_{H_p, i-})(e_{H_q, j+} - e_{H_q, j-}) | \mathcal{F}_{L\nu}] \right\}. \end{aligned} \quad (\text{B.96})$$

For the price-related term inside the bracket, we have

$$\mathbb{E}[(\Delta_{H_p} X_i)(\Delta_{H_q} X_j) | \mathcal{F}_{L\nu}] = \sigma_\nu^2 s(i, j) + o_p(H_q \Delta_n), \quad (\text{B.97})$$

where  $s(i, j) = H_p H_q \Delta_n \mathcal{K}_{p,q}(j - i)$  describes the overlapping time length of the increments, with  $\mathcal{K}_{p,q}$  defined in Equation (B.86). For the spot-volatility-related term inside the bracket, we use the similar decomposition as in the proof of Lemma 9. That is,  $e_{H_p, i+} = \tilde{e}_{H_p, i+} + \Delta_{H_p} \sigma_{i+H_p}^2$ , where the second term is negligible here. For the spot volatility on the right hand side, we have

$$\tilde{e}_{H_p, i+} = \frac{1}{k_p H_p \Delta_n} \left[ \left( \sum_{k \in S_{H_p}^+} \xi_{H_p, i, k} \right) + \eta_{H_p, i}^+ \right], \quad (\text{B.98})$$

where

$$\xi_{H_p, i, k} = \int_{(i+kH_p)\Delta_n}^{(i+(k+1)H_p)\Delta_n} 2(X_r - X_{i+kH_p}) dX_r, \quad \text{for all } k \in S_{H_p}^+, \quad (\text{B.99})$$

$$\eta_{H_p, i}^+ = \int_{(i+2H_p)\Delta_n}^{(i+(k_p+2)H_p)\Delta_n} (\sigma_r^2 - \sigma_{i+2H_p}^2) dr. \quad (\text{B.100})$$

The cross product of these terms are asymptotically negligible as before. Therefore, it suffices to consider

$$\mathbb{E}\left[\left(\sum_{k \in S_{H_p}^+} \xi_{H_p,i,k}\right)\left(\sum_{l \in S_{H_q}^+} \xi_{H_q,j,l}\right)\middle|\mathcal{F}_{L\nu}\right] \quad \text{and} \quad \mathbb{E}\left[\eta_{H_p,i}^+ \eta_{H_q,j}^+ \middle|\mathcal{F}_{L\nu}\right] \quad (\text{B.101})$$

terms. According to Lemma 7, we know that

$$\mathbb{E}\left[\left(\sum_{k \in S_{H_p}^+} \xi_{H_p,i,k}\right)\left(\sum_{l \in S_{H_q}^+} \xi_{H_q,j,l}\right)\middle|\mathcal{F}_{L\nu}\right] = 2\sigma_\nu^4 \text{SSOS}_{p,q}(i,j)\Delta_n^2 + o_p(k_q H_q^2 \Delta_n^2), \quad (\text{B.102})$$

and

$$\mathbb{E}\left[\eta_{H_p,i}^+ \eta_{H_q,j}^+ \middle|\mathcal{F}_{L\nu}\right] = \frac{1}{3} \frac{d\langle \sigma^2, \sigma^2 \rangle_t}{dt} \Big|_{t=L\nu} \text{COL}_{p,q}(i,j)\Delta_n^3 + o_p(k_q^3 H_q^3 \Delta_n^3). \quad (\text{B.103})$$

Therefore, we have

$$\begin{aligned} & \frac{u_n^2}{H_p H_q} \sum_{i \in J_{H_p}(\nu)} \sum_{j \in J_{H_q}(\nu)} \mathbb{E}\left[(\Delta_{H_p} X_i)(\Delta_{H_q} X_j) \middle|\mathcal{F}_{L\nu}\right] \mathbb{E}\left[\tilde{e}_{H_p,i} + \tilde{e}_{H_q,j} + \tilde{e}_{H_p,i} - \tilde{e}_{H_q,j} \middle|\mathcal{F}_{L\nu}\right] \\ & \approx \frac{u_n^2}{H_p H_q} \frac{1}{k_p H_p \Delta_n} \frac{1}{k_q H_q \Delta_n} \sum_{i \in J_{H_p}(\nu)} \sum_{j \in J_{H_q}(\nu)} \mathbb{E}\left[(\Delta_{H_p} X_i)(\Delta_{H_q} X_j) \middle|\mathcal{F}_{L\nu}\right] \mathbb{E}\left[\left(\sum_{k \in S_{H_p}^+} \xi_{H_p,i,k}\right)\left(\sum_{l \in S_{H_q}^+} \xi_{H_q,j,l}\right) + \eta_{H_p,i}^+ \eta_{H_q,j}^+ \middle|\mathcal{F}_{L\nu}\right] \times 2 \\ & \approx \frac{u_n^2}{k_p k_q H_p^2 H_q^2 \Delta_n^2} \sum_{i \in J_{H_p}(\nu)} k_q H_p H_q^3 \Delta_n^3 \cdot 4\sigma_\nu^6 v_{p,q}^{(1)} + k_q^3 H_p H_q^4 \Delta_n^4 \cdot \frac{2}{3} \sigma_\nu^2 \frac{d\langle \sigma^2, \sigma^2 \rangle_t}{dt} \Big|_{t=L\nu} v_{p,q}^{(2)} \\ & \approx \frac{u_n^2}{k_p} \cdot 4v_{p,q}^{(1)} \frac{H_q}{H_p} \cdot \sigma_\nu^6 L + u_n^2 k_p H_p \Delta_n \cdot \frac{2}{3} v_{p,q}^{(2)} \left(\frac{k_q H_q}{k_p H_p}\right)^2 \cdot \sigma_\nu^2 \frac{d\langle \sigma^2, \sigma^2 \rangle_t}{dt} \Big|_{t=L\nu} L. \end{aligned} \quad (\text{B.104})$$

This completes the proof of Lemma 10.  $\square$

Suppose  $k_p = \lfloor \beta[n/H_p]^b \rfloor$  holds for all  $p \in \{1, \dots, M_n\}$ , with some constant  $\beta > 0$  and  $b \in (0, 1)$ . Proposition 4 is a direct result of Lemma 10, and the first scenario of Theorem 4 follows directly from Proposition 4.

Next, we prove Proposition 5 on the asymptotic properties of the adjustment factors.

*Proof of Proposition 5.* Recall that, there are two sequences of scales  $H_p$  and  $H_q$  indexed by  $n$ , such that  $H_p \geq H_q$  for all  $n$ , and  $H_p, H_q \rightarrow \infty$ ,  $H_q/H_p \rightarrow c$  for some constant  $c \in (0, 1]$  as  $n \rightarrow \infty$ . Note the necessary condition for  $\mathcal{K}_{p,q}(d) > 0$  is that  $-H_q < d < H_p$ . It is easy to see that under this condition, we have  $\widehat{\text{COL}}_{p,q}(0, d) \rightarrow 1$  as  $n \rightarrow \infty$ , so  $v_{p,q}^{(2)} \rightarrow 1$  as  $n \rightarrow \infty$ . For  $v_{p,q}^{(2)}$ , note that asymptotically, the total length of overlapping region contains about

$$N_{p,q} = \frac{k_q H_q}{H_p} \approx \beta c^{1-b} (n/H_p)^b \rightarrow \infty \quad (\text{B.105})$$

increments of  $H_p$  in  $H_p$ -grids. In fact, across all  $j$  satisfying  $i - H_q < j < i + H_p$  for a fixed  $i$ , the number of  $H_p$ -intervals in  $H_p$ -grid, where the segments within it are full-filled and add up to  $H_p$ , is also about  $N_{p,q}$ . That is, we can regroup the SSOS defined in Equation (B.91) into approximately  $N_{p,q}$  groups, and therefore

$$\text{SSOS}_{p,q}(i, j) \approx \sum_{l=1}^{N_{p,q}} g_{p,q}(l; i, j), \quad (\text{B.106})$$

where  $g_{p,q}(l; i, j)$  is the SSOS within group  $l$ . Thus, we have

$$v_{p,q}^{(1)} \approx \frac{1}{k_q H_q^2} \sum_{d \in \mathbb{Z}} \mathcal{K}_{p,q}(d) \sum_{l=1}^{N_{p,q}} g_{p,q}(l; 0, d) = \frac{1}{k_q H_q^2} \sum_{l=1}^{N_{p,q}} \sum_{d \in \mathbb{Z}} \mathcal{K}_{p,q}(d) g_{p,q}(l; 0, d). \quad (\text{B.107})$$

Notice that,  $g_{p,q}(l; 0, d) = g_{p,q}(l; 0, d + H_q)$  for any valid  $d$ , because the pattern of grid points within the  $l$ th  $H_p$ -interval repeats itself when  $j$  shifts  $H_q$ . Another important observation is that, through direct calculation, we have

$$\sum_{d \in \mathbb{Z}} \mathcal{K}_{p,q}(d) 1_{\{d \equiv d_0 \pmod{H_q}\}} = \frac{1}{H_q}, \quad \text{for all } d_0 = 0, 1, \dots, H_q - 1, \quad (\text{B.108})$$

Therefore, we have

$$\begin{aligned} v_{p,q}^{(1)} &\approx \frac{1}{k_q H_q^2} \sum_{l=1}^{N_{p,q}} \sum_{d \in \mathbb{Z}} \mathcal{K}_{p,q}(d) g_{p,q}(l; 0, d) \\ &= \frac{1}{k_q H_q^2} \sum_{l=1}^{N_{p,q}} \sum_{d \in \mathbb{Z}} \mathcal{K}_{p,q}(d) g_{p,q}(l; 0, d) \sum_{d_0=0}^{H_q-1} 1_{\{d \equiv d_0 \pmod{H_q}\}} \\ &= \frac{1}{k_q H_q^2} \sum_{l=1}^{N_{p,q}} \sum_{d_0=0}^{H_q-1} g_{p,q}(l; 0, d_0) \sum_{d \in \mathbb{Z}} \mathcal{K}_{p,q}(d) 1_{\{d \equiv d_0 \pmod{H_q}\}} \\ &= \frac{1}{k_q H_q^2} \sum_{l=1}^{N_{p,q}} \frac{1}{H_q} \sum_{d_0=0}^{H_q-1} g_{p,q}(l; 0, d_0). \end{aligned} \quad (\text{B.109})$$

On the other hand, the property of  $H_q^{-1} \sum_{d_0=0}^{H_q-1} g_{p,q}(l; 0, d_0)$  has been well studied by Lemma 8. That is,

$$\begin{aligned} \frac{1}{H_q} \sum_{d_0=0}^{H_q-1} g_{p,q}(l; 0, d_0) &= H_p^2 \mathbb{E}_{\alpha_1 \sim \text{Unif}\{1/H_q, \dots, H_q/H_p\}} \left[ S_2(\alpha_1, H_q/H_p) \right] \\ &\rightarrow H_p^2 \mathbb{E}_{\alpha_1 \sim \text{Unif}(0,1]} \left[ S_2(\alpha_1, H_q/H_p) \right] \\ &= H_p H_q \left( 1 - \frac{H_q}{3H_p} \right), \end{aligned} \quad (\text{B.110})$$

as  $H_q \rightarrow \infty$ . Finally, we have

$$v_{p,q}^{(1)} \rightarrow \frac{1}{k_q H_q^2} \sum_{l=1}^{N_{p,q}} H_p H_q \left( 1 - \frac{H_q}{3H_p} \right) \approx \frac{1}{k_q H_q^2} \frac{k_q H_q}{H_p} H_p H_q \left( 1 - \frac{H_q}{3H_p} \right) = 1 - \frac{c}{3}, \quad (\text{B.111})$$

as  $n \rightarrow \infty$ . This completes the proof of Proposition 5.  $\square$

The second scenario of Theorem 4 follows directly from Proposition 4. This completes the proof of Theorem 4. The proof of Theorem 5 follows from Proposition 3 and Theorem 4 in the exactly same way as in Section B.3, so we omit the details here.